INFORMATION TO USERS

This manuscript has been reproduced from the microfilm master. UMI films the text directly from the original or copy submitted. Thus, some thesis and dissertation copies are in typewriter face, while others may be from any type of computer printer.

The quality of this reproduction is dependent upon the quality of the copy submitted. Broken or indistinct print, colored or poor quality illustrations and photographs, print bleedthrough, substandard margins, and improper alignment can adversely affect reproduction.

In the unlikely event that the author did not send UMI a complete manuscript and there are missing pages, these will be noted. Also, if unauthorized copyright material had to be removed, a note will indicate the deletion.

Oversize materials (e.g., maps, drawings, charts) are reproduced by sectioning the original, beginning at the upper left-hand corner and continuing from left to right in equal sections with small overlaps.

Photographs included in the original manuscript have been reproduced xerographically in this copy. Higher quality 6" x 9" black and white photographic prints are available for any photographs or illustrations appearing in this copy for an additional charge. Contact UMI directly to order.

Bell & Howell Information and Learning
300 North Zeeb Road, Ann Arbor, MI 48106-1346 USA
800-521-0600

UMI®

FUNCTIONAL PROPERTIES OF POST-SYNAPTIC DORSAL COLUMN NEURONS IN RACCOON

by

Susan H. Dick

Submitted in partial fulfillment of the requirements
for the degree of Doctor of Philosophy

at

Dalhousie University
Halifax, Nova Scotia
July 1999

DALHOUSIE UNIVERSITY

FACULTY OF GRADUATE STUDIES

The undersigned hereby certify that they have read and recommend to the Faculty of Graduate Studies for acceptance a thesis entitled "Functional Properties of Post-Synaptic Dorsal Column Neurons in Raccoon"

by Susan Dick

in partial fulfillment of the requirements for the degree of Doctor of Philosophy.

Dated: August 30, 1999

External Examiner

Research Supervisor

Examining Committee

DALHOUSIE UNIVERSITY

DATE: Sept 3/99

AUTHOR: Susan Dick

TITLE: Functional Properties of Post-Synaptic Dorsal Column Neurons in Raccoon

DEPARTMENT OR SCHOOL: Physiology & Biophysics

DEGREE: Ph.D. **CONVOCATION:** Oct. **YEAR:** 1999

Permission is herewith granted to Dalhousie University to circulate and to have copied for non-commercial purposes, at its discretion, the above title upon the request of individuals or institutions.

[redacted]

Signature of Author

TABLE OF CONTENTS:

LIST OF FIGURES:

LIST OF TABLES:

ABSTRACT:

The dorsal column medial lemnsicus (DC-ML) system is a critical pathway for discriminative aspects of light touch. The dorsal column nuclei (DCN) receive sensory input via direct and indirect pathways. The indirect pathway is characterized by a relay in the spinal cord dorsal horn and is referred to as the post-synaptic dorsal column (PSDC) system. To date, descriptions of PSDC neuronal properties have been limited to the rat and cat. The raccoon is an excellent alternative model in which to study the PSDC system because of the highly differentiated somatosensory system and the presence of large glabrous skin areas on the forepaw digits and palm.

In this study, single-unit extracellular recordings were made from 102 antidromically identified PSDC neurons and 51 cuneate neurons in response to receptive field (RF) stimulation and during spontaneous discharge. The PSDC neurons studied had RFs on glabrous skin of forepaw digits and/or palm. The RFs were discrete and well defined (9.4 mm^2) but were significantly larger than those observed for cuneate neurons in the same animals (6.7 mm^2). There was no difference in the latency of response of PSDC neurons (8.2 ms) vs. cuneate neurons (8.7 ms) in response to electrical stimulation of the RF (i.e. on-focus digit). Similarly, there was no difference between PSDC (9.9 ms) and cuneate (9.9 ms) neurons with respect the latency of response to off-focus stimulation.

Little is known about the contribution of the PSDC pathway to the DC-ML system in the processing of mechanosensory information. Using cross-correlation and frequency response analyses, a functional interaction between PSDC and cuneate neurons was identified that occurred only during spontaneous discharge. In 26 of the 51 neuron pairs examined, PSDC neuron activity appeared to be correlated with that of neurons in the cuneate nucleus. When the interaction between PSDC and cuneate neuron pairs was significant, most had overlapping RFs (19/26) and few did not (only 7/26). The mean coherence between PSDC input and cuneate output signals of the spinocuneate connection was 0.3, indicating partial linearity in the PSDC to cuneate interaction. One interpretation of these results is that the PSDC system exerts a somatotopically organized tonic facilitation of cuneate neuron activity, perhaps to control cuneate mechanosensory neuron RF size and excitability.

It is known that reorganization of the cuneate nucleus occurs following permanent deafferentation in raccoon. The mechanisms responsible for these changes are unknown but could involve the unmasking of ineffective input to PSDC neurons from an adjacent digit. In this way, deafferented cuneate neurons could become responsive to input from an adjacent digit via a PSDC to cuneate connection. To test this hypothesis, lidocaine was injected into the digit containing the PSDC neuron RF and the response of these cells to stimulation of the adjacent digit was monitored before and during temporary deafferentation. The results indicated that PSDC neurons become even less responsive to stimulation of the adjacent digit during deafferentation, indicating that immediate unmasking of connections does not occur.

LIST OF ABBREVIATIONS:

C	cervical spine
C_{single}	single event connection strength
C_{peak}	peak connection strength
CCG	cross-correlogram
CL	central lateral thalamus
DC-ML	dorsal column-medial lemniscal
DCN	dorsal column nuclei
DLF	dorsolateral funiculus
DRG	dorsal root ganglia
FAI	fast adapting type I
FAII	fast adapting type II
FFT	fast Fourier transform
GABA	gamma-amino-n-butyric acid
HRP	horseradish peroxidase
Hz	Hertz
ISI	inter-spike interval
LCN	lateral cervical nucleus
LTM	low threshold mechanical
PO_m	medial posterior complex
P(r)	probability of response
PSDC	post-synaptic dorsal column
PSTH	peri-stimulus time histogram

RA	rapidly adapting
RF	receptive field
SAI	slowly adapting type I
SAII	slowly adapting type II
SCT	spinocervical tract
SMT	spinomesencephalic tract
SRT	spinoreticular tract
STT	spinothalamic tract
T	thoracic spine
VPL	ventral posterolateral thalamus
WDR	wide dynamic range

ACKNOWLEDGEMENTS:

I would like to extend a special thank you to my supervisor, Dr. Douglas Rasmusson, for his tremendous support and guidance throughout my degree. I would also like to express my gratitude to Liisa Tremere for helping me in so many ways and for being a true friend. Thanks to Julie Jordan and Wendy Ruigrok for all their assistance and for bringing laughter to the lab!

I would also like to thank Dr. Andrew French for the many hours he spent patiently explaining mathematical concepts to me and for the use of his specialized software package (ASF Software, Halifax, Canada). Thank you to Dr. John Downie for teaching me many of the surgical procedures that were critical to my project. I would also like to acknowledge and thank Drs. Croll, Hagg and Fine for their supervision and words of wisdom. Many thanks to Dr. Kazue Semba and all the members of her lab, especially Bill Fortin and Leticia Materi, for helping to broaden my scientific focus and for extending the hand of friendship.

I would like to thank my parents, Ruth and Alf Dick and my sisters Colleen, Martha and Alison for their love and support and for always being there when I need it most. I would also like to thank the O'Connor family for all their encouragement and for making Nova Scotia feel like home. I would especially like to thank Mary Clare O'Connor for being such an unwavering source of inspiration and support from start to finish.

Chapter 1: INTRODUCTION

1.1 Historical perspective

It has been accepted since the time of Aristotle that there are five basic senses - hearing, vision, taste, touch and smell - that allow us to perceive the world in which we live (Herrnstein and Boring, 1973). It was based on the Aristotelian concept of sensory perception that Johannes Müller developed his 'doctrine of specific nerve energies' (Boring, 1942). Müller devoted the entire fifth book (256 pages) of his famous *Handbuch der Physiologie des Menschen* (1833-1840) to the discussion of nerve substances and their specific energies (Boring, 1942). In the *Handbuch*, Müller proposed that there are five different types of nerve, one for each of the five Aristotelian senses. Individual nerve types were proposed to have an "intrinsically different nervous mechanism" that would produce a characteristic sensation or 'specific energy' upon stimulation (Sinclair, 1981).

Expanding on the Müllerian theory of specific nerve energy, Natanson (1844) and Volkmann (1844) proposed that separate nerve fibers were responsible for different sensory qualities within the five senses. For example, Natanson posited that separate nerve fibers were responsible for temperature and touch; sweet, sour and bitter; and for the colors red, yellow and blue. Natanson proposed that the five senses could be broken up into simple sensations, each of which was subserved by a separate nerve fiber. Natanson's proposal represented the anatomical underpinnings of the concept of 'sensory modality', a term that had not yet been coined (Boring, 1942). It was not until 1863 that Helmholtz defined the term 'sensory modality' as "a class of sensations connected by a qualitative continuum" (Boring, 1942; Sinclair, 1981). In

other words, sensations of two different modalities are perceived as being qualitatively different (e.g. hearing vs. vision), whereas sensations within the same modality are only quantitatively different (e.g. different intensities of two sounds) (Willis and Coggeshall, 1991).

Helmholtz's concept of sensory modality was readily extended to include cutaneous sensibility and resulted in the formation of four major categories: touch, warm, cold and pain (Sinclair, 1981). The idea of an anatomical substrate for each different sensory modality was independently furthered by Blix (1883) and Goldscheider (1884) (Boring, 1942). Blix discovered the existence on normal skin of sensory 'spots', each of which preferentially responded to touch, cold, warm or pain (Sinclair, 1981).

Even before the discoveries of Blix and Goldschedier, histologists had begun to examine the sensory innervation of skin and underlying tissue. The major types of nerve endings that were discovered during the period between 1834 and 1892 were the Pacinian corpuscle (1834), Meissner's corpuscle (1853), Krause end-bulb (1859), Merkel's disc (1875) and Ruffini ending (1891). In addition, ubiquitous free nerve endings were found to permeate skin and surrounding hairs (Sinclair, 1981). The knowledge of different receptor types and the sensory spots of Blix and Goldscheider undoubtedly provided the impetus for von Frey's speculation about the anatomical basis of cutaneous sensory perception (Boring, 1942).

Von Frey (1894, 1895, 1896) put forth the idea that underlying each sensory spot was a specialized end organ (or group of end organs) that responded to a particular type of stimulus. Von Frey hypothesized that there was a different end

organ for each cutaneous modality (i.e. touch, warm, cold, pain) and that it was connected to a fiber that carried information from the periphery to a specific brain region. Von Frey proposed that pain was subserved by free nerve endings, warm by Ruffini ending, cold by Krause end-bulbs and touch by Meissner corpuscles in glabrous skin (Sinclair, 1981).

Von Frey's theory was met with heavy criticism because the anatomical details of his work were allegedly poor (Hagen et al. 1953). Further, his theory did not account for the wide range of sensations that can be derived from the skin (e.g. roughness, greasiness, stickiness etc.). The theory of 'sensory blends' was forwarded by Alrutz (1900) in an attempt to allay objections and salvage von Frey's theory, but this idea also met with criticism. As stated by Stevens and Green (1978), the "idea of differentiating separate skin senses in terms of four and only four separate receptors and separate nerve supplies turns out to appear embarrassingly naïve".

Sherrington took an intermediary approach, circumventing the anatomical rigidity of Von Frey's theory when he wrote:

> The sensorial end-organ is an apparatus by which an afferent nerve fiber is rendered distinctively amenable to some particular physical agent, and at the same time rendered less amenable to, i.e. is shielded from, other excitants. It lowers the value of the limen of one particular kind of stimulus, it heightens the value of the limen of stimuli of other kinds (Sinclair, 1981).

As pointed out by Sinclair (1981), the words of Sherrington aptly embodied the notion of an 'adequate stimulus', a term originally proposed by Lotze in 1948 (Woodward, 1975). It should be noted that the substance of Sherrington's statement

(1900) stood for 50 years without the benefit of experimental evidence. It was not until the advent of modern electrophysiological techniques that the stimulus-specificity of different receptor types could be resolved, providing proof for Sherrington's earlier supposition (Sinclair, 1981).

Following Von Frey's theory, Head (1908) conceived the idea of 'dual sensibilities' that was initially embraced as "holding fresh promise for understanding somesthetic function" (Stevens and Green, 1978). Head's theory was based on the results of a self-experiment in which he transected a cutaneous nerve in his forearm. The return of sensation was carefully documented in the days and weeks that followed the nerve transection and it reportedly occurred in two distinct phases (Stevens and Green, 1978; Sinclair, 1981). Head claimed that the first sensibility to return was primitive, enabling him to feel only heavy pressure and the extremes of temperature and pain. During this time, Head reported his inability to discriminate stimulus qualities such as intensity, quality or spatial location (Stevens and Green, 1978). The early primitive sensation was called 'protopathic sensibility' and the later returning refined perception was called 'epicritic sensibility'. Epicritic sensibility was said to include light touch, fine discrimination of temperature, and localization of tactile stimulation (Sinclair, 1981). The notion of dual sensibility never received general acceptance; however the terms 'protopathic' and 'epicritic' found their way into clinical usage and remain as modern day remnants of Head's fallen theory.

In more recent times, the pattern theory of sensation has been considered as an alternative or adjunct to the specificity theory. Development of the pattern theory was based on the observation that stimulation of sensory receptors set up trains of impulses

in the nerve fibers that supply them (Adrian, 1946; Willis and Coggeshall, 1991). It was suggested by Nafe (1927, 1929) that a sensation results from a patterned input from sense organs in the skin that is "usually but not necessarily always, associated with a particular kind of stimulus". In Nafe's opinion, there "need be no specific fibers within a given sense, but only a shifting flux of impulses arriving in the brain dispersed in both time and space" (Sinclair, 1955).

The pattern theory, in its purest form, lost credibility when it was found that large nerve fibers are preferentially involved in light touch and small myelinated and unmyelinated fibers in pain and temperature sensations (Heinbecker et al., 1933, 1934; Lewis and Pochin, 1938a,b; Torebjörk and Hallin, 1973). The pattern theory fell further out of favor when electrophysiological evidence (single-unit recordings) demonstrated that mechanoreceptors are primarily supplied by large myelinated fibers and nociceptors and thermoreceptors are supplied by small myelinated and unmyelinated fibers (Hensel and Zotterman, 1951; Dodt, 1952; Dodt and Zotterman, 1952; Iggo, 1959, 1960; Hensel et al., 1960; Hunt and MacIntyre, 1960; Iriuchijima and Zotterman, 1960; Willis and Coggeshall, 1991).

The specificity, dual control and pattern theories are not the only ones to have been conjured up in recent history; however, they are undoubtedly among the most influential with respect to our current thinking about cutaneous sensibility. This is especially true for the specificity theory which "proposed by Müller and clothed in detail by von Frey, still permeates our thinking about the sensory nervous system" (Sinclair, 1981).

1.2 Peripheral mechanoreceptors and primary afferent neurons

Adrian and Zotterman (1926) were the first to record the electrical response of a single sensory nerve fiber to various grades of stimulation (Burgess and Perl., 1973). The muscle spindle was used in this landmark study to demonstrate that the nerve fiber transmits information using the principle of impulse frequency modulation. The study was of additional importance because it highlighted the fact that peripheral receptors are essential first order transducers of sensory information. Before peripheral nerves can transmit sensory information to central brain structures, the information must be coded in a way that the brain can interpret. Adrian and Zotterman (1926) were the first to show that the peripheral receptor is critical in the coding process and that it is the first step in somatosensory perception.

Sensory receptors are sorted and classified in a variety of ways. One of the broadest categorizations divides sensory receptors with respect to the three essential functions of the somatosensory system, i.e. exteroceptive, proprioceptive and interoceptive (Hendry et al., 1999). Exteroceptive functions include the sensations of touch, temperature and pain and involve the skin and subcutaneous tissue. Proprioceptive functions include the kinesthetic senses of body/limb position and movement that require input from muscle, tendon and joint receptors (i.e. muscle spindles, Golgi tendon organs, pressure-pain endings, receptors in the fascial planes) (Barker, 1962; Clark et al., 1985). Interoceptive functions result from sensory receptors in the viscera that provide information about the state of the body's internal organs (Hendry et al., 1999). The functional categorization of sensory receptors is rooted in a psychological perspective that deals with the perceptual aspects of

sensation. However, some classifications take a more physiological approach and are based on the type of stimulus for which the receptor shows the greatest responsiveness, i.e. the adequate stimulus (Sherrington, 1906, Skoglund, 1973).

1.2.1 Peripheral nerves

All sensory receptors are innervated by primary sensory neurons (synonym: primary afferent neurons) that extend from the skin and other tissues to the central nervous system (Burgess and Perl, 1973). Primary sensory neurons travel as part of a peripheral nerve that is composed of the axons of sensory neurons as well as somatic and autonomic motor neurons. A network of connective tissue (endoneurium, perineurium and epineurium) ensheaths the axons which can be either myelinated or unmyelinated (Landon, 1976; Willis and Coggeshall, 1991).

Primary sensory neurons are divided into categories based on their diameter and degree of myelination. Most nerves supplying the skin fall into three major fiber classes: Aαβ, Aδ and C. The largest sensory axons belong to the Aαβ fiber class which are heavily myelinated and conduct impulses at 30-100 m/s (Boivie and Perl, 1975; Erlanger and Gasser, 1937). The smaller myelinated Aδ fibers conduct at 4-30 m/s and the unmyelinated small C-fibers conduct at less than 2.5 m/s (Boivie and Perl, 1975; Gasser, 1950). Nerves that supply visceral structures share the same terminology as those supplying the skin.

A different terminology is used to describe axons innervating muscle and joints. The myelinated fibers innervating muscle are divided into groups I, II, III and

IV whose axons conduct at velocities of 72-120, 24-71, 6-23 and less than 2.5 m/s respectively (Hunt, 1954; Lloyd and Chang, 1948; Rexed and Therman, 1948; Stacey, 1969).

1.2.2 Cutaneous receptors

There are two anatomical families of cutaneous receptors, the 'free' terminals and the 'organized' corpuscular receptors (Sinclair, 1981). The free nerve endings are functionally diverse and found universally throughout the body. In the skin, the free nerve endings permeate the dermis and are comprised of C-fiber terminals. The Aδ fibers are often included as members of the free nerve ending family but this is inappropriate because the terminals are largely ensheathed by Schwann cells (Kruger et al., 1981). The fact that both C and Aδ fibers are involved in thermal and nociception likely contributes to the common usage of the term 'free nerve ending'.

The word 'noxious' is derived from the Latin word *noxius* which means hurtful, harmful or damaging (Burgess and Perl, 1973). Sherrington (1906) was the first to introduce the term 'nociceptor' to describe those primary afferent neurons that can be activated by harmful or potentially harmful stimuli and then give rise to the sensation of pain. Nociceptors include both unmyelinated C-fibers and lightly myelinated Aδ fibers. There are two major classifications of nociceptors: those that respond exclusively to noxious mechanical stimuli and those that respond to both mechanical and thermal noxious input (Burgess and Perl, 1973). Progress with respect to our understanding of the neurobiology of pain continues to proceed at a great rate.

The identification of membrane receptors for capsaicin, protons and heat represents an achievement that will undoubtedly provide insights into the "molecular machinery of nociceptor activation and sensitization" (Kress and Zeilhofer, 1999).

Mechanoreceptors, the other major family of cutaneous receptor, are those which respond most readily to mechanical forces applied to the skin (Willis and Coggeshall, 1991). There are different sub-types of mechanoreceptor that can be classified in several different ways. One classification system divides mechanoreceptors into three groups than encode information about different stimulus properties, i.e. position detection, velocity detection and detection of rapid transients (Burgess and Perl, 1973). Another system of classification uses the adaptation rate of mechanoreceptors to a maintained stimulus as the defining characteristic (e.g. rapidly adapting vs. slowly adapting) (Adrian and Zotterman, 1926a,b; Adrian, 1928).

Slowly adapting mechanoreceptors discharge repetitively in the presence of a maintained stimulus and are thought to encode information about stimulus position, intensity and duration; the discharge rate is accordingly a function of skin displacement or position. In contrast, rapidly adapting receptors discharge upon initial application of the stimulus, and sometimes when it is removed. As a result of these response properties, rapidly adapting mechanoreceptors are thought to encode higher derivatives of skin position (i.e. velocity and acceleration of skin displacement) as well as rapid transients (Adrian and Zotterman, 1926a,b; Adrian, 1928).

There are two major types of slowly adapting receptors in the skin, SAI and SAII (slowly adapting type I and II respectively). SAI receptors are associated with Merkel cells, which are specialized cells in the epidermis adjacent to the basement

membrane. The Merkel cell receptor is sometimes called the tactile dome, touch corpuscle or Haarscheibe because of its dome-like morphology in the skin of some animals (Smith, 1968). SAI mechanoreceptors are normally silent in the absence of a stimulus but are very sensitive to low threshold skin indentation directly over the ending (Willis and Coggeshall, 1991).

SAII cells have been identified in association with Ruffini endings in the dermis. These endings respond to small displacements of skin either directly over the receptor or as a result of skin stretch in an adjacent region. The response properties of SAII receptors differ from their SAI counterparts in a variety of ways, including the fact that they often exhibit a resting discharge in the absence of an overt stimulus (Burgess and Perl, 1973).

The velocity detector in glabrous skin is the rapidly adapting FAI receptor. This receptor is associated with Meissner's corpuscles in primates (including humans) and with Krause's end bulbs in cat. The hairy skin has four types of velocity detectors: G_2 hair follicle receptors, D hair follicle receptors, field receptors, and C mechanoreceptors.

In addition to velocity detectors, both glabrous and hairy skin have receptors that are specialized for the detection of transient stimuli. In hairy skin this function is carried out by the G_1 hair follicle receptor and in glabrous skin by the Pacinian corpuscle. In the skin, Pacinian corpuscles are located subcutaneously and respond best to frequencies of vibration in the range of 60-300 Hz but are capable of following frequencies of 500 Hz and greater (Hunt, 1961; Burgess et al., 1968; Talbot et al., 1968; Iggo and Ogawa, 1977; Willis and Coggeshall, 1991).

1.2.3 Muscle receptors

Muscles have receptors that are responsive to stretch and those that respond preferentially to pressure and pain. The pressure-pain endings are found in the fascia and in the adventitia of muscles and blood vessels and may comprise up to 75% of the sensory innervation of skeletal muscle (Stacey, 1969). These receptors can be excited by both innocuous and noxious mechanical stimulation of muscle as well as by muscle stretch and contraction (Mense and Stahnke, 1983; Mense and Meyer, 1985). The fibers innervating pressure-pain endings tend to be smaller (group III and IV), but some are innervated by larger (group II) afferents.

A muscle spindle has two types of sensory endings, a single primary and one or more secondary endings. The primary muscle spindle ending gives rise to a large, myelinated Ia fiber that carries information about changes in muscle length (dynamic response). The secondary muscle spindle endings signal stationary muscle length and position (static response) and give rise to type II fibers. The sensitivity of the dynamic and static responses are maintained by input from dynamic and static γ motor axons respectively (Appelberg et al., 1966; Skoglund, 1973; Rothwell, 1992).

Golgi tendon organs are found intertwined with the connective tissue of muscle tendons and aponeuroses (Schoultz and Swett, 1972). These receptors are innervated by large, myelinated Ib fibers and they respond to both passive muscle stretch (high threshold response) and contraction of muscle fibers ending on the

tendon containing the receptor (low threshold response) (Houk and Henneman, 1967; Willis and Coggeshall, 1991).

1.2.4 Joint receptors

Joint receptors are comprised of both mechanoreceptors and nociceptors. The mechanoreceptors are slowly adapting Ruffini (SAII) endings, thought to signal joint position, and Pacinian corpuscles (FAII) that are presumed to signal transient mechanical input to the joint (Skoglund, 1956, 1973). Nociceptors within the joints respond to movement beyond the limits of normal range and to intra-articular inflammation (Coggeshall et al., 1983; Schaible and Schmidt, 1983a,b; Grigg et al., 1986).

1.2.5 Visceral receptors

Visceral receptors traveling to the spinal cord include mechanoreceptors and nociceptors. The afferents of these receptor types reach the spinal cord by way of the splanchnic nerves and sympathetic chain or via the pelvic parasympathetic nerves (Willis and Coggeshall, 1991). Pacinian corpuscles (mechanosensory receptors) have been identified in the connective tissue and mesentery surrounding visceral organs and are thought to signal movement and/or distension of visceral structures (Sheehan, 1932; Morrison, 1977). The visceral nociceptors include fibers in the Aδ and C range that respond to mechanical, thermal and chemical stimuli (Clifton et al., 1976; Kumazawa et al., 1987).

1.3 Structure of the spinal cord dorsal horn

1.3.1 Lamina I

In his original treatise on spinal cord cytoarchitecture, Rexed (1952) divided the feline dorsal horn into six different laminae (Rexed's laminae I-VI). Lamina I was described as "a thin veil of gray substance forming the dorsal-most part of the spinal gray matter" (Rexed, 1952, Willis and Coggeshall, 1991). Lamina I, also known as the marginal zone, is not usually more than one cell thick. The triangular or spindle-shape cells are loosely distributed and range in size from small to large (Rexed, 1952, 1954). In cats, Burgess and Perl (1967) identified a set of cells in lamina I that were responsive to stimulation of high threshold mechanoreceptors supplied by Aδ afferents. A second set of cells was found that responded to noxious pressure and temperature input from Aδ and C-fibers and a third set that was additionally responsive to innocuous temperature input from small unmyelinated C-fibers (Burgess and Perl, 1967). In addition to cutaneous input, lamina I is also thought to receive muscle and visceral afferent fibers (Willis and Coggeshall, 1991).

In rat, approximately 50% of the synapses in lamina I are lost following dorsal rhizotomy and are presumably from primary afferent fibers (McNeill et al., 1988b; Chung et al., 1989). It is assumed that the remaining synapses are formed by propriospinal and/or descending input (Willis and Coggeshall, 1991).

Since the original descriptions by Rexed, the largest of lamina I cells, the marginal neurons, have been sub-divided into two types: P (projection) and type A

(association) (Narotzky and Kerr, 1978). The type P neurons are thought to project to other parts of the spinal cord as well as to the mid-brain, brain stem reticular formation, thalamus and cerebellum. Included in the type P category are spinothalamic (STT) spinoreticular (SRT) and spinomesencephalic (SMT) tract neurons (Snyder et al., 1978; Lima and Coimbra, 1988; Willis, 1999).

1.3.2 Lamina II

Rexed's lamina II is commonly referred to as the 'substantia gelatinosa', a term coined by Rolando to describe its distinctly gelatinous appearance (Cervero and Iggo, 1980). The striking feature of this lamina is the predominance of small, densely packed cells and lack of myelinated axons (Rexed, 1952, 1954; Willis and Coggeshall, 1991).

It was Szentagothai (1964) who first proposed that the substantia gelatinosa was a closed system, claiming that all axons originating here also ended within its boundaries. He believed that there were two types of cells in lamina II: cells with intrinsic axons and cells with extrinsic axons that projected into the white matter but ultimately returned to terminate within the substantia gelatinosa. In this way, Szentagothai believed that there was no 'forward transmission' of information from lamina II but that output was achieved through contact with dorsally projecting dendrites of cells in laminae IV and V (Szentagothai, 1964). It has since been shown that the substantia gelatinosa is not a closed system as was claimed by Szentagothai (Willis et al., 1978; Giesler et al., 1978). However, his ideas were important because

they had a great influence on the development of modern ideas about the organization of Rexed's lamina II (Willis and Coggeshall, 1991).

The current terminology with respect to cell types in lamina II was developed in detail by Gobel in cat (Gobel 1975, 1978a, 1978b, 1979; Gobel et al., 1980). Stalked cells were defined by Gobel as interlaminar interneurons whose axons ramified primarily in lamina I, although terminations have since been identified in deeper layers of the dorsal horn (Schoenen, 1982; Light and Kavookjian, 1988). Although not verified, it was Gobel's contention that stalked cells formed excitatory connections with "long transmission neurons involved in nociception" (Willis and Coggeshall, 1991).

Aside from stalked cells, the other major cell type identified by Gobel was the islet cell, thought to be an inhibitory interneuron receiving both nociceptive and mechanoreceptive input from the periphery (Gobel, 1978b; Bennett et al., 1980). Other interneurons identified by Gobel include the arboreal cells, the II-III border cells and the spiny cells (Willis and Coggeshall, 1991).

The primary afferent input to lamina II is largely via unmyelinated fibers from cutaneous and visceral regions of the body, although sparse Aδ projections are also known to terminate here (Scheibel and Scheibel, 1968; Rethelyi, 1977; Rethelyi and Capowski, 1977; Light and Perl, 1979). With respect to output, it is now known that Szentagothai (1964) was incorrect in his assumption that the substantia gelatinosa does not possess a forward projection i.e. does not send axons to terminate outside its own boundaries. According to Willis and Coggeshall (1991), most of the axons of

lamina II cells project to other laminae or to other segments of the spinal cord (i.e. propriospinal). Few lamina II cells are thought to be true intralaminar interneurons as originally thought by Szentagothai (1964) and few seem to project out of the spinal cord, although terminations in the brainstem and thalamus have been noted (Willis et al., 1978; Giesler et al., 1978; Willis and Coggeshall, 1991).

1.3.3 Lamina III

The cells in layer III are "a little larger than those of layer II but they are still uniformly small" (Rexed, 1954). The most distinctive of the cell types in this region are the spinocervical tract (SCT) and post-synaptic dorsal column (PSDC) cells (Brown et al., 1977b; Brown and Fyffe, 1981; Brown, 1981). There are other cell types in lamina III, including some cells of origin of the spinothalamic tract (STT), but they remain less well understood in comparison to the distinct SCT and PSDC populations (Carstens and Trevino, 1978: Craig et al., 1989; Pubols and Haring, 1995).

Neurons in lamina III receive afferent input from receptors including hair follicles, Meissner's corpuscles (FAI), Pacinian corpuscles (FAII), Merkel's cells (SAI) and Ruffini endings (SAII) (Willis and Coggeshall, 1991). The major output from Rexed's lamina III is to the DCN (PSDC cells), lateral cervical nucleus (SCT cells) and deeper layers of the dorsal horn (Matsushita 1969, 1970; Brown et al., 1977b; Brown and Fyffe, 1981; Brown, 1981; Bennett et al., 1984).

1.3.4 Lamina IV

Lamina IV constitutes a thick band across the dorsal horn and is characterized by "its mixture of cells of all sizes up to fairly large ones" (Rexed, 1954). Although the large cells are relatively infrequent, their morphology is so striking that they are considered to be the hallmark of this layer (Willis and Coggeshall, 1991). Similar to lamina III, lamina IV contains neurons that belong to the PSDC system and others that are SCT cells. STT cells are also situated in lamina IV, although they are more predominant in layers I and V (Willis and Coggeshall, 1991).

Afferent input to lamina IV neurons is difficult to discern because, as stated by Rethelyi and Szentagothai (1973), "the cytoarchitectonic borders do not match with those of dendroarchitectonics and neuropil architectonics." It should be noted that Szentogothai (1964) had previously described antenna-type neurons in laminae IV and V with dendrites projecting dorsally into the substantia gelatinosa. The primary afferent input to lamina IV is thought to be from large myelinated afferents similar to those that terminate in lamina III (Ralston and Ralston, 1982).

With respect to output, Scheibel and Scheibel (1968) noted that the axons of lamina IV neurons often bifurcate and send collaterals to deeper layers of the dorsal horn before entering the white matter. The final destination of lamina IV neurons includes the DCN (PSDC), lateral cervical nucleus (SCT) and thalamus (STT).

1.3.5 Lamina V

As described by Rexed (1954), lamina V "goes straight across the dorsal cell column" and is composed of a medial and a lateral zone. The border of the lateral zone "is reticulated, and has a number of large, dark-staining cells in addition to many medium-sized, lighter cells." The cell population in lamina V is more heterogenous with respect to soma size as compared to lamina IV (Rexed, 1954). Another distinguishing feature between lamina IV and V neurons involves the shape of the dendritic tree. In lamina V, the dendrites "radiate along the dorsoventral and mediolateral planes with little or no extensions along the longitudinal axis of the cord" and are often described as flattened disks (Scheibel and Scheibel, 1968). In contrast, the dendrites of lamina IV cells often radiate in all directions from the soma (i.e. medially, laterally, ventrally and dorsally), often in a cone-shaped configuration with the apex directed ventrally (Scheibel and Scheibel, 1968). The STT, SCT, PSDC, SRT and SMT systems are known to have cells of origin within the boundaries of lamina V (Willis and Coggeshall, 1991; Willis, 1999).

The terminals of primary afferent axons in laminae V and VI are not as somatotopically organized as those of laminae III and IV, although they are thought to arise from a similar source (i.e. large myelinated axons) (Sterling and Kuypers, 1967; Willis and Coggeshall, 1991). In addition, the axons of lamina V cells are oriented dorsoventrally as opposed to the longitudinal direction that typifies laminae III and IV neurons (Scheibel and Scheibel, 1968; Rethelyi and Szentagothai, 1973). The output

of lamina V neurons is presumed to be similar to that of layers III and IV, (i.e. the DCN, lateral cervical nucleus and thalamus) (Willis and Coggeshall, 1991).

1.3.6 Lamina VI

Lamina VI exists only in the lumbosacral and cervical enlargements and is characterized by small to medium sized cells in the medial zone and larger, star shaped cells in the lateral zone (Rexed, 1954). The cells situated medially lie "in a relatively compact group" while the lateral zone is, on the whole, "more loose in its structure" (Rexed, 1954).

According to Willis and Coggeshall (1991), the primary afferent input to lamina VI is very complex. The complexity arises from the fact that many collaterals from primary afferent fibers terminate here, particularly those from Ia fibers (Scheibel and Scheibel, 1968; Maxwell and Bannatyne, 1983).

Most of the cells in lamina VI are probably propriospinal, although some have been shown to project to the lateral cervical nucleus or thalamus (Willis and Coggeshall, 1991). According to Matsushita (1969), the small cells of lamina VI have "abundantly ramifying" axon collaterals that end primarily in laminae IV, V, VI and VII.

1.4 Spinothalamic and spinocervicothalamic tracts

The STT and SCT represent two major ascending somatosensory pathways whose cells of origin lie in the dorsal horn of the spinal cord. Electrophysiological recording studies have shown that both light tactile and nociceptive information may

be transmitted by the STT and SCT systems (Handwerker et al., 1975; Sorkin et al., 1986). Although the DC-ML pathway is thought to be the primary conveyor of modality and place specific light tactile information, the STT and SCT systems also provide somatosensory information to the thalamus (Pubols and Haring, 1995; Willis, 1999).

1.4.1 Spinocervicothalamic tract

The spinocervicothalamic pathway, first described by Morin (1955), originates in the spinal cord and projects to the thalamus by way of a relay in the lateral cervical nucleus (LCN) (Willis and Coggeshall, 1991). The SCT constitutes the first segment of the spinocervicothalamic pathway, having cells of origin in Rexed's laminae III and IV in cat and monkey (Bryan et al., 1973, 1974; Craig, 1978; Brown et al., 1980a). Before leaving the gray matter, most SCT neurons give off one or more axon collaterals within 500μm of the cell body, presumably to influence the activity of nearby dorsal horn neurons. PSDC neurons are thought to be affected by SCT collaterals because axoaxonal, axodendritic and axosomatic connections from SCT to PSDC neurons have been identified anatomically (Rastad, 1981b). In addition, Jankowska et al. (1979) have found physiological evidence for a disynaptic excitation of PSDC neurons via a circuit containing SCT cells.

To date, most electrophysiological studies of SCT neurons have involved the hindlimb of the cat. In cat, most SCT neurons have excitatory light touch RFs that are exclusively on hairy skin, although some include a glabrous skin component (Brown

and Franz, 1969). The responsiveness of SCT neurons to heat, cold and high threshold mechanical stimuli has also been identified in cat and demonstrated to be under tonic descending inhibition via the dorsolateral, ventral and dorsal funiculi (Brown, 1973; Brown et al., 1973b,c). Similarly, SCT responses to high-threshold muscle and joint afferents in cat are heavily influenced by descending inhibition which arises, at least in part, from cytoarchitetonic areas 4, 3a, 3b, 1 and 5 of the cerebral cortex (Lundberg and Oscarsson, 1961; Hongo et al., 1968; Brown et al., 1977a).

Mendell (1966) recorded from the axons of SCT neurons in cat and found that they could be monosynaptically activated by electrical stimulation of Aβ, Aδ, and C-fiber afferents. Convergence of A and C-fiber inputs onto SCT cells has been confirmed in cats, with 29% of SCT cells excited by just A fiber stimulation and 71% excited by both A and C-fibers (Fetz, 1968; Brown et al., 1973a,b, 1975; Cervero et al., 1977). With regard to C-fiber input, Mendell (1966) observed an increased responsiveness of SCT axons in cat to repeated C-fiber volleys, a phenomenon known as 'windup' (Willis and Coggeshall, 1991).

In monkey, most SCT cells (78%) were found by Downie et al. (1988) to include regions of glabrous skin. The SCT neurons studied responded to a series of mechanical stimuli such as brushing, pressure, pinch and squeeze, low frequency vibration and/or to noxious heat. The cells were classified as high-threshold, low-threshold or wide dynamic range, although most SCT cells were found to be in the low-threshold or wide dynamic range classes (Downie et al., 1988).

In raccoon, SCT neuron RFs have been found in large number on glabrous surfaces of forelimb digits and palm (Hirata and Pubols, 1989). These findings are similar to the results in monkey, but are in sharp contrast to those in cat where the majority of mechanosensitive SCT RFs are found on hairy skin. The majority (39/45) of raccoon SCT neurons with glabrous skin RFs showed RA responses to low threshold mechanical stimuli, although some (6/45) showed characteristic SA responses. Of 11 cells tested, 2 showed enhanced responses to nociceptive pinch and thermal (heat) stimuli and were considered to be multireceptive (Hirata and Pubols, 1989). The RF sizes of raccoon SCT neurons were found to be larger on the glabrous palm as compared to the digits and were comparable in size to those previously reported in raccoon cuneate nuclear cells (Rowinski et al., 1981, 1985; Hirata and Pubols, 1989). The RF size and response properties of raccoon SCT cells led Hirata and Pubols (1989) to conclude that the SCT system was "at least as precise" as the DC-ML system with respect to submodality, spatial and dynamic characteristics of responses to light mechanical stimulation of the forelimb glabrous skin in raccoon.

The SCT projects to the LCN via the ipsilateral DLF, although some axons ascend for a short distance in the dorsal columns before entering the DLF (Enevoldson and Gordon, 1989b). The SCT projection is somatotopically organized, terminating on LCN cells whose axons form the thalamic projection segment of the spinocervicothalamic pathway (Svensson et al., 1985). The LCN projection crosses the midline at the level of C1/C2 to join the medial lemniscus and terminate in various regions of the contralateral thalamus, including the ventral posterior lateral (VPL) and

medial posterior complex (PO_m) in rats, cats and monkeys (Berkley, 1980; Boivie, 1970, 1980; Giesler et al., 1988).

Morin et al. (1963) measured the activity of single LCN neurons in cat and showed that they respond to tactile stimulation of the skin and to joint movement. The majority of RFs were located on the limb and were large in size, although some moderate to small RFs were noted (Morin et al., 1963). In agreement with the findings of Morin, Horrobin (1966) found that most (90%) of the feline LCN neurons he tested responded to tactile stimuli (touch, pressure). However, the author also found that noxious stimuli applied to large areas of the ipsilateral body surface were effective for some cells in this nucleus. In one study involving decerebrate, spinalized cats, 41% of the LCN cells tested were characterized as low-threshold, 49% as wide-dynamic-range and 9% as high-threshold neurons (Kajander and Giesler, 1987). The low-threshold neurons were responsive to touch and pressure, whereas the wide dynamic range and high-threshold LCN neurons typically responded in a graded fashion to increasing levels of heat, including noxious heat (Kajander and Giesler, 1987).

In monkey, Downie et al. (1988) found that many neurons in the LCN had RFs on hairy skin, although some included a glabrous skin component. The response properties of monkey LCN neurons were similar to those of SCT neurons, indicating that input from SCT cells converges onto LCN cells (Downie et al., 1988).

In raccoon, Simone and Pubols (1991) compared the response properties of SCT neurons to cells in the LCN. Based on the results of this comparison, the authors concluded that Hirata and Pubols (1989) had overestimated the content and precision of mechanosensory information reaching the thalamus via the spinocervicothalamic

system as a whole (Simone and Pubols, 1991). They found that raccoon LCN neurons had digital RFs that were 8.5X larger than SCT neurons, indicating a lack of 'place specificity' (Simone and Pubols, 1991). In addition, the somatotopy of the raccoon LCN was found to be far less precise in comparison to the cervical dorsal horn, a region that includes the cells of origin of the SCT (Hirata and Pubols 1989; Simone and Pubols, 1991). Simone and Pubols (1991) concluded that the place specificity attributed to the peripheral and central afferent projections of forepaw mechanoreceptors was not a characteristic of the SCT system in the raccoon. They further speculated that "although the SCT system probably makes significant contributions to properties of ventrobasal thalamic (VB) neurons, these properties primarily reflect those of neurons in the DC-ML system" (Simone and Pubols, 1991).

1.4.2 Spinothalamic tract

Brown-Sequard (1860) and Gowers (1878) are credited with the first clinical evidence that fiber tracts in the anterolateral quadrant of the spinal cord mediate pain and temperature sensation. However, the first anatomical evidence of a direct spinothalamic projection came from work by Edinger (1889, 1890) in cats (as cited by Keele, 1957). The spinothalamic tract is a major conveyor of nociceptive information to the thalamus in many species including rat, cat, raccoon and a variety of primates, including humans (Mehler, 1962, 1966, 1969, 1974; Craig and Burton, 1985). In addition to nociceptive information, neurons of the STT tract are also known to convey non-noxious input from the periphery (Willis and Coggeshall, 1991).

The cells of origin of the spinothalamic tract (STT) lie predominantly in Rexed's laminae I and V, although some cells are found in laminae II, III and VI-X (Carstens and Trevino, 1978; Craig et al., 1989; Willis and Coggeshall, 1991; Pubols and Haring, 1995). Most of the axons of STT cells cross to the contralateral side of the spinal cord and travel to the thalamus in the anterolateral white matter. In the cat and monkey, some projections from STT cells (approximately 25% in the lumbar enlargement) ascend to the thalamus in the dorsolateral funiculus (M.W. Jones et al., 1985, 1987; Apkarian and Hodge, 1989a,c). According to Stevens et al. (1989), most of the STT cells projecting in the dorsolateral STT in cat are in laminae I-III, whereas most projecting via the anterolateral spinal cord reside in deeper laminae. Despite the different route of travel, it has been found that the dorsolateral and ventral components of the STT terminate in the same thalamic nuclei (Apkarian and Hodge, 1989b).

Thalamic target sites of STT neurons in rat, cat, raccoon and monkey include the ventral posterolateral (VPL), central lateral (CL) and posterior complex (Lund and Webster, 1967b; Mehler, 1960, 1969; Zemlan et al., 1978; Boivie, 1971a, 1979; Peschanski et al., 1983; Craig and Burton, 1981, 1985). STT projections to the medial thalamus are thought to be involved in the mediation of motivational-affective components of pain because of this region's projections to the frontal lobe and limbic areas of the cerebral cortex. In contrast, STT projections to the lateral tier are thought to be involved in sensory-discriminative aspects of pain because of the heavy projection of lateral tier neurons to the primary (SI) and secondary (SII) somatosensory cortices (Craig, 1989; Willis, 1999).

The RF sizes of STT cells vary depending on their laminar position in the dorsal horn. For example, STT neurons in lamina I of the spinal cord typically have smaller RFs than those found in deeper layers, the implication being that these cells provide useful information for stimulus localization (Applebaum et al., 1975; Ferrington et al., 1987; Willis et al., 1989). In contrast, STT neurons in laminae IV-VI of the monkey dorsal horn often have RFs that encompass the entire limb, indicating that they are probably not critically involved in stimulus localization (Giesler et al., 1981).

Many STT neurons respond best to noxious stimuli and are classified as high threshold. Others respond best to innocuous mechanical input such as hair movement or brushing of the glabrous skin; these are termed low threshold STT neurons. Another type, the wide dynamic range STT neurons, can be activated by innocuous mechanical stimuli, but are more responsive to noxious ones (Willis et al., 1974, 1975; Price et al., 1978; Chung et al., 1979, 1986; Blair et al., 1981; Surmeier et al., 1988). It has been estimated in monkey that 15% of STT neurons projecting to the VPL thalamus are tactile (low-threshold or wide dynamic range) and 85% are nociceptive (high-threshold). The tactile VPL-projecting STT neurons have cell bodies that are predominantly in laminae IV-VI, whereas the cell bodies of nociceptive STT neurons lie in lamina I (Christensen and Perl, 1970; Willis and Coggeshall, 1991).

In raccoon, there are approximately 4-6 times as many SCT cells as STT cells in the dorsal horn cervical enlargement. Approximately 67% of raccoon STT cells were found to be located in laminae I and V of the dorsal horn. Less than 25% of STT cells in raccoon are found in the medial 2/3 of the cervical enlargement, the region of

glabrous skin representation in this animal (Pubols and Haring, 1995). Based on the relative distribution of SCT and STT neurons in raccoon, Pubols and Haring (1995) have proposed that "the STT plays a more significant role for noxious information transmission from the forelimb as a whole, but the SCT is more important for relaying discriminative light tactile and nociceptive information from the glabrous surfaces of the forepaw".

1.5 Dorsal column-medial lemniscal system

Ramon y Cajal (1909) was the first to identify ascending branches of DRG cells in the spinal cord dorsal funiculus. Since that time, the dorsal column-medial lemniscal (DC-ML) pathway has been described in a variety of species, including amphibia, reptiles, birds and mammals (Ferraro and Barrera, 1935a,b; Kappers et al., 1936; Kruger and Witkovsky, 1961; Valverde, 1966; Joseph and Whitlock, 1968; Johnson et al., 1968; Imai and Kusama, 1969). Notably absent in fish, it is speculated that the DC-ML evolved upon the emergence of vertebrates onto land where sensory stimulation of the body's surface is likely to be more complex (Willis and Coggeshall, 1991). The DC-ML system is thought to play a critical role in the perception of tactile stimuli that require a spatiotemporal transformation (Azulay and Schwartz, 1975).

As initially described by Cajal, the dorsal columns contain branches of primary afferent fibers that enter the spinal cord via the dorsal roots (Ramon y Cajal, 1909; Sprague and Ha, 1964; Carpenter et al., 1968; Imai and Kusama, 1969; Rethelyi and Szentagothai, 1973). The long system of primary afferent fibers travels uninterrupted within the dorsal columns to terminate in the medulla (Glees and Soler, 1951; Horch

et al., 1976). In addition to long projection fibers, the dorsal columns contain descending branches of primary afferent fibers, the axons of propriospinal and post-synaptic dorsal column neurons as well as pathways that descend from the brain (Erulkar et al., 1966; Valverde, 1966; Sterling and Kuypers, 1967; Shriver et al., 1968; Kerr, 1968; Uddenberg, 1968; Rustioni, 1973, 1974; Hancock, 1982).

The dorsal columns are sub-divided into two components, the fasciculus gracilis and the fasciculus cuneatus (Latin for thin and wedge-shaped bundles, respectively). The fasciculus gracilis in monkeys contains ascending branches of primary afferent fibers from the lower part of the trunk and lower extremities (i.e. dorsal roots T8 and below). The fasciculus cuneatus carries afferents innervating the upper part of the trunk and upper extremities (i.e. dorsal roots T7 and above) (Walker and Weaver, 1942; Carpenter et al., 1968; Shriver et al., 1968). Fibers within the fasciculus gracilis travel medially within the dorsal columns to terminate in the nucleus gracilis (gracile nucleus), whereas the fasciculus cuneatus ascends lateral to the fasciculus gracilis to terminate in the nucleus cuneatus (cuneate nucleus). In some species with a prominent tail, there exists a nucleus of Bischoff that is located medial to the gracile nucleus and which receives input from afferent fibers supplying the tail (Kappers et al., 1936). Collectively, the gracile and cuneate nuclei comprise the dorsal column nuclei (DCN) (Willis and Coggeshall, 1991).

The majority of long primary afferents ascending to the DCN are large myelinated fibers, although small myelinated and unmyelinated fibers have also been identified in the dorsal columns (Burgess and Horch, 1978; McNeill et al., 1988; Tamatani et al., 1989; Patterson et al., 1989, 1990). Within the DCN, the fibers

terminate in an orderly, somatotopic manner. Werner and Whitsel (1967, 1970) demonstrated in monkey that fiber sorting occurs as the primary afferent fibers ascend within the dorsal columns, progressing from a dermatomal to a somatotopic organization. Pubols and Pubols (1973) found an incomplete somatotopic organization at the cervical level of the dorsal columns in raccoon, suggesting that final sorting occurs in the DCN.

The somatotopic organization of the DCN has been well described in a number of species including rats, cats, raccoon and monkey (Kruger et al., 1961; Nord, 1967; Johnson et al., 1968; Millar and Basbaum, 1975; Beck, 1981; Nyberg and Blomqvist, 1982; Hummelsheim et al., 1985; Nyberg, 1988; Culberson and Brushart, 1989; Florence et al., 1989; Rasmusson, 1989). The dorsal funiculus divides into several fiber bundles as it approaches the dorsal surface of the DCN. The bundles dive ventrally to enter the appropriate target (i.e. gracile or cuneate nucleus), with individual fibers giving off several collaterals before terminating (Gulley, 1973; Fyffe et al., 1986). Within the gracile nucleus, the most caudal regions of the body are represented medially and more proximal representations, including the lower trunk, are found in progressively more lateral regions. The somatotopic organization is similar in the cuneate nucleus i.e. the progression from caudal to rostral representations is also in the medial to lateral direction (Kruger et al., 1961; Nyberg and Blomqvist, 1982).

In the cat, the DCN is divided into rostral, middle and caudal zones (Hand, 1966). The cell cluster region in the middle zone provides the highest density DCN projection to the thalamus, although rostral and caudal regions of the DCN also

project to this site (Berkley, 1975; Blomqvist and Westman, 1975; Cheek et al., 1975; Blomqvist, 1980; Ellis and Rustioni, 1981). In addition to the cluster region, the middle zone also contains dorsal and ventral regions that bear a close resemblance to the rostral and caudal zones (Kuypers and Tuerck, 1964). Ellis and Rustioni (1981) found that over 92% of cells within the cluster region of cat could be retrogradely labeled following HRP injection into the contralateral thalamus. The thalamic sites known to receive input from the DCN are the VPL nucleus, medial posterior complex (PO_m) and the zona incerta (Boivie, 1971b; Berkley, 1975, 1980; Groenewegen et al., 1975; Hand and van Winkle, 1977). Within the ventrobasal thalamus, the terminations of DCN afferents are somatotopically organized. The thalamic map is basically an inverted copy of that in the DCN; i.e. the cuneate projection is medial to that of the gracile nucleus within the VPL (Hand and van Winkle, 1977; Berkley and Hand, 1978).

The cluster region has a distinctly different cytoarchitecture as compared to all other regions of the DCN, including the dorsal and ventral middle regions. Cell cluster neurons are typically round with short, bushy dendrites as opposed to the stellate, fusiform or triangular neurons in other regions of the DCN (Ramon y Cajal, 1909). Neurons in the cluster region of cats are known to receive input from cutaneous afferent fibers, including both slowly adapting and rapidly adapting populations (Dykes et al., 1982). In contrast, muscle afferents have been shown to terminate in ventral or dorsal regions of the middle zone, avoiding the cell cluster region (Nyberg and Blomqvist, 1982; Fyffe et al., 1986). In addition to primary muscle afferents, non-cluster regions of the DCN receive input from the sensorimotor cortex, reticular

formation, red nucleus and spinal cord grey matter (Kuypers and Tuerk, 1964; Edwards, 1972; Rustioni, 1973, 1974, 1977; Sotgiu and Marini, 1977; Weisberg and Rustioni, 1979; Brown and Fyffe, 1981; Gordon and Grant, 1982; Cheema et al., 1983).

The monkey DCN resembles that of the cat in that there are rostral, middle and caudal zones, with the middle zone containing a cell cluster-like region. In the monkey cuneate nucleus, the cluster region is called the pars rotundus and the remainder of the middle zone is referred to as the pars triangularis (Ferraro and Barrera, 1935b; Boivie, 1978; Rustioni et al., 1979). The pars rotundus, like the cluster region in cat, receives predominantly cutaneous input, whereas most of the muscle afferent input terminates in the pars triangularis and the deep part of the caudal zone (Hummelsheim et al., 1985; Culberson and Brushard, 1989; Florence and Kaas, 1989). The target of DCN projection neurons in monkey is similar to that in cats, with the predominant output being from the pars rotundus to the contralateral VPL thalamus (Boivie, 1978; Berkley, 1980).

The DCN of raccoon has been thoroughly characterized, starting with an anatomical and physiological description by Johnson, Welker and Pubols (1968). The location of the DCN is easily identifiable as a prominent bulge or tubercle on the dorsal medullary surface in raccoon (Johnson et al., 1968). As in cat and monkey, the raccoon DCN can be sub-divided into rostral, middle and caudal regions. The middle region can be further divided into the dorsal cap, cluster region and basal cuneate nucleus (Johnson et al., 1968). In the cluster region, relatively large cell bodies have been described that extend rostrocaudally as "slender, laterally compressed, irregular

columns of cells". Each cluster contains neurons that respond to input from the glabrous skin of a single digit and are separated from each other by fibrous laminae (Welker and Johnson, 1965; Johnson et al., 1968). The dorsal cap, which overlies the cluster region, contains neurons responding to input from the claws and hairy skin of the forepaw. Ventral to the cluster region is the basal cuneate nucleus that contains neurons responding to input from the hairy skin of the paw and forearm (Johnson et al., 1968; Rasmusson and Northgrave, 1997).

Pubols and Pubols (1973) examined the different types of mechanosensory afferent fibers in the cuneate fasciculus that innervate glabrous skin regions of the raccoon forepaw. Within the cuneate fasciculus, they found two types of rapidly adapting and two types of slowly adapting mechanoreceptive afferent fibers that responded to stimulation of the glabrous skin. In addition, fibers that responded to stimulation of joints or hairy skin were noted, but were not included in the study (Pubols and Pubols, 1973). These findings are in agreement with those of Rowinski et al. (1985) who showed that, in response to mechanical stimulation of the glabrous skin, neurons of the middle cuneate nucleus could be classified as receiving input from rapidly adapting receptors (76%), including Pacinian corpuscles, or slowly adapting receptors (24%).

1.6 Anatomical studies of post-synaptic dorsal column neurons

Using Golgi staining techniques in the spinal cord, it was shown by Edinger (1885) that some dorsal horn neurons have axons that project in the dorsal columns (as cited by Nathan and Smith, 1959). However, the existence of post-synaptic dorsal

column axons was not proven unequivocally until Uddenberg (1966) provided an electrophysiological description in cat. The first evidence that post-synaptic dorsal column fibers reach the level of the DCN came from the anatomical work of Rustioni (1973, 1974) in cat. Since the early work of Uddenberg, investigations of the PSDC system have been extended to include the rat and monkey, but most work to date has been done in cat.

Giesler et al. (1984) studied the laminar distribution of PSDC neurons in rat by examining the retrograde transport of horseradish peroxidase (HRP) from the DCN to the spinal cord. They found that the cell bodies of rat PSDC neurons predominated in the nucleus proprius (i.e. lamina III and IV) of the spinal cord dorsal horn. They also determined that most PSDC neurons are in the cervical and lumbar enlargements, with cervical PSDC neurons situated more medially than those in more caudal regions of the spinal cord. The PSDC system was determined to be a major projection to the DCN in rat, constituting over 38% of cells (including DRG) that project to the cuneate and 30% of those projecting to the gracile nucleus. Most of the PSDC projections from the cervical dorsal horn (90%) were found to reach the cuneate nucleus via the dorsal columns, whereas a further 8% were found in the dorsolateral funiculus. In contrast, it was estimated that the PSDC projection from lumbar regions travels entirely within the dorsal columns (Giesler et al., 1984).

In a similar study in cat, Enevoldson and Gordon (1989) implanted HRP pellets into either the dorsal columns or DCN after destruction of the dorsolateral funiculus on one side. After HRP retrograde transport, the authors were able to examine the number, location and dendritic morphology of PSDC neurons in the

feline spinal cord (Enevoldson and Gordon, 1989a). PSDC neurons were found predominantly in the lumbar and cervical enlargements, similar to the finding of Giesler et al. (1984) in rat. Within the dorsal horn, the cells were largely found in lamina IV but some cells were identified in laminae III, V, VI and VII (Enevoldson and Gordon, 1989a).

Three different types of PSDC neuron morphology (A, B and C) were characterized by Enevoldson and Gordon (1989) which matched Brown and Fyffe's (1981) previously described types 1, 2 and 3 in cat. The most prevalent type of cell (Enevoldson and Gordon type C; Brown and Fyffe type 3) was found centered in lamina IV, with dendritic trees that extended in the rostrocaudal direction but restricted mediolaterally. These neurons had mainly dorsally directed dendritic trees that were seen to penetrate as far as lamina II and occasionally lamina I (Brown and Fyffe, 1981). Type B cells (Brown and Fyffe type 2) were described as being "dramatically different" from type C cells, with large perikarya in medial lamina V and long straight dendrites in the transverse plane. Type A cells (Brown and Fyffe type 1) were found to be confined to medial regions of laminae II and IV and with dendritic fields that were restricted in both the rostrocaudal and mediolateral direction (Enevoldson and Gordon, 1989).

Bennett et al. (1984) also provided a description of PSDC neuronal morphology in cat. In this study, HRP was injected intracellularly into antidromically identified neurons in the lumbosacral enlargement (Bennett et al., 1984). As in previous studies, the PSDC neurons were found to be located primarily in laminae III-IV of the dorsal horn. Four different neurons types were described with respect to

PSDC dendritic morphology (neuron types A-D) (Bennett et al., 1984). The classifications made by Bennett et al. (1984) are not unlike those made in a previous intracellular HRP injection study in cat, but the small number of cells used in both studies precludes a definitive comparison (Brown and Fyffe, 1981).

The cell body diameter of cat PSDC neurons was found to be variable depending on the type of labeling used. For example, in studies that injected HRP intracellularly the soma diameter reportedly ranged from 12-60 μm in one study to 25.6-70.2 μm in another (Brown and Fyffe, 1981; Bennett et al., 1984). In contrast, when retrograde filling was used to identify PSDC neurons, the cell body diameter was reported to range between 13.7-49.2 μm (Bennett et al., 1984). It has been suggested that the soma of intracellularly stained neurons may swell, causing artificially high measures of cell body diameter (Bennett et al., 1984).

In monkey, Rustioni et al. (1979) reported that PSDC neurons are located primarily in laminae IV-VI. In contrast, Bennett et al. (1983) determined that they were found more superficially than in cats, mostly in lamina III but with some in laminae I, II and VII. In both studies, the PSDC cells were concentrated medially within the cervical enlargement and laterally within the lumbar enlargement (Rustioni et al., 1979; Bennett et al., 1983; Cliffer and Willis, 1994).

Based on the results of degeneration experiments, it was originally thought that the PSDC system projected to non-cluster regions of the DCN in cat and monkey (Rustioni, 1973, 1974, 1979). The PSDC projection was reportedly concentrated in the rostral and caudal zones of the DCN, sparing the cluster region of the middle zone that

projects heavily to the thalamus. These findings were in sharp contrast to studies in rat that described a widespread projection of PSDC fibers throughout the entire DCN (Cliffer and Giesler, 1989). However, it has more recently been shown using *Phaseolus vulgaris* leucoagglutinin and intra-PSDC fiber injections of HRP, that there is at least a sparse projection to the cluster region in cats (Pierce et al., 1990). Furthermore, when the distribution of PSDC fiber terminals in the cuneate nucleus of monkeys was re-examined by Cliffer and Willis (1994), a distinct projection to the pars rotunda (analogous to the cuneate cluster region in cat) was noted. The more recent findings are thought to result from the use of more advanced methodological techniques, including the use of the sensitive anterograde tracers such as *Phaseolus vulgaris* leucoagglutinin (Cliffer and Willis, 1994).

1.7 Electrophysiological studies of the PSDC system

Following his landmark paper in 1966, Uddenberg continued to investigate feline PSDC neurons, establishing a comprehensive description of their physiological properties (Uddenberg, 1968). Recording from identified PSDC axons in the cervical spinal cord, Uddenberg (1968) was the first to establish that post-synaptic fibers receive convergent input from low and high threshold cutaneous afferents as well as from low and high threshold muscle and joint afferents. The PSDC axons in the experiment were estimated to conduct at 40-70 m/s, a velocity thought to correspond with myelinated fibers ranging in diameter from 7-12 μm (Uddenberg, 1968). Uddenberg found that the cutaneous RFs varied in size between 1 and 10 cm^2, with the

smallest on distal regions of the forearm (i.e. paw and toes). The fields were described as being sharply delimited and with no evidence of surround inhibition (Uddenberg, 1968). The resting discharge of PSDC units ranged from 1-5 impulses per second, and it was noted that "following strong activation either by natural or electrical stimulation, the activity often increased above the resting level and remained high for some minutes" (Uddenberg, 1968). In reference to PSDC fibers, Uddenberg commented that they are "remarkable in combining lack of modality specificity with a high degree of spatial discrimination" (Uddenberg, 1968). He postulated the main function of PSDC neurons to be the spatial discrimination of exteroceptive information, noting that PSDC fiber RFs were only slightly larger than the smallest fields of relay cells in the gracile nucleus of cats (Uddenberg, 1968).

Angaut-Petit (1975) reported similar findings in cat with respect to the response properties of PSDC fibers in the dorsal columns. Using the same recording technique as employed by Uddenberg (1966, 1968), Angaut-Petit estimated that the conduction velocity of PSDC fibers ranged from 16-55 m/s, overlapping with those of primary afferent fibers (Hursh, 1939; Angaut-Petit, 1975). The fibers of PSDC neurons were found intermingled amongst those of primary afferent, roughly situated between primary fibers of cutaneous origin and those responding to proprioceptive input (Angaut-Petit, 1975). This finding was important because it demonstrated that PSDC fibers are incorporated into the general somatotopic projection to the DCN and do not constitute a specific bundle within the dorsal columns. Another novel finding was the observation that PSDC fibers can exhibit the phenomena of 'wind-up', an increased activity in response to repeated stimulation. This phenomenon is usually

produced by C-fiber activation, although Angaut-Petit postulated the additional involvement of small myelinated fibers in the PSDC system (Angaut-Petit, 1975).

The first report of intracellular recording from PSDC neurons came from Jankowska et al. (1979) in cat who used this technique to corroborate the previous findings of Uddenberg (1968) and Angaut-Petit (1975). In addition to finding responses to both high and low threshold cutaneous afferents, Jankowska et al. found that over 50% of the PSDC cells tested responded to electrical stimulation of muscle nerves. Based on the results of their study, the authors suggested that PSDC neurons receive either mono- or disynaptic input from group Ia and Ib muscle afferents (Jankowska et al., 1979). The PSDC conduction velocities were judged to range between 30-80 m/s, with most (32/37) occurring between 50-80 m/s (Jankowska et al., 1979). These estimates are higher than in previous reports, a discrepancy that was attributed to differences in recording technique and/or a sampling bias (Jankowska et al., 1979).

Brown and Fyffe (1981) recorded intracellularly from PSDC neurons and injected them with HRP to gain anatomical information about the recorded cells (Brown and Fyffe, 1981). The conduction velocity of PSDC neurons in their study reportedly ranged from 30-47 m/s, similar to reports by Uddenberg (1968) and Angaut-Petit (1975) but different to those of Jankowska et al. (1979) (Brown and Fyffe, 1981). In light of these findings, it is probable that inter-study differences in PSDC neuron conduction velocity can be attributed to sampling biases and not to differences in recording technique.

Brown and Fyffe (1981) found that approximately 33% of their PSDC neuron sample had a subliminal excitatory RF, an area of higher threshold surrounding the low threshold firing zone. The subliminal RF typically responded to the same kinds of stimulation that evoked impulses from the firing zone, but occasionally responded only to noxious mechanical input (Brown and Fyffe, 1981). In addition, they often found inhibitory RFs in association with the PSDC neuron excitatory RFs, some of which were within the excitatory RF. In other cells, the inhibition was evoked by stimulation of a large region of skin that was proximal to and contiguous with the excitatory RF (Brown and Fyffe, 1981).

Following the intracellular PSDC neuron recordings of Jankowska et al. (1979) and Brown and Fyffe (1981), Lu et al. (1983) also used this technique to study the feline PSDC system. The authors antidromically identified a large number (n=120) of PSDC neurons and subsequently characterized their response to both natural and electrical RF stimulation (Lu et al., 1983). Approximately one-half of the PSDC neurons studied responded exclusively to innocuous tactile stimuli and were classified as low-threshold mechanoreceptive (LTM). The remaining one-half were classified as wide-dynamic-range neurons as they responded to both innocuous and noxious stimuli. None of the PSDC neurons examined responded only to noxious stimuli (Lu et al., 1983).

The types of LTM input that Lu et al. (1983) found to be effective for PSDC neuron excitation included deflection of guard hairs and brush strokes on the skin surface. The authors postulated that G_1, G_2 and slowly adapting receptors were the most likely contributors to the observed LTM response of PSDC neurons. Effective

wide dynamic range input included those sufficient to excite LTM units as well as noxious pinch (Lu et al., 1983). In response to electrical RF stimulation, an EPSP alone or an EPSP in combination with an IPSP could be identified for PSDC neurons. The IPSP amplitude and duration varied as a function of stimulus intensity but never lasted in excess of 100 ms (Lu et al., 1983).

Maxwell et al. (1985) provided direct anatomical evidence in support of Lu et al.'s proposal with respect to afferent types that influence PSDC cells. In this study, the authors retrogradely labeled PSDC neurons in the feline dorsal horn with HRP and injected this tracer into isolated primary afferent axons of the same animals. Using light and electron microscopy, it was established that SAI (Merkel discs), hair follicle, Krause, and group Ia muscle afferents as well as Pacinian corpuscles form monosynaptic contacts with PSDC neurons (Maxwell et al., 1985). All neurons contacted by cutaneous axons were found in laminae III-V, whereas those contacted by group Ia muscle spindle afferents were located in lamina VI (Maxwell et al., 1985). The primary afferents formed both terminal and en passant contacts, with individual collaterals giving rise to single or multiple contacts with proximal dendrites and/or the somata of PSDC neurons (Maxwell et al., 1985).

Brown et al. (1983) used extracellular recording techniques to supplement the results of their previous (1981) intracellular study of PSDC neurons. Extracellular recording was used in the more recent investigation because of the poor sample size obtained using intracellular techniques. PSDC neurons are difficult to find and impale because of their small extracellular field potential and soma size, making extracellular techniques a more fruitful alternative (Brown and Fyffe, 1981; Brown et al., 1983). In

the new study, the conduction velocity of PSDC neurons was estimated to vary between 22-61 m/s, similar to their previous estimation of 30-47 m/s (Brown and Fyffe, 1981; Brown et al., 1983). Also similar to the previous study was the observation that many PSDC neurons have complex RFs with excitatory and inhibitory regions, some of which are discontinuous. The regions of high and low threshold previously described by Brown and Fyffe (1981), were often found to be discontinuous in the later study, prompting the authors to comment that "very few units behaved as if they received excitatory input from a single class of mechanoreceptor" (Brown et al., 1983).

Electrical stimulation of cutaneous nerves was found by Brown et al. (1983) to produce inhibition in many cells (9/15) even though they were not excited by the stimulation. The time course of inhibition was similar to that of primary afferent excitation (PAD), with a peak at 20-40 ms and duration up to 100-200 ms (Brown et al., 1983). Some inhibitory time courses, however, were longer with a peak at 100-150 ms and a total duration up to 400 ms. The shorter time course of inhibition was proposed to involve pre-synaptic mechanisms in the spinal cord and the longer to possibly involve supraspinal loops (Brown et al., 1983). A similar inhibition following electrical RF stimulation was reported by Jankowska et al. (1979) and by Lu et al. (1983), both of whom used intracellular recording techniques.

Noble and Riddell (1988) found that, in addition to light tactile and noxious mechanical stimuli, some PSDC neurons in cat were responsive to noxious thermal stimuli. In the large sample of PSDC neurons tested, the authors found that 66 of 75 units tested (88%) responded to both light tactile and noxious mechanical stimuli and

22 of 39 units (50%) also responded to noxious heat (Noble and Riddell, 1988). In addition to convergent excitatory input, 56 of 75 units tested (75%) had an inhibitory field on the ipsilateral hindlimb. Most of the units (69%) had RFs that were confined to hairy skin, but 27% had RFs that encompassed regions of both hairy and glabrous skin (Noble and Riddell, 1988). The conduction velocity of the PSDC neurons in this study ranged between 14-69 m/s and all were found to have a background discharge, similar to previous reports (Uddenberg, 1966, 1968; Angaut-Petit, 1975; Jankowska et al., 1979; Brown and Fyffe, 1981; Brown et al., 1983). The observed spontaneous PSDC neuron activity typically consisted of high frequency bursts of 4-12 impulses that were interspersed with single or paired action potentials (Noble and Riddell, 1988). The finding that noxious heat can excite feline PSDC neurons is interesting in light of the fact that Giesler and Cliffer (1985) did not find any nociceptive PSDC neurons in rat. In unanaesthetized, decerebrate, spinalized rats, the authors tested the response of PSDC neurons to noxious pinch and several intensities of sustained, repeated noxious heating of their RFs. Despite repeated attempts, the only responses that could be elicited from these neurons were those to innocuous mechanical stimuli (Giesler and Cliffer, 1985). However, more recently PSDC neurons have been proposed to mediate visceral pain in rats, presumably receiving input from visceral nociceptive afferents (Al-Chaer et al., 1996a,b, 1998).

Another interesting aspect of Noble and Riddell's work was their confirmation that PSDC neuron RF characteristics in cat depend on the type of anaesthetic used (Noble and Riddell, 1988). Specifically, the authors highlighted the fact that studies using chloralose-anaesthetized animals report more complex PSDC neuron RFs than

those using pentobarbitone-anaesthetized animals (Uddenberg, 1968; Angaut-Petit, 1975; Brown and Fyffe, 1981; Brown et al., 1983; Noble and Riddell, 1988). For example, several previous studies in pentobarbitone-anaesthetized cats failed to detect inhibitory input to PSDC neurons (Uddenberg, 1968; Angaut-Petit, 1975; Lu et al., 1983). The anaesthetic based discrepancies are important because the general impression based on experiments in pentobarbitone-anaesthetized animals is that PSDC and SCT neurons are very similar with respect to RF characteristics. However, studies using chloralose-anaesthetized animals have described PSDC RFs that are much different in their organization as compared to SCT neurons (Hongo et al., 1968; Uddenberg, 1968; Brown and Franz, 1969; Angaut-Petit, 1975; Brown and Fyffe, 1981; Brown et al., 1983; Brown et al., 1987; Noble and Riddell, 1988). One of the major differences between PSDC and SCT neurons, as identified in chloralose-anaesthetized animals, is that SCT neurons commonly have inhibitory RFs on the contralateral limb and not the ipsilateral limb as in the PSDC system. Another difference between the two sets of neurons is that PSDC neurons respond to input from SAI and Pacinian corpuscles, whereas SCT cells do not (Brown and Franz, 1969; Willis et al., 1974).

Despite their functional differences, it has been postulated that PSDC and SCT neurons interact within the spinal cord dorsal horn (Jankowska et al., 1979; Brown and Fyffe, 1981; Brown et al., 1986). It has been shown that SCT neurons have axon collaterals that ramify extensively within the dorsal horn and synapse on the dendrites and somata of neurons in Rexed's laminae IV-V (Brown, 1976, 1977; Rastad et al., 1977; Rastad, 1978a,b). Jankowska et al. (1979) used electrophysiological methods in

an attempt to show that collaterals of the spinocervical tract terminate on PSDC neurons in the dorsal horn. The authors showed that stimulation of the ipsilateral dorsolateral funiculus could produce EPSPs in PSDC neurons whereas stimulation at C1 is much less effective. From these results, they concluded that the EPSPs in the PSDC neurons were being evoked via spinal collateral branches of axons of SCT neurons that terminate at the level of C1-C2 (Jankowska et al., 1979). There is anatomical evidence to support this postulate. Maxwell and Koerber (1986) found anatomical evidence that SCT neurons in the spinal cord dorsal horn make connections with an identified population that likely includes PSDC neurons. Although strengthened by anatomical findings, the electrophysiological evidence itself was inconclusive because of an alternative explanation that could account for the results. Jankowska et al. could not rule out the possibility that PSDC neurons were excited by stimulation of the dorsolateral fasciculus, not because of synaptic connections between PSDC and SCT neurons in the dorsal horn, but because the two projections are not completely independent.

The question of PSDC-SCT projection independence was investigated by Lu et al. (1985) using intracellular recording techniques. Their study was based on a previous observation that many PSDC neurons could be antidromically activated by stimulation of the dorsolateral funiculus (Lu et al., 1983). Of 56 dorsal horn neurons, 23 could be driven antidromically by both the dorsal columns and the dorsolateral funiculus (DC+DLF neurons). Of the remaining neurons, 22 could be driven exclusively from the dorsal columns and 11 only from the dorsolateral funiculus (Lu et al., 1985). Approximately half of the DC+DLF neurons responded exclusively to

low threshold mechanosensory input, whereas the remainder were additionally responsive to noxious input (Lu et al., 1985). The results of the study were taken as evidence that many cells in the dorsal horn contribute axons to both the PSDC and SCT projection and that they "do not constitute morphologically and physiologically distinct populations" (Lu et al., 1985). Jiao et al. (1984) provided anatomical evidence in support of the latter contention. Following injections of fluorescent retrograde tracers into the DCN and LCN, some of the neurons in laminae III-V were found to be double labeled (Jiao et al., 1984).

Brown et al. (1986) challenged the findings of Lu et al. (1985) in light of the high intensity antidromic stimuli used by this group. It was argued that the antidromic stimuli used by Lu et al. was of sufficiently high magnitude (0.2-0.5 ms, 30V) that it likely spread from the intended funiculus to the other, leading to incorrect conclusions about the independence of PSDC and SCT neuronal populations (Brown et al., 1986). Brown et al. (1986) also challenged the anatomical findings of Jiao et al. (1984) based on previous reports that some PSDC neurons project axons to the DCN via the dorsolateral funiculus (Dart and Gordon, 1973; Gordon and Grant, 1982). According to Brown et al., "if these axons give off collateral branches to the LCN, as suggested by Craig and Tapper (1978), then such double labeling would be expected" (Brown et al., 1986).

Brown et al. were themselves unable to antidromically activate PSDC neurons from the ipsilateral dorsolateral funiculus, even with stimuli up to 70 times the threshold for PSDC excitation via the dorsal columns (Brown et al., 1986). Approximately 50% of SCT neurons could be excited via the dorsal columns with

antidromic stimuli up to 30 times the threshold for excitation via the dorsolateral funiculus. However, the authors cited many reasons why this finding was likely to be the result of current spread. Based on their study, Brown et al. concluded that PSDC and SCT neurons constitute separate populations of neurons, although they probably interact with one another in the dorsal horn (Brown et al., 1986).

1.8 Descending influences on PSDC neurons

Noble and Riddell (1989) have shown that PSDC neurons in the feline dorsal horn are under tonic inhibitory control, which is at least partly due to descending projections. Using reversible cold block of the spinal cord, the authors established that the PSDC sensitivity to noxious pinch and radiant heat was increased, as was the area of skin from which a nociceptive response could be elicited (Noble and Riddell, 1989). In contrast, the response of PSDC neurons to low threshold mechanical stimuli was unchanged following the disruption of descending pathways. In addition, the spontaneous activity of PSDC neurons is affected by descending influences, either directly or indirectly. During the cold block, the spontaneous activity of 15 of 19 PSDC neurons increased to between 2-19 times the resting level. In two cases, the spontaneous activity decreased and in another two it was unchanged during the cold block. These results suggest that nociceptive afferent input to PSDC neurons is under the influence of tonic descending inhibition. One explanation for the finding is that peripheral input (via spontaneously active C-fibers) drives the spontaneous activity of PSDC neurons. In this scenario, descending presynaptic inhibition of afferent C-fiber input to PSDC neurons would be expected to indirectly affect the spontaneous

discharge of these cells. It is also possible that descending inhibition could affect the spontaneous activity of PSDC neurons via a multisynaptic pathway in the dorsal horn that is independent of a tonic afferent excitation.

Other potential sources of descending influence on PSDC neurons include the somatosensory cortex (SI and SII), the DCN, the periaqueductal gray, raphe and juxta-raphe regions of the medial reticular formation and the brainstem lateral reticular formation (Engberg et al., 1968; Dart, 1971; Hall et al., 1982; Morton et al., 1983; Gray and Dostrovsky, 1983; Enevoldson and Gordon, 1984).

1.9 Pharmacological studies of the PSDC system

To date, there have been relatively few investigations into specific neurochemical features of PSDC neurons. According to the findings of Maxwell et al. (1995), glutamate is the primary excitatory neurotransmitter with respect to input to PSDC neurons. Of the 60 synaptic profiles associated with PSDC cell bodies or proximal dendrites, 53% were found to contain glutamate (Maxwell et al., 1995). In a different set of PSDC neuron-associated synaptic profiles (n=114), the authors reported that 42% contained the inhibitory neurotransmitter, GABA (Maxwell et al., 1995). In an experiment where sections were labeled for both GABA and glutamate, it was demonstrated that these neurotransmitters are not co-localized within the same synaptic profile (Maxwell et al., 1995). In contrast, the co-localization of GABA and glycine, both inhibitory neurotransmitters, has been demonstrated with respect to PSDC neuron-associated synaptic terminals (Maxwell and Kerr, 1995).

It has been demonstrated that the excitatory responses of PSDC neurons to cutaneous input can be modulated by noradrenaline and serotonin in cat (Fleetwood-Walker et al., 1985; Jankowska et al., 1997). Fleetwood-Walker et al. (1985) examined the effect of iontophoretically-applied L-noradrenaline on PSDC neurons in the cat dorsal horn. The authors found that in 3 of 5 PSDC neurons noradrenaline produced a potent, selective inhibition of nociceptive responses (to heat, pinch), but had no effect on the response to innocuous mechanosensory input or spontaneous activity (Fleetwood-Walker et al., 1985). The effect was mimicked by α_2- but not α_1-selective agonists and reversed by α_2 antagonists, indicating its dependence on the α_2 receptor (Fleetwood-Walker et al., 1985).

Jankowska et al. (1997) tested the response of PSDC neurons to electrical stimulation of low threshold cutaneous afferents following iontophoretic application of noradrenaline and serotonin into the feline dorsal horn. It was found that serotonin had an excitatory effect on PSDC neuron responses, whereas noradrenaline had an inhibitory effect (Jankowska et al., 1997). The results of this study are clearly different than those of Fleetwood-Walker with respect to the effects of noradrenaline. One reason for the discrepancy could be the use of electrical stimulation in the work of Jankowska et al. versus the use of natural stimuli by Fleetwood-Walker et al. (1985). Changes in the number and timing of responses evoked by single electrical stimuli provide a more sensitive measure of the modulation of synaptic actions than the total number of responses evoked by longer-lasting natural stimuli (Jankowska et al., 1997). Furthermore, the amplitude of electrical stimulation can be adjusted to

excite specific afferent types, facilitating the identification of modality-specific drug effects.

1.10 Putative function of PSDC neurons

The role of PSDC neurons in somatosensation is not known although there is indirect evidence to suggest that they could be involved in modulating the responsiveness of DCN neurons to mechanosensory input. Dykes and Craig (1998) found that blocking synaptic transmission in the cat dorsal horn resulted in an almost immediate increase in the receptive field (RF) size and responsiveness of DCN neurons. Although the cobalt chloride-induced synaptic blockade used by Dykes and Craig (1998) did not specifically target PSDC neurons, these cells were presumably affected along with all others in the spinal cord dorsal horn. Furthermore, since PSDC neurons provide the only known direct spinal cord projection to the DCN, they are likely to have contributed to the observed effect in the cuneate nucleus.

The results of Dykes and Craig (1998) suggest that DCN neurons were released from tonic inhibition following the blockade of synaptic transmission at the level of the spinal cord. The authors postulated that disinhibition of DCN neurons occurred because the balance of excitatory drive to PSDC neurons was disrupted in the spinal cord, causing a decrease in the excitatory drive of PSDC neurons to DCN inhibitory interneurons (Dykes and Craig, 1998). An alternative explanation for the findings of Dykes and Craig (1998) should be considered given the fact that cobalt chloride indiscriminately blocks all synaptic transmission, both excitatory and inhibitory. Disruption of tonic glycinergic and/or GABA-ergic inhibition of PSDC

neurons in the dorsal horn could increase the excitatory drive from PSDC to DCN neurons, resulting in altered DCN neuron RF and response properties. The latter explanation is feasible in light of the recent findings of Sherman et al. (1997). When the authors blocked glycinergic transmission in the spinal cord of rats, they observed marked increases in the receptive field size and evoked responses of low-threshold mechanical neurons in the VPL thalamus (Sherman et al., 1997). The authors concluded that there is a significant low-threshold input to low-threshold mechanical neurons in the VPL thalamus that arises from the spinal cord, the source of which could include PSDC neurons acting on VPL neurons via the DCN (Sherman et al., 1997).

Other studies have indicated a role for PSDC neurons in the transmission of noxious visceral input to the DCN in both rat and monkey (Al-Chaer et al. 1996, 1998). Al-Chaer et al (1996) recorded separately from PSDC and DCN neurons in rat to characterize the response of these cells to noxious viscerosensory input (i.e. colorectal distension and mustard oil-induced inflammation). The results clearly indicate that both PSDC and gracile neurons fire in response to nociceptive visceral input, an effect that was reversibly blocked by administration of morphine or CNQX (a non-NMDA glutamate receptor antagonist) in the dorsal horn. In addition, a lesion of the dorsal columns blocked the response of gracile neurons to nociceptive visceral input, suggesting an intermediary role for PSDC neurons in this relay. In a separate study, the authors demonstrated a significant decrease in the response of VPL neurons to visceral nociceptive input following a lesion of the dorsal columns but not after a ventrolateral spinal cord lesion (Al-Chaer et al. 1996). Similar findings were obtained

when the experiment was later repeated in monkey (Al-Chaer et al., 1998). Taken together, the results indicate the importance of the dorsal column pathway in relaying noxious viscerosensory information to neurons in the gracile nucleus.

The results of these recent studies support the existence of a functional connection between PSDC and DCN neurons. It has been previously shown using anatomical techniques that PSDC axons terminate in widespread regions of the DCN in rat, cat and monkey (Cliffer and Giesler, 1989; Pierce et al., 1990; Cliffer and Willis, 1994). However, the synaptic relationship between PSDC terminations and thalamic-projecting neurons in the DCN has not been clearly established. In fact, early anatomical work seemed to indicate the absence of PSDC neuron terminations in the vicinity of cuneothalamic neurons, except perhaps in rat. PSDC axon terminals were found largely in regions of the cuneate nucleus that project to targets including the cerebellum, inferior olive, tectum and pontine nuclei, leading to the suggestion that PSDC neurons are involved in motor control (Cliffer and Giesler 1989; Rustioni 1973, 1974, 1979).

More recently, Pierce et al. (1990) found sparse PSDC input to the cluster region of the cuneate nucleus in cats. Similarly, Cliffer and Willis (1994) demonstrated that axons of PSDC neurons terminate in all regions of the monkey DCN, including those that project to the thalamus. These recent findings in cat and monkey are important because they introduce the possibility of an anatomical connection between PSDC and cuneothalamic neurons. There is immunocytochemical evidence to suggest that at least 20% of PSDC terminals within the rat cuneate nucleus are glutamatergic, providing an excitatory drive to cuneate neurons (De Biasi

et al., 1995). It is not known whether the excitatory drive is imparted to cuneothalamic neurons, neurons in non-thalamic projecting regions or both. It is also possible that PSDC neurons excite inhibitory interneurons in the basal region of this nucleus, providing an indirect inhibition on other cuneate neurons, including cuneothalamic neurons in the cluster regions (Dykes and Craig, 1998). The neurotransmitter utilized by most PSDC neurons is currently unknown (Willis, 1999).

It is possible that PSDC neurons play a role in the reorganization that occurs in the raccoon cuneate nucleus following peripheral denervation (Rasmusson and Northgrave, 1997). Rasmusson and Northgrave (1997) observed reorganization within the cuneate nucleus of adult raccoons at two to five months after amputation of a single digit. The authors discussed two general mechanisms that could account for their findings, i.e. the growth of new connections (sprouting) and the strengthening of preexisting connections. The strongest evidence for sprouting comes from a study in which the growth of new connections within the cuneate nucleus was observed following amputation of the entire hand in monkeys (Florence and Kaas, 1995). In this study, forearm afferents of animals that had undergone therapeutic forearm amputation were labeled and found to innervate a more extensive area of both the dorsal horn and cuneate nucleus as compared to normal animals. However, sprouting of afferents was not observed in raccoon following the amputation of a single digit. Rasmusson (1988) did not find any new projections from intact adjacent digits to the deafferented digit region of the cuneate nucleus after amputation. The discrepant findings could result from differences in the degree of peripheral denervation used in

the studies, i.e. the entire hand in the monkey vs. a single digit in raccoon (Rasmusson, 1988; Florence and Kaas 1995).

In addition to sprouting, the strengthening of preexisting connections could explain the reorganization of the cuneate nucleus following peripheral denervation in raccoon. If unmasking of preexisting synapses is responsible for cuneate reorganization, new RFs should become apparent on adjacent digits immediately following peripheral deafferentation. However, Rasmusson and Northgrave (1996) did not find any evidence of new RFs on adjacent digits when they temporarily blocked afferent input from the digit containing the normal RF. The authors concluded that ineffective synapses from adjacent digits are not suddenly unmasked following the removal of afferents from the denervated digit (Rasmusson and Northgrave, 1996).

However, it remains a possibility that unmasking of ineffective synapses onto PSDC neurons could occur in the dorsal horn following removal of the dominant input to these cells. In this scenario, unmasked synapses from adjacent digits would become functionally relevant, able to contribute to PSDC neuron activity. In this way, cuneate neurons would indirectly become responsive to input from adjacent digit, secondary to unmasking in the dorsal horn and not the cuneate nucleus. The results of Rasmusson and Northgrave (1996) indicate that neurons in the deafferented region of the cuneate nucleus do not immediately become responsive to input from adjacent digits. Therefore, it is possible that unmasked synapses onto PSDC neurons are weak and must be strengthened before a sufficient number of PSDC are excited and capable of driving neurons in the cuneate nucleus.

1.11 Purpose of the thesis and statement of hypotheses

1.11.1 Purpose

Most investigations of the mammalian PSDC system have been in cat, although some work has been done in rat and monkey. The almost exclusive use of cats in physiological studies of the PSDC system is problematic because of limitations in the degree to which results can be generalized to other species, including human. The hind and forelimbs of cats are suitably adapted for their primary role in balance and locomotion. In contrast, rats, monkeys, raccoons and humans have forelimbs that are, to varying degrees, specialized for fine spatiotemporal discrimination tasks involving glabrous skin surfaces of the forepaw. Given the existence of inter-species functional differences, it is conceivable that the PSDC system is adapted to suit the specific needs of the animal. For example, it is possible that PSDC neurons in cat receive a large proportion of input from muscle and joint receptors, because they provide critical proprioceptive information for finely tuned balance and movement. In animals with forelimbs that are adapted for skilled object manipulation, PSDC neurons may receive their primary input from both high and low threshold cutaneous receptors in glabrous skin. Another example of species differences in the PSDC system is the well documented difference in responsiveness of rat vs. cat PSDC neurons to noxious stimuli (Cliffer and Giesler, 1985; Kamogawa and Bennett, 1986).

The SCT system is also known to have very pronounced species differences. While the SCT path has been postulated to be a major somatosensory projection in carnivores, it is much smaller and presumably less important in other animals such as rats, monkeys and humans (Ha et al., 1965; Kitai et al., 1965; Muzuno et al., 1967). In

monkeys, many SCT cells have RFs on glabrous skin, whereas in cats, the majority of SCT RFs are on the hairy skin and do not incorporate regions of the footpad (Brown and Franz, 1969; Bryan et al., 1973,1974).

As a result of species variation, it is important to study different aspects of PSDC neuron function in different animals. For example, the study of proprioceptive input to PSDC neurons may be best suited to cats because of their propensity for skilled balance and locomotion. In contrast, the lemniscal properties of the PSDC system are best studied in animals that have forepaws that are specialized for use as sensitive tactile organs and for the dexterous manipulation of objects. Consequently, one purpose of this thesis was to study the lemniscal properties of PSDC neurons in the raccoon because this animal has large regions of forepaw glabrous skin and can manipulate objects with great manual dexterity.

To date, there have been no studies that directly test the functional connections between PSDC and cuneate neurons. One way to test for the existence of a functional connection between two populations of neurons involves simultaneous recording of both populations and complex post hoc analyses using cross-correlation and frequency response analyses. This has recently been done to demonstrate functional interactions between mechanosensory neurons in the cuneate nucleus and VPL thalamus and between thalamus and SI cortex (Alloway et al. 1993, 1994). Therefore, a second purpose of this thesis was to use cross-correlation analysis to address the question of PSDC-cuneate interaction.

The mechanisms responsible for the reorganization of somatosensory maps within the cuneate nucleus are currently unknown. It is possible that PSDC neurons

contribute to cuneate reorganization via the unmasking of ineffective synapses onto these cells. Therefore, a third purpose of this thesis was to test for ineffective synapses onto PSDC neurons and to look for evidence of increased effectiveness (i.e. unmasking) during temporary deafferentation.

1.11.2 Statement of hypotheses

Based on the literature described in the introduction, the experiments in this thesis will test the following hypotheses:

1A. Raccoon PSDC neurons are more similar to PSDC neurons in rat and monkey than they are to cat PSDC neurons in terms of their location of their cell bodies, RF characteristics and response properties.

1B. Raccoon PSDC neurons with RFs on forepaw glabrous skin are similar to published reports of raccoon SCT neurons with respect to RF size and responsiveness to innocuous mechanosensory stimulation.

2A. There is a functional connection between PSDC and cuneate neurons that can be detected using cross-correlation and frequency response analyses.

2B. A functional connection exists only between PSDC and cuneate neurons that have overlapping RFs.

2C. The functional connection is excitatory and in the PSDC to cuneate direction.

2D. The responses of PSDC neurons can be well approximated by a linear model.

2E. A functional connection between PSDC and DCN neurons is present during the response of PSDC neurons to RF stimulation.

2F. A functional connection between PSDC and DCN neurons is present during spontaneous discharge of PSDC neurons.

3A. Removing all afferent activity from the digit that provides a PSDC neuron's major input (the 'on-focus' digit) causes a decrease in spontaneous activity similar to that seen in the cuneate nucleus.

3B. Temporary deafferentation of the on-focus digit destroys any functional connection between PSDC and cuneate neurons.

3C. Temporary deafferentation of the on-focus digit reveals an increased responsiveness of PSDC neurons to electrical stimulation of the off-focus digit (i.e. adjacent to the on-focus digit).

Chapter 2: METHODS

2.1 Experiment 1: Characterization of raccoon PSDC neurons

2.1.1 Animals

Recordings were made from 23 adult raccoons (*Procyon lotor*) of either sex that were trapped in the wild and housed communally with ad lib food and water. At the time of recording, the animals weighed between 4 and 12 kg.

2.1.2 Recording procedure

Induction of anesthesia was carried out using ketamine hydrochloride (100 mg, i.m.; MTC Pharmaceuticals, Cambridge, ON) followed by 2% halothane. The radial or cephalic vein (opposite to the forepaw of interest) was catheterized to allow intravenous injection of α-chloralose (5% in propylene glycol; Sigma, St. Louis, MO). An initial dose of 2 ml α-chloralose, followed by 0.5 ml/h was sufficient to maintain the animal in an areflexic state throughout the experiment.

To stabilize the preparation, the animal was placed in a Kopf stereotaxic frame and the neck was ventroflexed. The skull was secured in this position by cementing a bar to the top of the skull using dental caulk. The spine was supported by clamping the spinous process of one of the thoracic vertebrae and securing it to the stereotaxic frame. The skin and muscles overlying the medulla and C5-T1 were reflected and parts of the atlas, axis, occipital bone and C5-T1 were removed to expose the dorsal surface of the medulla and spinal cord. A dam was created around each opening using gauze soaked in 3% agar before opening the dura. Penetrations at the level of the medulla were concentrated in the region caudal to the obex where the cuneate nucleus

produces a visible bulge on the dorsal surface. Penetrations in the cervical spine were made ipsilateral to the recording site in the medulla.

Isolated extracellular neuronal responses were recorded simultaneously from the cuneate nucleus and ipsilateral cervical spinal cord. Recordings were made using Parylene-C insulated tungsten electrodes (1-2 MΩ impedance, A-M Systems, Everett, WA). The signals were amplified (model 1 CWE, Ardmore, PA and model 2 A-M Systems, Everett, WA) and monitored on an oscilloscope and an audio speaker. Signals recorded in the cervical spinal cord were included only if they could be antidromically identified using a concentric bipolar electrode (FHC, Brunswick, ME) placed in the middle of the ipsilateral dorsal columns rostral to C1. A Master-8 stimulator (AMPI, Jerusalem, Israel) was used to deliver a single 0.1-ms constant current pulse (< 100 μA) or a train of 4 pulses at 400 Hz. Criteria for antidromic activation were i) a constant latency of response to single pulses, ii) the ability to follow a high frequency train of pulses (> 400 Hz) and iii) responsiveness to pulses less than 100 μA in amplitude.

Prior to microelectrode insertion in the spinal cord, pia was carefully removed with jeweler's forceps to facilitate penetration without spinal cord dimpling. Microelectrodes were advanced in the spinal cord in 25- to 50 μ steps and responses to tapping the skin and deep tissues of the forearm or touching the skin with a fine-tipped glass probe were assessed. When a PSDC neuron was antidromically identified, its RF was carefully mapped using Semmes-Weinsten von Frey monofilaments (Stoelting, Wood Dale, IL). The lowest threshold von Frey monofilament that could

elicit a PSDC neuron response in more than 50% of the test trials was used in the RF mapping procedure. A similar procedure was carried out in the cuneate nucleus, relying on the clear mediolateral somatotopy of this structure in the raccoon to locate cuneate neurons having RFs overlapping those of the isolated spinal cord neuron (Johnson et. al., 1968). For each neuron recorded, a RF map was drawn on a scaled representation of the raccoon paw. The RF area was then calculated using a two-dimensional calibrated grid that could be placed over the RF drawing. The percentage of RF overlap was calculated using the formula:

$$\frac{\text{(RF area common to both neurons)}}{\text{(PSDC area + cuneate neuron area) – (area common to both neurons)}} \times 100$$

In the cases where the cuneate neuron RF was totally contained within the PSDC neuron RF (or vice versa), the formula was not used and the PSDC-cuneate neuron pair was considered to have a 100% RF overlap.

Once the spinal cord-cuneate neuron pair were identified, their responses to electrical stimulation of the overlapping RF were tested. Electrical stimulation of the digits was accomplished via two Teflon-coated stainless steel wires (0.003 in) inserted subcutaneously into the center of the overlapping region of the RFs. The times of the stimuli were stored on a microcomputer using the DataWave A/D and software package (Thornton, CO). Activity was sampled at 40 kHz in trials that were 250 ms in duration with the stimulus delivered at 50 ms. The timing of individual spikes was measured with 0.1-ms resolution.

A Master-8 stimulator was used to deliver a 0.2-ms constant-current pulse to the digit every 2 s. In each trial responses of the neuron pair to digit stimulation at

1000 μA were alternated with recordings of spontaneous discharge. At least 100 trials were recorded for each neuron pair using this stimulation paradigm.

2.1.3 Histology

At the termination of each experiment, the animal was transcardially perfused with 1500ml of 0.9% NaCl followed by 1500ml 4% paraformaldehyde in 0.1M phosphate-buffered saline (PBS). The spinal cord was removed, postfixed overnight, and then placed in a cryoprotective 30% sucrose solution in 0.1 PBS at 4°C. Blocks of tissue were cut in 50μm-thick sections through the spinal cord region containing the recording sites using a freezing microtome. Free-floating sections were placed in 0.1 PBS and serial sections were mounted, air dried and stained with cresyl violet. The slides were then coverslipped in preparation for examination using light microscopy.

2.1.4 Data analysis

The data analysis used here was the same as described by Northgrave and Rasmusson (1996). Briefly, all data were analyzed off-line using the DataWave software. Digitized waveforms were examined to confirm neuronal isolation and to remove any spurious signals. Spontaneous firing rates were calculated from the trial periods without stimulation. The presence of an excitatory response to stimulation was determined from the peristimulus time histogram (PSTH), and the first 1-msec bin above background was used to define the start of a 10-msec window. The latency of the first spike within this window was determined for each trial. The mean latencies of the first spike were calculated from multiple trials. The probability of a response, P(r),

was defined as the proportion of trials containing at least one action potential within the 10-msec window. Threshold was defined as the lowest level of electrical stimulation that produced a response in greater than 50% of the trials. All values except thresholds were determined at 1000 μA stimulation.

Most comparisons between groups were made by means of the paired or unpaired Student's *t* test and by repeated measures ANOVA. The chi-square test was also used. The α level used to determine statistical significance was 0.05.

2.2 Experiment 2: Correlation between PSDC and cuneate neuron activity

2.2.1 Cross-correlation analysis

Antidromically identified PSDC neurons were included in the cross-correlation analysis if they had a RF located on glabrous skin of a digit and/or palmar region, responded to mechanical stimulation of the RF and responded to electrical stimulation of the RF in greater than 50% of the trials. Cuneate neurons were included if they were located in the digit cluster region, had a RF on the same or an adjacent digit as the paired PSDC neuron and responded to electrical stimulation in greater than 50% of the stimulation trials. Simultaneously recorded pairs of PSDC and cuneate neurons were assessed for temporal interactions using cross-correlation techniques that have been described previously (Alloway et al. 1993; Gochin et al. 1989; Perkel et al. 1967). Raw cross-correlograms (CCGs) were constructed to display the temporal probability that a cuneate neuron (target event) would fire as a function of a PSDC neuron spike (reference event) at time zero (Alloway et al. 1993). To remove the

effects of the stimulus, a linear shift-predictor was subtracted from the raw CCG, resulting in the neural CCG that was used for analytical purposes. The shift predictor was constructed by averaging 5 raw CCGs produced by pairing the reference event with target events shifted by 1, 2, 3, 4 and 5 stimulus intervals. Correlations between the stimulus and events in the PSDC and cuneate neurons are preserved in the shifted CCG but inter-neuronal interactions (i.e. between the PSDC and cuneate neuron pair) are destroyed because they are thought to occur at a much shorter time course. Therefore, when the shifted CCG is subtracted from the raw CCG, what is left are inter-neuronal interactions and not those resulting from stimulus effects. The shift predictor was further smoothed using a 3 bin boxcar and subtracted from the raw CCG to produce the 'neural CCG'. The smoothed shift predictor was used to estimate the 95% confidence intervals by taking the square root of each bin value and multiplying it by 1.96 (Aertsen et al. 1989, Alloway et al 1993, Gochin et al. 1989). The neural CCG was broken down into quadrants as defined by perpendicular lines through the zero values of the ordinate and abscissa. Each of the four quadrants represented a possible type of neural interaction and was analyzed within ±50 ms of the reference spinal cord event. Neural interactions were considered to be statistically significant if they had three or more contiguous 1 ms bins that exceeded the 95% confidence limits. Using these criteria, one would expect 5 bins to exceed the 95% confidence limits purely by chance within the 100 ms time window used in the cross-correlation analysis. Following this argument, in the 50 ms to the right of zero (i.e. in the 'forward' direction), one would expect 2.5 bins to exceed the confidence limits by chance (i.e. a probability of 0.025). Therefore, the probability that three contiguous

bins would be incorrectly assumed to be statistically significant would be 0.025 x 0.025 x 0.025 = 0.000016.

The presence of a statistically significant interaction in quadrant I (upper right) of the neural CCG would indicate an *excitatory* interaction with the cuneate neuron firing at times *after* the PSDC spike at time zero. An interaction in quadrant II (upper left) would indicate an *excitatory* interaction with the cuneate neuron firing at times *before* the PSDC neuron spike at time zero. In quadrant III (lower left), an interaction would indicate the occurrence of an *inhibitory* interaction with the cuneate neuron stopping firing at times *before* the PSDC neuron at time zero. Finally, an interaction in quadrant IV (lower right) of the neural CCG would signify an *inhibitory* interaction in which the cuneate neuron stops firing at times *after* the PSDC event at time zero. Figure 1 shows the type of interaction that can occur between PSDC and cuneate neurons in each of the four quadrants.

To estimate the functional strength or efficacy of interactions between PSDC and cuneate neuron pairs, single event and peak connection strengths were determined (Aertsen et al. 1989; Alloway et al. 1993; Levick et al. 1972). To estimate the effectiveness of a PSDC neuron in evoking a single cuneate discharge, the number of interactions in the peak bin and its highest contiguous neighbor was divided by the sum by the total number of reference events (PSDC spikes). This ratio was called the single-event connection strength (C_{single}) because based on their interspike interval (ISI), cuneate neurons are not expected to discharge more than once during a 2 ms time interval. Peaks and valleys in the neural CCG were often greater than 2 ms in

Fig. 1. Diagram indicating how a significant interaction within each of the four quadrants would best be interpreted. A spinocuneate interaction means that the PSDC neuron firing is influencing the cuneate neuron firing. A cuneospinal interaction means that the cuneate neuron firing is influencing the PSDC neuron firing. An excitatory interaction means that the probability of firing of the second neuron is increased following the firing of the first (or influential) neuron. An inhibitory interaction means that the probability of firing of the second neuron is decreased following the firing of the first neuron.

QUADRANT II:	QUADRANT I:
Excitatory Cuneospinal Interactions	Excitatory Spinocuneate Interactions
QUADRANT III:	QUADRANT IV:
Inhibitory Cuneospinal Interactions	Inhibitory Spinocuneate Interactions

Figure 1

width and peak connection strength was also calculated to estimate the maximum strength of connection between a PSDC and cuneate neuron pair. The peak connection strength (C_{peak}) was calculated by summing all contiguous significant interactions in the largest significant peak and dividing by the total number of PSDC reference events. Because two or more significant bins are used in the estimation of C_{peak}, it is important to note that more than one cuneate event could occur, yielding a result above a unitary value (Alloway et al. 1993).

2.2.2 Frequency response analysis

Cross-correlation measurements are inherently contaminated by the auto-correlation of the input signal. Frequency response measurements avoid this problem by dividing the cross-spectrum by the input power spectrum (Bendat and Piersol, 1980). Therefore spike trains of neuron pairs with significant interactions in the time domain (i.e. significant neural CCGs) were further analyzed in the frequency domain. This analysis was performed to substantiate results obtained from the time based cross-correlation analysis. Using frequency response analysis, it was also possible to test for linearity in the PSDC-cuneate neural interactions using the coherence function. In essence, the frequency response analysis served to corroborate evidence for neural interactions detected in the time domain.

Using specialized software (ASF Software, Halifax, Canada) the frequency responses of cuneate neurons (system output) were measured as functions of PSDC neuron input. The simultaneously recorded spike trains were each separately filtered

by convolution with the sin(x)/x function to band-limit them to 0-100 Hz (French and Holden 1971). The convolved signals were then re-sampled to give equally spaced points in time that could be transformed into the frequency domain using the fast Fourier transform (FFT) (Cooley and Tukey 1965). The PSDC signal was treated as the input and the cuneate spike train treated as the output of the system. The frequency response of the output with respect to the input PSDC signal was analyzed and represented by a Bode plot of gain and phase vs. frequency. The coherence between the input and output signals was calculated and used to assess the linearity of the relationship between the PSDC neuron input and the cuneate neuron output.

2.3 Experiment 3: Temporary deafferentation of on-focus digit

2.3.1 Temporary deafferentation

After normal responses of PSDC neurons had been characterized, the on-focus digit (i.e. the digit containing the RF) was temporarily deafferented by injecting approximately 0.2 ml of lidocaine hydrochloride (Xylocaine 2%; Astra, Mississauga, Ontario) into the ulnar and radial sides of the digit. A 30-gauge needle was inserted deeply into the base of the digit and then slowly withdrawn as the lidocaine was injected. The response of the isolated PSDC neuron to mechanical RF stimulation was monitored frequently following lidocaine injection to determine the time during which afferent input from the on-focus digit was completely blocked. Responses to electrical stimulation of both on- and off-focus digits and spontaneous activity were continuously recorded during deafferentation.

Chapter 3: RESULTS - Experiment 1

3.1 Identification of PSDC neurons

A total of 102 cells in the spinal cord dorsal horn satisfied the criteria used for antidromic identification of PSDC neurons. The antidromically identified PSDC neurons represented approximately 2/3 of the total number of neurons tested. In 27 of the 102 neurons studied, the response latency to antidromic stimulation was measured and the conduction velocity along the dorsal columns was calculated. The mean antidromic latency of PSDC neurons was found to be 3.4 (±0.7 s.d.) ms and the mean conduction velocity along the dorsal columns was calculated to be 16.8 (±3.5) m/s (range 9-23 m/s) (Fig. 2). The mean conduction velocity indicates that PSDC axons in the cervical enlargement are myelinated and have a small to medium diameter, similar to Aδ fibers in the periphery.

Within the cervical enlargement and between 1000-3000 μm from midline, there was approximately a 50% chance of finding at least one PSDC neuron per penetration. The probability of finding a PSDC neuron in the raccoon cervical enlargement may have been underestimated in this study because, when searching for these neurons, mechanical stimuli were applied almost exclusively to glabrous skin on the forepaw digits and palm. It is likely that PSDC neurons responding to stimulation of forepaw hairy skin, which covers the sides and dorsal surface of the digits and palm, were not included or tested for antidromicity as a result of the search methods employed here.

Fig. 2. A histogram of the conduction velocities for 27 PSDC neurons. The approximate distance between the stimulating and recording electrodes was measured on the surface of the spinal cord. This distance was divided by the antidromic latency obtained from the oscilloscope. The conduction velocities had a mean of 16.8 (±3.5) m/s (range 9-23 m/s).

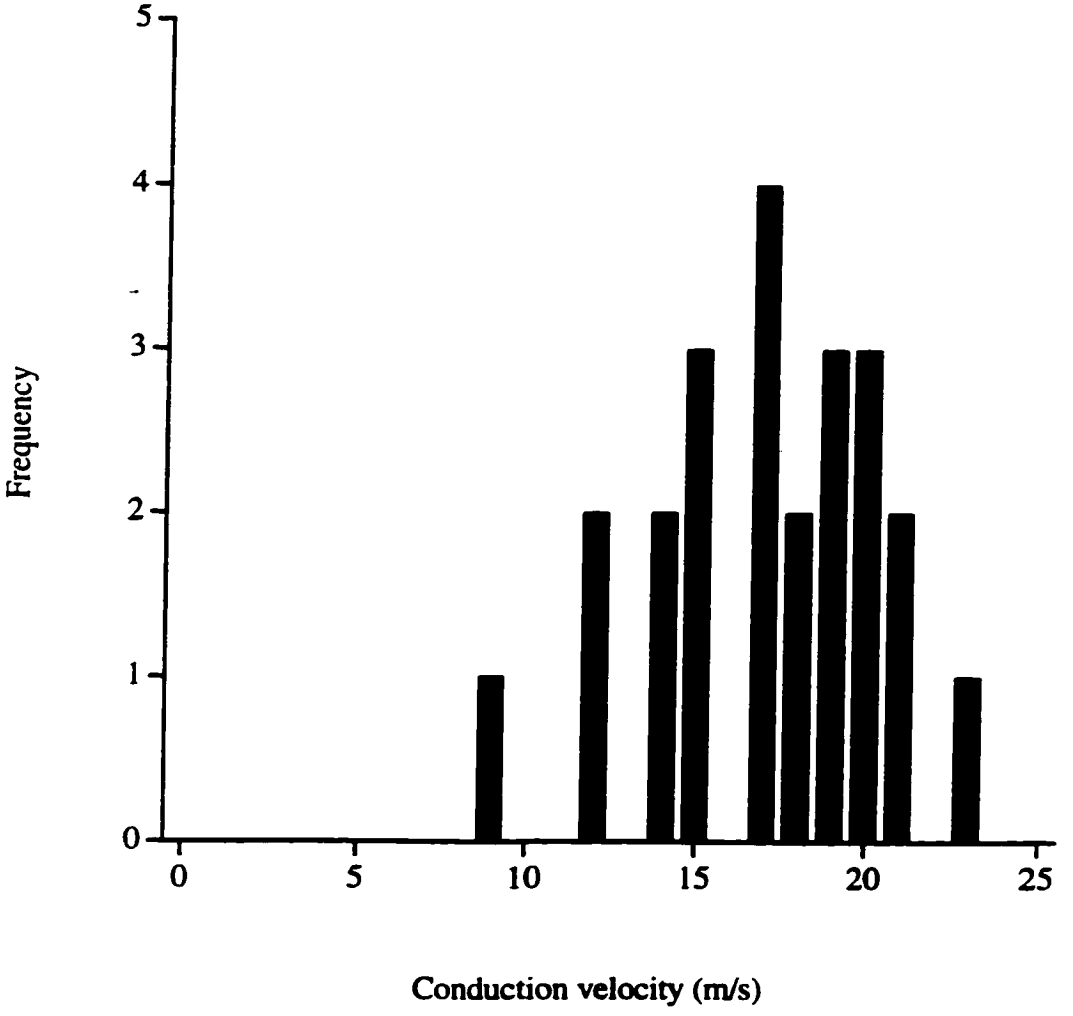

Figure 2

3.2 Somatotopic organization of PSDC neurons in the cervical enlargement

The PSDC neurons studied were located in segments C5-T1 of the spinal cord dorsal horn. Post-experiment visualization of electrode penetrations and/or related tissue damage made it possible to estimate the position of recording sites within the dorsal horn for approximately 30 cells. Figure 3A shows an example of the histology from one animal with four penetrations passing into the dorsal horn and Figure 3B is a representative drawing of the raccoon dorsal horn showing the location of Rexed's laminae (Rexed, 1954). PSDC neurons were organized somatotopically with digit 1 represented in the most rostral location and digits 2-5 represented in progressively more caudal locations within the cervical enlargement. PSDC neurons with RFs on digit 5 were consistently found at recordings sites at the level between where the C8 and T1 dorsal roots could be seen entering the spinal cord. PSDC neurons with RFs on digit 4 were generally located at or near the level between where C7 and C8 dorsal roots entered the spinal cord. It is not possible to comment accurately on the dermatomal organization of digits one to three because fewer PSDC neurons were recorded in more rostral regions of the cervical enlargement. Figure 4 is a drawing of the surface of the spinal cord showing the location of all penetrations in one representative animal labeled according to the RFs of the PSDC neurons. As can be seen in Figure 4, the representation of a single digit within the cervical enlargement extended from 3000-6000 μm along the rostrocaudal axis. In regions of the spinal

Fig. 3. Coronal view of the dorsal horn. A: Photomicrograph of a 50 μm thick coronal section taken through the cervical enlargement at the level between where C7 and C8 dorsal roots entered the spinal cord. On the right is shown the tissue damage associated with three penetrations passing through the dorsal horn (labeled 1, 2 and 3). Penetration 1 extended to 1900 μm and penetrations 2 and 3 extended to 2000 μm. In penetration 2, a PSDC neuron was recorded with a receptive field on the distal portion of digit three. By comparing the size and distribution of cells in the dorsal horn with the descriptions of Rexed (1954) in cat, it is possible to estimate the lamina to which the electrode penetrated in the dorsal horn. It is estimated that the electrode penetrations in this example extend into Rexed's lamina III and/or IV. B: A drawing of the approximate location of Rexed's layers at this level of the raccoon spinal cord (Rexed, 1954).

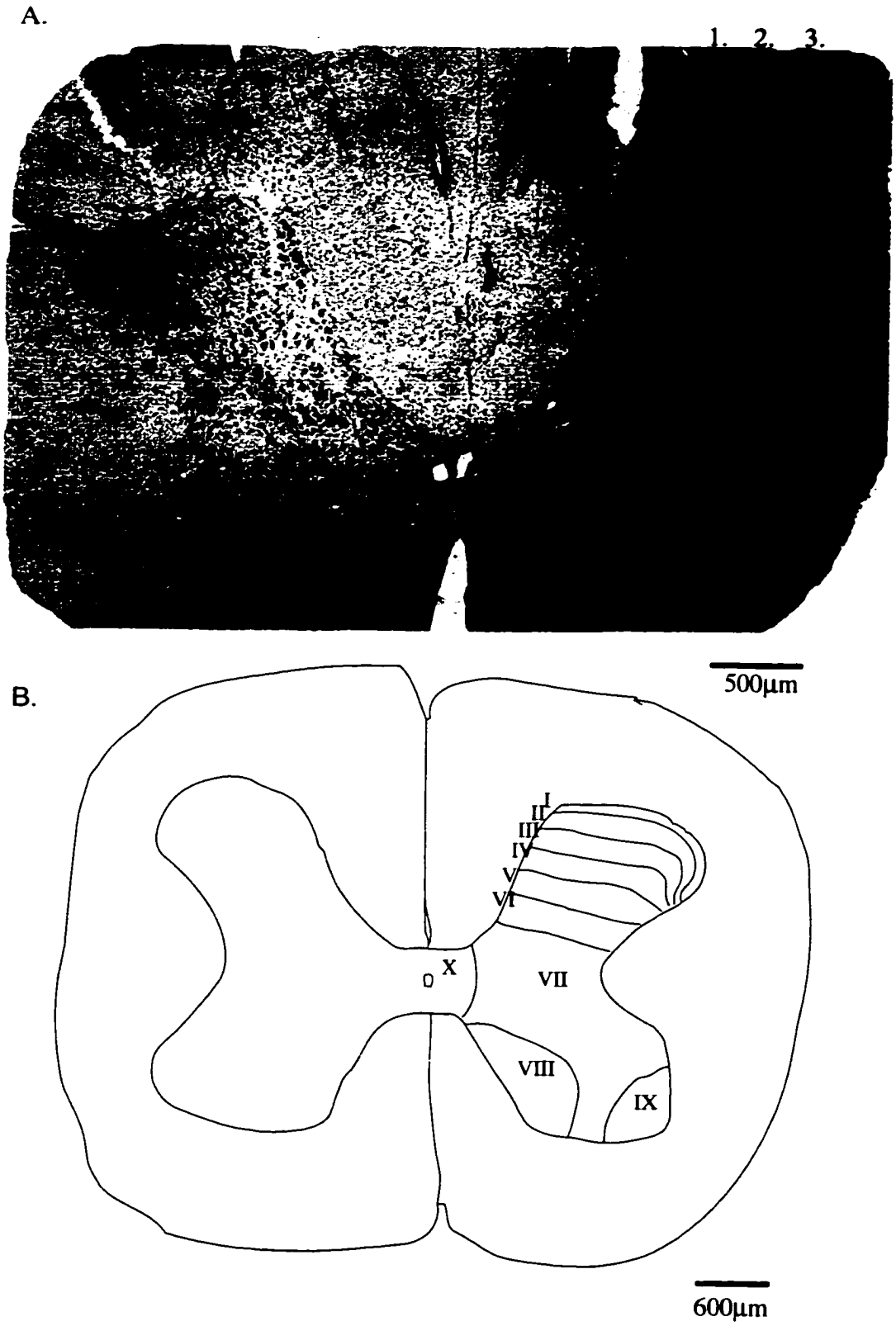

Figure 3

Fig. 4. Location of all PSDC neurons recorded in one representative animal. The inset shows a representation of the raccoon forepaw with the digits and palmar regions labeled. The rostrocaudal organization of PSDC neurons follows a dermatomal pattern, with digit 5 represented at the level of entry of the C8 and T1 dorsal roots. PSDC neurons with RFs on digits 3 and 4 are located between the level of C7 and C8. With respect to the mediolateral organization, PSDC neurons with RFs on the pads were generally found medial to cells with RFs on the digits. Where representative letters and/or numbers are immediately atop one another in the diagram, the upper character indicates the location of the RF of the most superficial neuron within a penetration and the lower character indicates the RF location of the second and deeper neuron in the same penetration. Note that the neuron with the RF on the forearm (labeled FAr) was not antidromically identified as a PSDC neuron. FA = forearm; D = pad D; E = pad E; 3 = digit 3; 4 = digit 4; 5 = digit 5; d = distal; p = proximal; r = radial; u = ulnar.

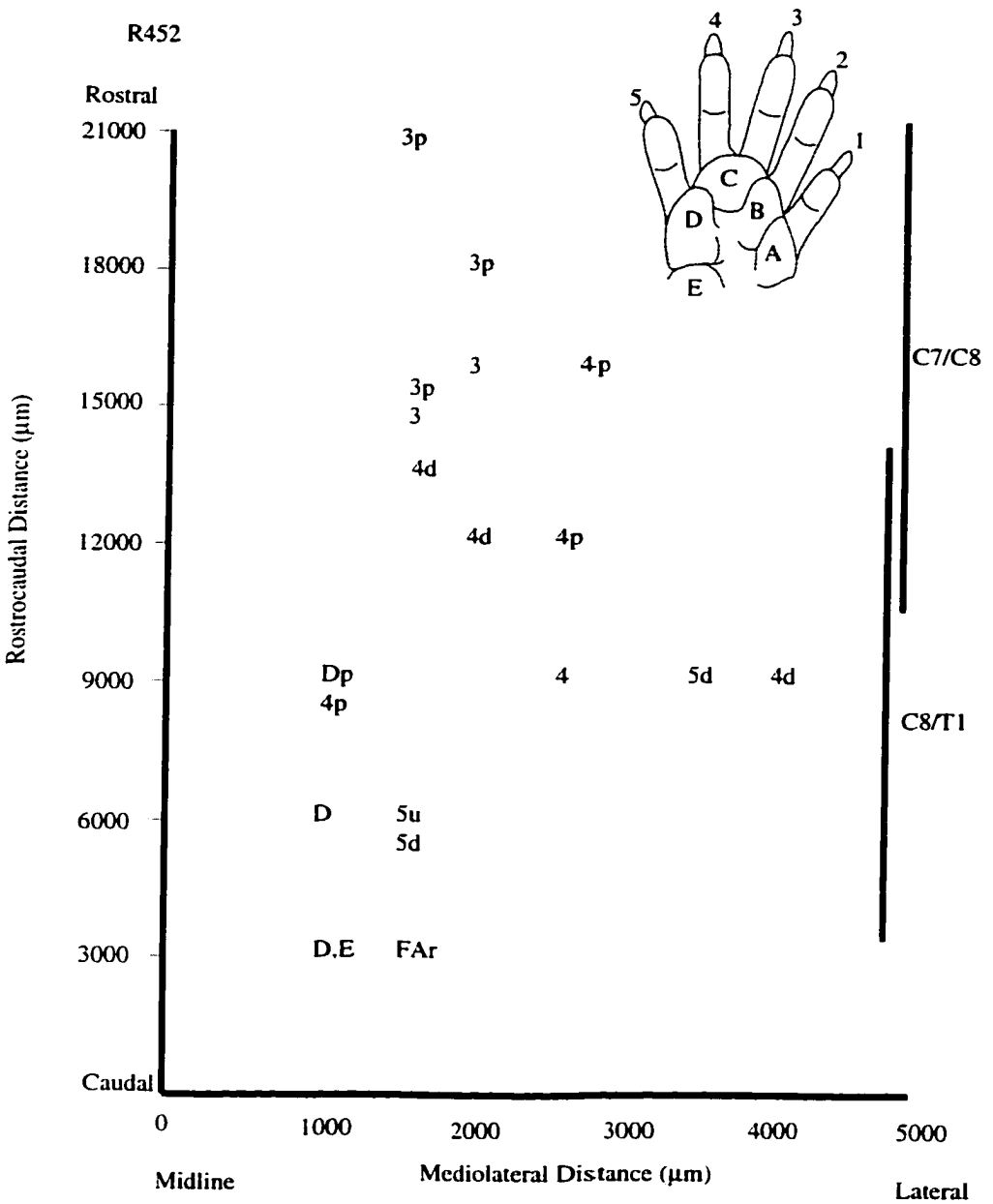
R452
Rostral
21000
18000
15000
12000
9000
6000
3000
Caudal
Rostrocaudal Distance (µm)
3p
3p
3
4p
3p
3
4d
4d
4p
Dp
4p
4
5d
4d
D
5u
5d
D,E
FAr
4
3
2
1
5
A
B
C
D
E
C7/C8
C8/T1
0
1000
2000
3000
4000
5000
Midline
Mediolateral Distance (µm)
Lateral

Figure 4

cord caudal to the digit representations, neurons with RFs on the hairy skin of the forearm were found but these were not identified as PSDC neurons.

A mediolateral organization of raccoon PSDC neurons could be observed for the paw representation, which extended from 1000 μm to 4000 μm lateral to midline. PSDC neurons with digit RFs were found along the entire mediolateral extent of the paw representation but neurons with RFs on the pads of the palm were generally restricted to more medial regions (Fig. 4). However, in some penetrations, the digit and palm representations were intermingled. PSDC neurons were most commonly found at depths of between 1500-3000 μm. In penetrations where more than one PSDC neuron was found, cells with RFs on the palm were generally found superficial to cells with RFs on the digit, although this was not true in approximately 20% of the cases. The distance between successive PSDC neurons within the same penetration was usually between 100-500 μm, and it was often the case that only one PSDC neuron could be found per penetration. The mean depth of PSDC neurons with RFs on distal regions of the digit (1821.9 ±455.6 μm, range 1100-3200 μm) was not significantly different than that of PSDC neurons with RFs on proximal regions of the digit and/or palm (1790.8 ±421.3 μm, range 1010-3100 μm, $t=0.4$, $df=89$, $p>0.05$). Figure 5 is a scatter plot of depth versus mediolateral location of all PSDC neurons recorded in this study. PSDC neurons were never found at depths more superficial than 1010 μm and were never found closer than 1000 μm from the midline. PSDC neurons with RFs on the digits were generally found deeper and more lateral to those with RFs on the palm.

Fig. 5. Depth and mediolateral location of all PSDC neurons recorded at all levels of the cervical enlargement. There was no significant difference in the depth of neurons with RFs on distal vs. proximal regions of the forepaw. PSDC neurons with RFs on the palm were generally found medial to those with RFs on the digits. Note that the vertical axis was expanded to facilitate visualization of neurons that were located at similar depths. Also note that neurons with RFs on the palm were found medial to cells with RFs on the digits.

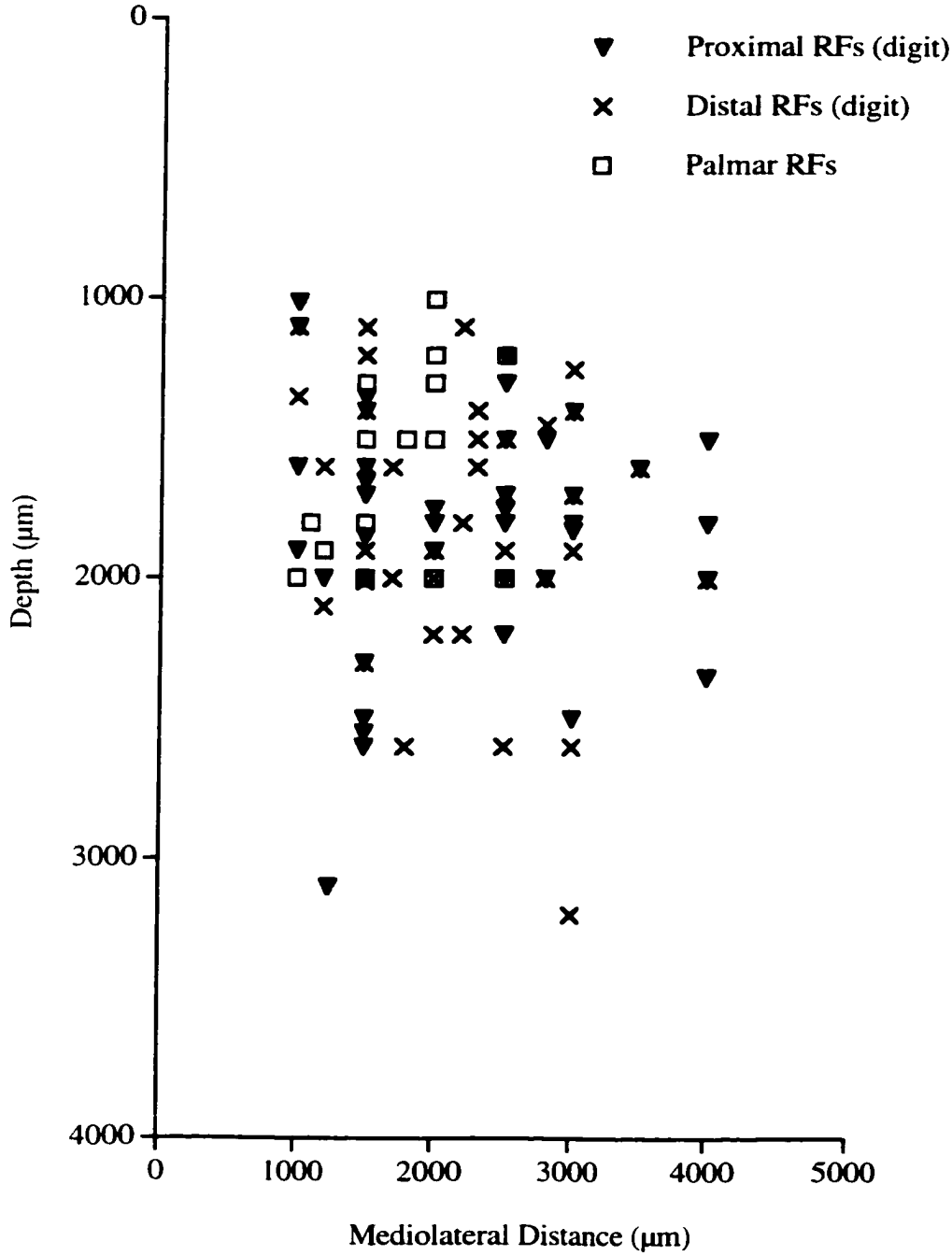
Proximal RFs (digit)
Distal RFs (digit)
Palmar RFs
Depth (μm)
0
1000
2000
3000
4000
0
1000
2000
3000
4000
5000
Mediolateral Distance (μm)

Figure 5

3.3 Receptive fields of PSDC neurons

All of the PSDC neurons studied had RFs on glabrous skin regions of the forepaw digits and/or palm. In 29 representative cases, the RF size was carefully measured using the lowest caliber von Frey monofilament that exceeded the neuron's firing threshold on more than 50% of the test trials. Using this criterion, the RFs had a mean area of 9.4 (±4.2) mm^2. Fig. 6A shows the distribution of RF areas for these PSDC neurons. The average size of RFs on distal regions of the digit (e.g. Fig. 7A) (8.8 ±3.4 mm^2, range 3.8-18.7 mm^2) was not significantly different than on proximal regions of the digit (e.g. Fig. 7B) or on the palm (mean 11.1 ±5.8 mm^2, range 5.1-24.5 mm^2, $t=1.7$, $df=27$, $p>0.05$). The majority of qualitatively studied PSDC RFs (99 of 102) were confined to a single digit. In only two of 102 cases, the RF extended onto the palm and base of an adjacent digit (e.g. Fig. 7C) and in another case, the RF was split and included discrete distal regions of two adjacent digits (e.g. Fig. 7D). All of the PSDC neurons examined (n=102) had excitatory RFs with no discernable inhibitory regions within or surrounding the RF border. However, the presence of inhibitory regions was difficult to assess in PSDC neurons because of their low spontaneous rate. Furthermore, the PSDC neurons in this study were not brought to supra-threshold levels of excitation for the express purpose of testing for inhibitory RFs. Therefore, it is possible that inhibitory RFs or inhibitory regions in association with excitatory RFs exist in raccoon but were not detected using the current methodology. The majority of PSDC RFs consisted of a uniform low-threshold region that was delineated by a sharply defined edge; however some cells (<30%) had RFs

Fig. 6. RF areas of 29 representative PSDC and cuneate neurons. The mean and range of RF areas was greater for PSDC neurons than for cuneate neurons. The largest PSDC neuron RF (25 mm^2) was almost twice the size of the largest cuneate neuron RF (13 mm^2) in the sample.

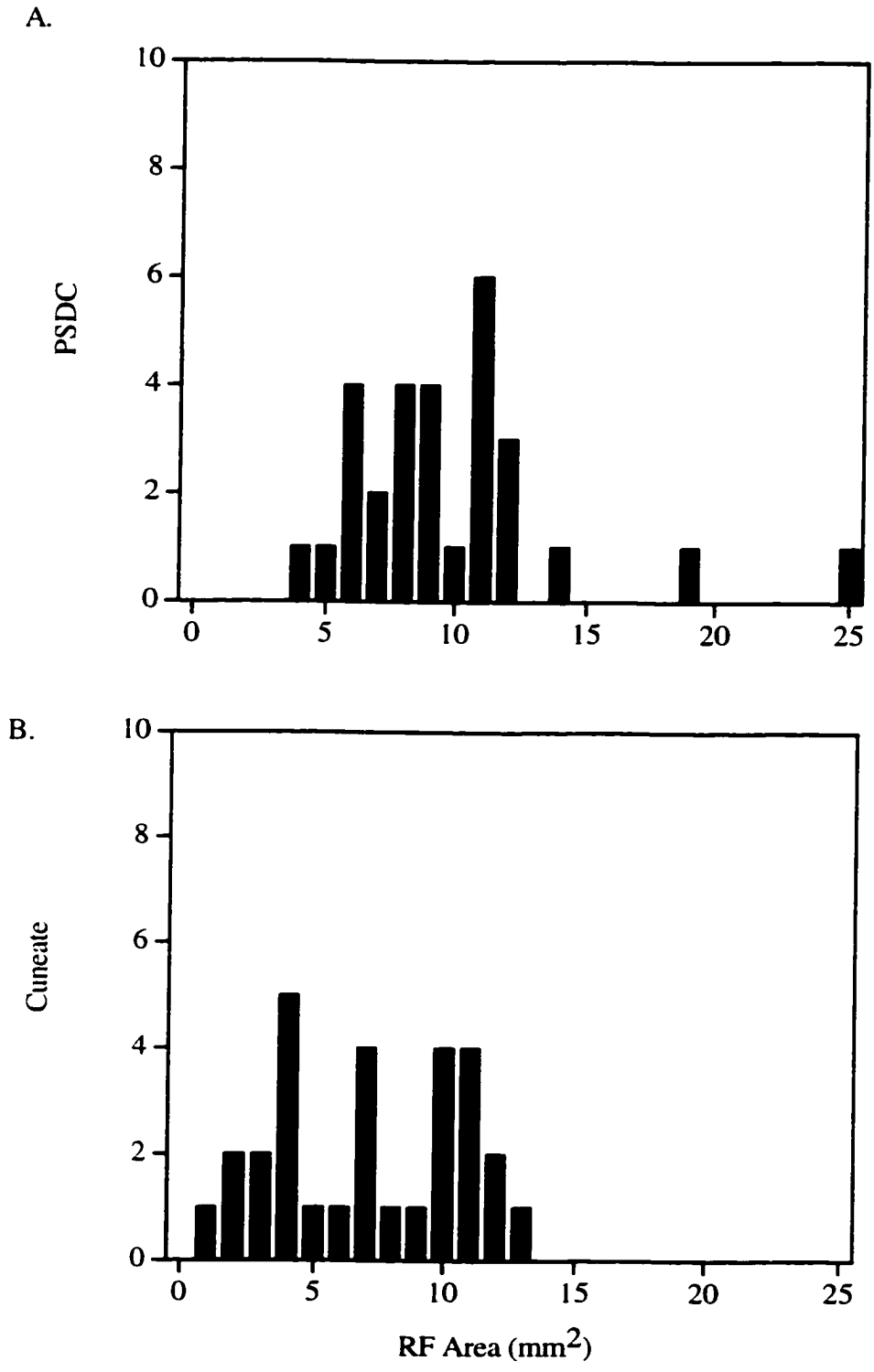
A.
PSDC
10
8
6
4
2
0
0
5
10
15
20
25
B.
Cuneate
10
8
6
4
2
0
0
5
10
15
20
25
RF Area (mm2)

Figure 6

Fig. 7. A-D: Representative drawings of four types of PSDC neuron RFs on glabrous skin of the forepaw. A: A small, well-delineated RF (solid shading) confined to the distal portion of a single digit. B: A larger, well-delineated RF located proximally on the digit. C: A large, proximal RF that has a small low-threshold region and a larger 'subliminal fringe' (hatched shading) of higher threshold that extended onto the palm and an adjacent digit. This type of RF was rare, seen in only two of 102 cases. D: A RF that is divided into two well-delineated regions on adjacent digits. This type of receptive field was also rare, occurring in only one of 102 cases.

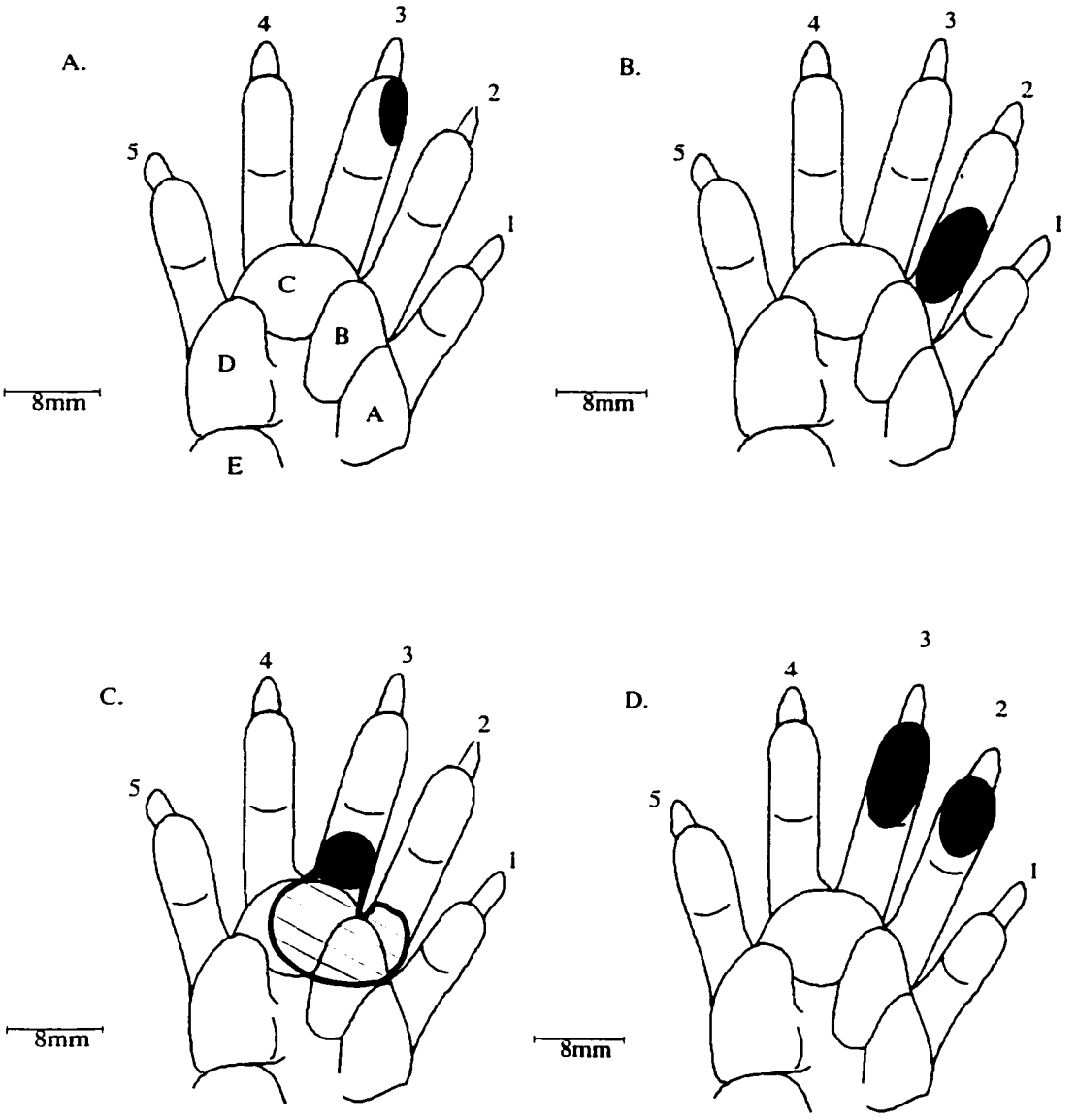

Figure 7

with low threshold centers and a contiguous subliminal fringe (i.e. region of higher threshold). The subliminal fringe was always found to be larger than the low threshold region and could be excited only by mechanical stimulation with a glass probe.

3.4 Response of PSDC neurons to on-focus stimulation

The PSDC neurons responded reliably to mechanical stimulation of the on-focus digit. The median threshold of response to mechanical stimulation (von Frey hair) was 0.2 grams (range 0.1-13.7 grams, n=61) (Fig. 8). In all cases (102/102) the PSDC neurons adapted rapidly to sustained mechanical stimulation of the RF. The PSDC neurons responded reliably to electrical stimulation (1000 μA) of the on-focus digit with a mean latency of 8.2 (±1.1) ms. The mean probability of response was 96% and the mean threshold of response to on-focus electrical RF stimulation was 306.7 μA. Figure 9 shows the electrical threshold of PSDC neurons in response to electrical RF stimulation. In all cases (102/102), the PSDC neurons responded to stimulation of the RF with a burst of action potentials (mean 6 spikes/30 ms) which, in 25% of the test cases (15/60), was followed by a brief period of inhibition which lasted approximately 50-100 ms (e.g. Fig. 10A). The mean inter-spike interval (ISI) of PSDC neurons in response to electrical stimulation of the on-focus digit was 1.6 ms. A summary of PSDC neuron activity in response to electrical stimulation of the on- and off-focus digits and during spontaneous discharge is shown in Table 1A.

Fig. 8. Histogram showing the distribution of mechanical thresholds for 61 representative PSDC neurons. Von Frey monofilaments of different caliber were used to mechanically stimulate the PSDC neuron RFs. For each cell, the force (g) of the lowest caliber von Frey monofilament that could elicit a response in greater than 50% of the test trials was considered to be the mechanical threshold. The majority of PSDC neurons tested (72%) had low thresholds of between 0.1 and 0.5 grams (median 0.5 grams).

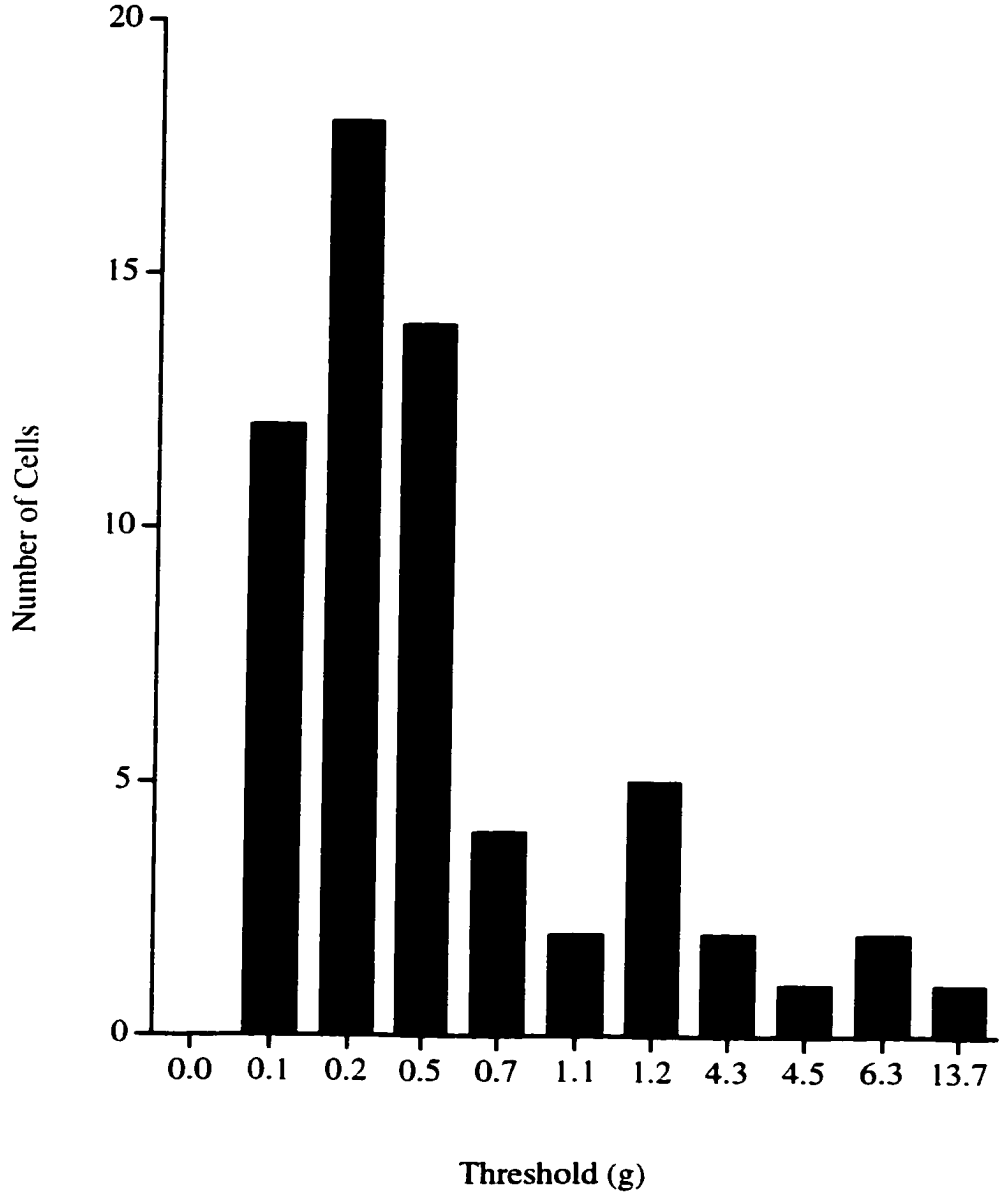
20
15
10
5
0
Number of Cells
0.0
0.1
0.2
0.5
0.7
1.1
1.2
4.3
4.5
6.3
13.7
Threshold (g)

Figure 8

Fig. 9. Graph showing the thresholds for electrical stimulation of the on- and off-focus digits for both PSDC and cuneate neurons. A,C: Distribution of PSDC neuron thresholds for electrical stimulation of the on- and off-focus digits, respectively. The mean threshold for off-focus stimulation (553.3 μA) was significantly higher than that for on-focus stimulation (306.7μA, ANOVA, $p<0.001$). B,D: Cuneate neuron thresholds for electrical stimulation of the on- and off-focus digits, respectively. As in PSDC neurons, the mean threshold for off-focus stimulation in cuneate neurons (797.8 μA) was significantly higher than that for on-focus stimulation (391.3 μA, $p<0.001$). The thresholds for both on- and off-focus electrical stimulation were significantly lower for PSDC neurons than cuneate neurons ($p<0.01$).

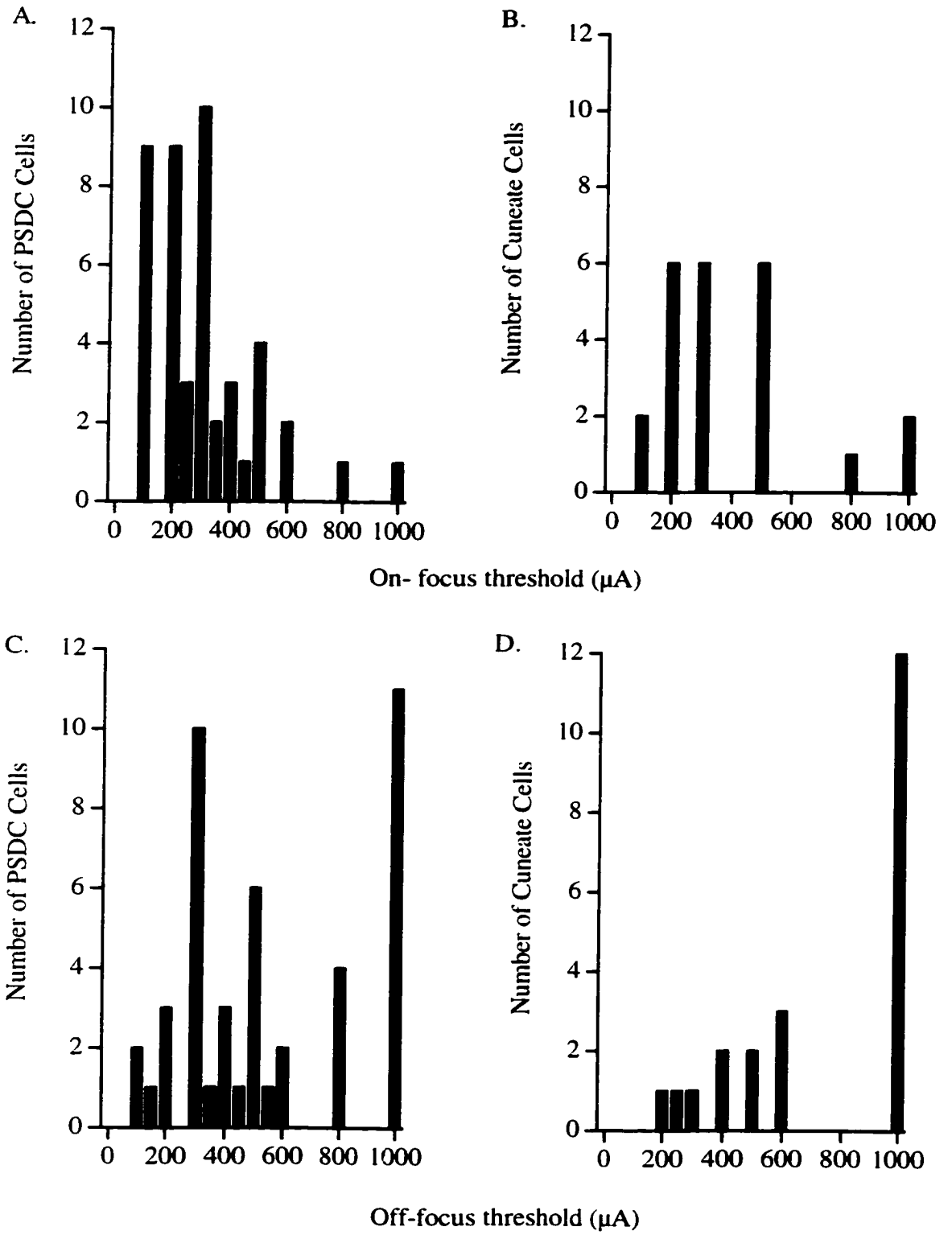
A.
B.
Number of PSDC Cells
Number of Cuneate Cells
0
2
4
6
8
10
12
0 200 400 600 800 1000
On- focus threshold (μA)
C.
D.
Number of PSDC Cells
Number of Cuneate Cells
Off-focus threshold (μA)

Figure 9

Fig. 10. Peristimulus time histograms (PSTHs) and dot rasters for a representative PSDC neuron in response to electrical digit stimulation. A: PSTH (upper) and dot raster (lower) for a PSDC neuron in response to electrical stimulation of the on-focus digit. The neuron responded at a mean latency of 7.6 (±0.6) ms with an average of 3.5 spikes per response. Note the narrow, sharp peak in the PSTH and the tightly aligned dot raster, indicating a consistent stimulus-linked response of the PSDC neuron to on-focus electrical stimulation. B: PSTH (upper) and dot raster (lower) for the same PSDC neuron shown in 10A in response to electrical stimulation of the off-focus digit. The mean latency of response to off-focus stimulation was 8 (±1.6) ms with an average of 1.8 spikes per response. The probability of response to off-focus stimulation (89%) was lower than the probability of response to on-focus stimulation (94%). Note the smaller, wider peak in the PSTH as well as the more sparse and less tightly constrained dot raster, indicating a greater variability in the response to off-focus as compared to on-focus stimulation.

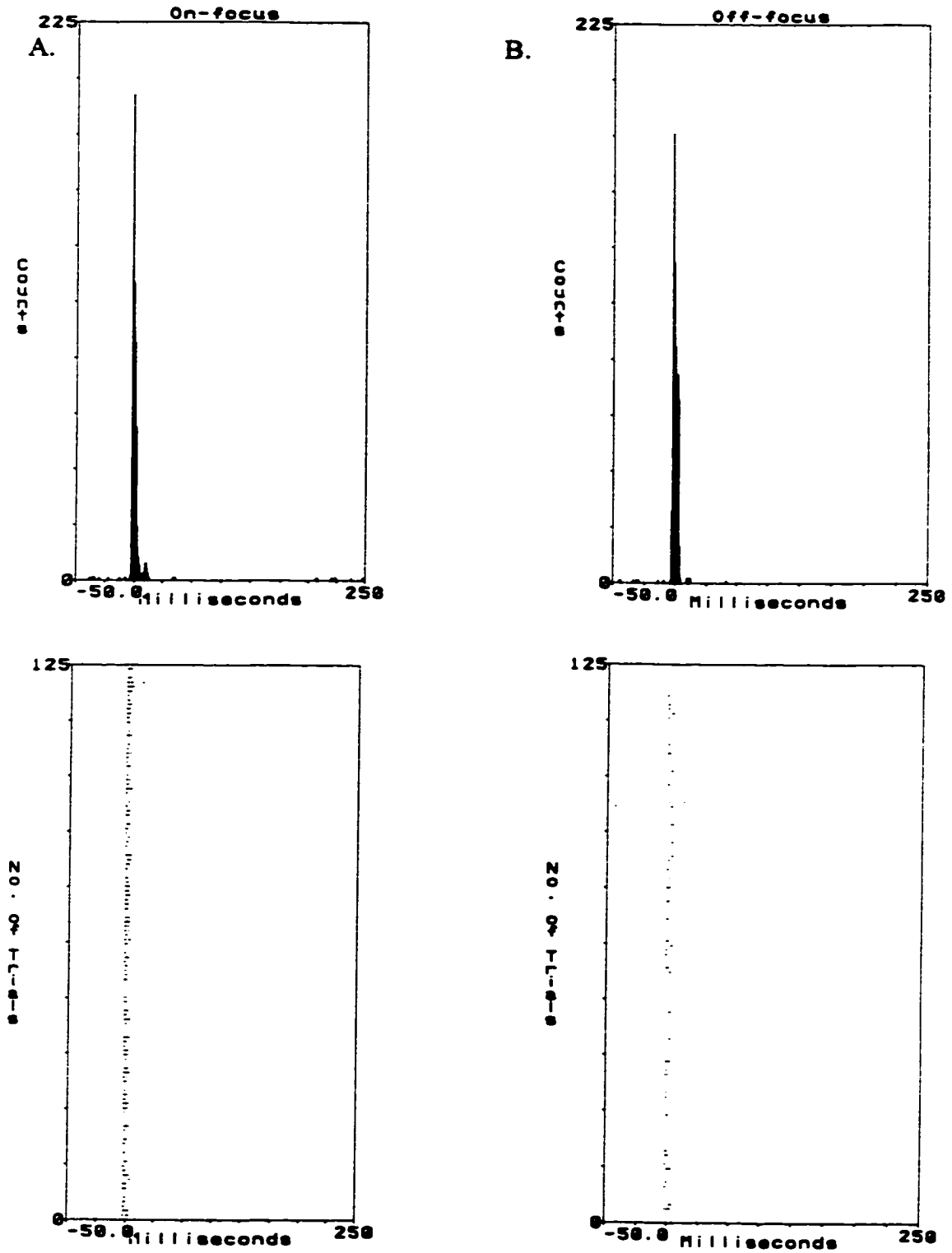
A.
On-focus
225
Counts
0
-50.0
Milliseconds
250
B.
Off-focus
225
Counts
0
-50.0
Milliseconds
250
125
No. of Trials
0
-50.0
Milliseconds
250
125
No. of Trials
0
-50.0
Milliseconds
250

Figure 10

3.5 Response of PSDC neurons to off-focus stimulation

In 96% of the cases, PSDC neurons fired in response to electrical stimulation of the off-focus digit (e.g. Fig. 10B) but at a significantly longer latency (mean 9.9 ms, $F=1.7$, $df=1, 72$, $p<0.001$) than on-focus stimulation (Fig. 11A). In addition, the variability of the off focus response latency (s.d. 2.9 ms) was greater than for on-focus (s.d. 1.1 ms) ($F=9.9$, $df=1, 73$, $p<0.01$) (Fig. 11B). The thresholds for off-focus stimulation (mean 553.3 μA) were significantly higher than those for on-focus digits ($F=46.3$, $df=1, 66$, $p<0.001$) (Figs. 9C and 11C). In addition, the probability of response of PSDC neurons to off-focus stimulation (mean 87%) was found to be significantly lower in comparison to stimulation of the on-focus digit ($F=25.3$, $df=1, 72$, $p<0.001$) (Fig. 11D).

PSDC neurons responded to off-focus stimulation with a burst of action potentials, similar to characteristic burst that followed on-focus digit stimulation (e.g. Fig. 10B). However, there were significantly fewer spikes per burst (mean 4.1 spikes/30 ms, $t=1.7$, $df=50$, $p<0.01$) following off-focus stimulation than on-focus digit stimulation. The mean ISI of PSDC neurons in response to off-focus stimulation (1.9 ms) was significantly longer than for on-focus stimulation ($t=1.7$, $df=73$, $p<0.001$).

3.6 Spontaneous activity of PSDC neurons

In the absence of stimulation PSDC neurons discharged at a mean rate of 7.4 spikes/s (Fig. 12). The spontaneous activity was largely composed of bursts of

Fig. 11. Group means of the response properties of PSDC vs. cuneate neurons to on- and off-focus electrical stimulation. A: Response latency. There was no significant difference between PSDC and cuneate neurons with respect to the latency of response to either on- or off-focus electrical stimulation (ANOVA, $p>0.05$). However, both PSDC and cuneate neuron responses to on-focus stimulation had significantly shorter latencies than their off-focus responses ($p<0.001$). B: Variability in latency of the first spike. There were no differences between PSDC and cuneate neurons ($p>0.05$); however there were significant within group differences between on- vs. off-focus stimulation ($p<0.01$). C: Thresholds for electrical stimulation. PSDC neurons had significantly lower thresholds to both on- and off-focus stimulation than cuneate neurons ($p<0.01$). Thresholds for on-focus stimulation were significantly lower than for off-focus for both PSDC and cuneate neurons ($p<0.001$). D: Response probability. There were no differences between PSDC and cuneate neurons ($p>0.05$). However, the probability of response for on-focus was significantly higher than for off focus ($p<0.001$). Error bars = ±s.d.

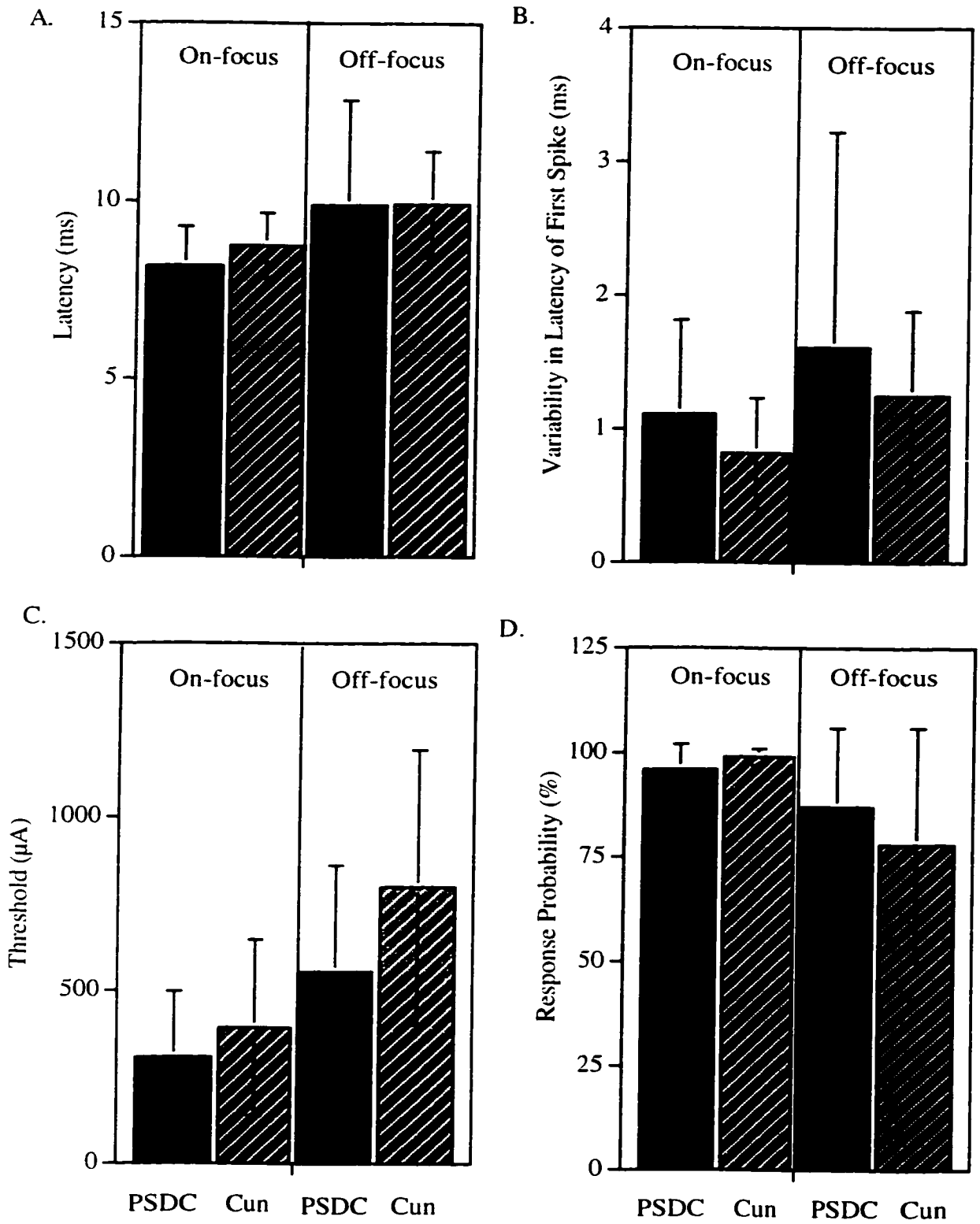
A.
15
10
5
0
Latency (ms)
On-focus
Off-focus
B.
4
3
2
1
0
Variability in Latency of First Spike (ms)
On-focus
Off-focus
C.
1500
1000
500
0
Threshold (μA)
On-focus
Off-focus
PSDC
Cun
PSDC
Cun
D.
125
100
75
50
25
0
Response Probability (%)
On-focus
Off-focus
PSDC
Cun
PSDC
Cun

Figure 11

2-5 spike events separated by irregular time intervals; however single spikes were not uncommon. The mean ISI for the PSDC neurons during spontaneous firing was 2.17 ms and was significantly longer than the ISI following on-focus stimulation ($t=1.7$, $df=75$, $p<0.001$).

3.7 Comparison of cuneate and PSDC response properties

A total of 51 cuneate neurons were simultaneously recorded with PSDC neurons in the present study. There was no statistically significant difference between PSDC and cuneate neurons in the latency of response to on-focus stimulation (mean 8.7, t-test, $p>0.05$) (Fig. 11A). Figure 13 shows a normalized cumulative frequency distribution of the response latencies of PSDC vs. cuneate neurons. This type of graph was used to highlight the similarity between PSDC and cuneate neurons with respect to their latency in response to electrical on-focus digit stimulation. This graph also shows (dashed line) the minimum time at which impulses traveling along PSDC axons would reach the cuneate nucleus assuming a 3 ms conduction time.

Cuneate neurons responded reliably to on-focus stimulation (mean P(r)=99%) with a burst of action potentials (mean 4.5 spikes/30 ms) and an interspike interval (mean 1.6 ms) that were similar to the on-focus response of PSDC neurons (t-test, $p>0.05$). In addition, the mean latency of response to off-focus stimulation was not significantly different for PSDC and cuneate neurons (cuneate: 9.9 ms, ANOVA, $p>0.05$) (Fig. 11A). The variability in the latency of the first spike in response to both on- and off- focus was also similar for PSDC and cuneate neurons (ANOVA, $p>0.05$) (Fig. 11B). Thresholds for on- and off-focus electrical stimulation were significantly

Fig. 12. Histograms showing the spontaneous rate of discharge for PSDC and cuneate neurons. A: Distribution of PSDC neuron spontaneous firing rates. B: Distribution cuneate neuron spontaneous firing rates. Cuneate neurons had more widely distributed and significantly higher rates of spontaneous discharge than PSDC neurons (t-test, $p<0.001$).

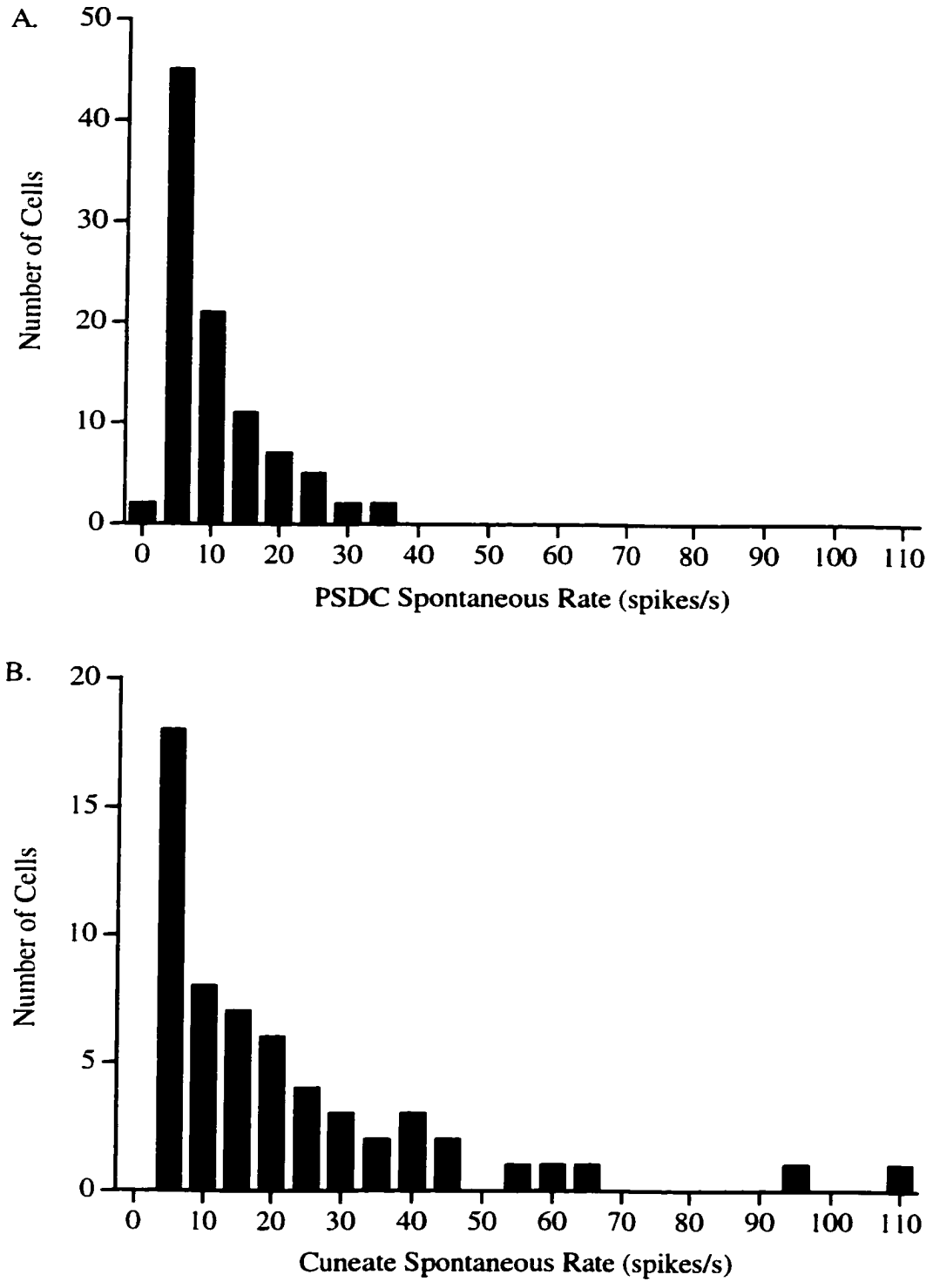
A.
Number of Cells
0
10
20
30
40
50
0 10 20 30 40 50 60 70 80 90 100 110
PSDC Spontaneous Rate (spikes/s)
B.
Number of Cells
0
5
10
15
20
0 10 20 30 40 50 60 70 80 90 100 110
Cuneate Spontaneous Rate (spikes/s)

Figure 12

Fig. 13. Normalized cumulative frequency plot of PSDC vs. cuneate neuron latencies in response to on-focus digit stimulation. Note the similarity in shape between PSDC and cuneate neuron plots. There was no statistically significant difference between the latency of response for PSDC and cuneate neurons (t-test, $p>0.05$). The dashed line shows the minimum latencies at which PSDC neuron action potentials could reach the cuneate nucleus in response to on-focus digit stimulation.

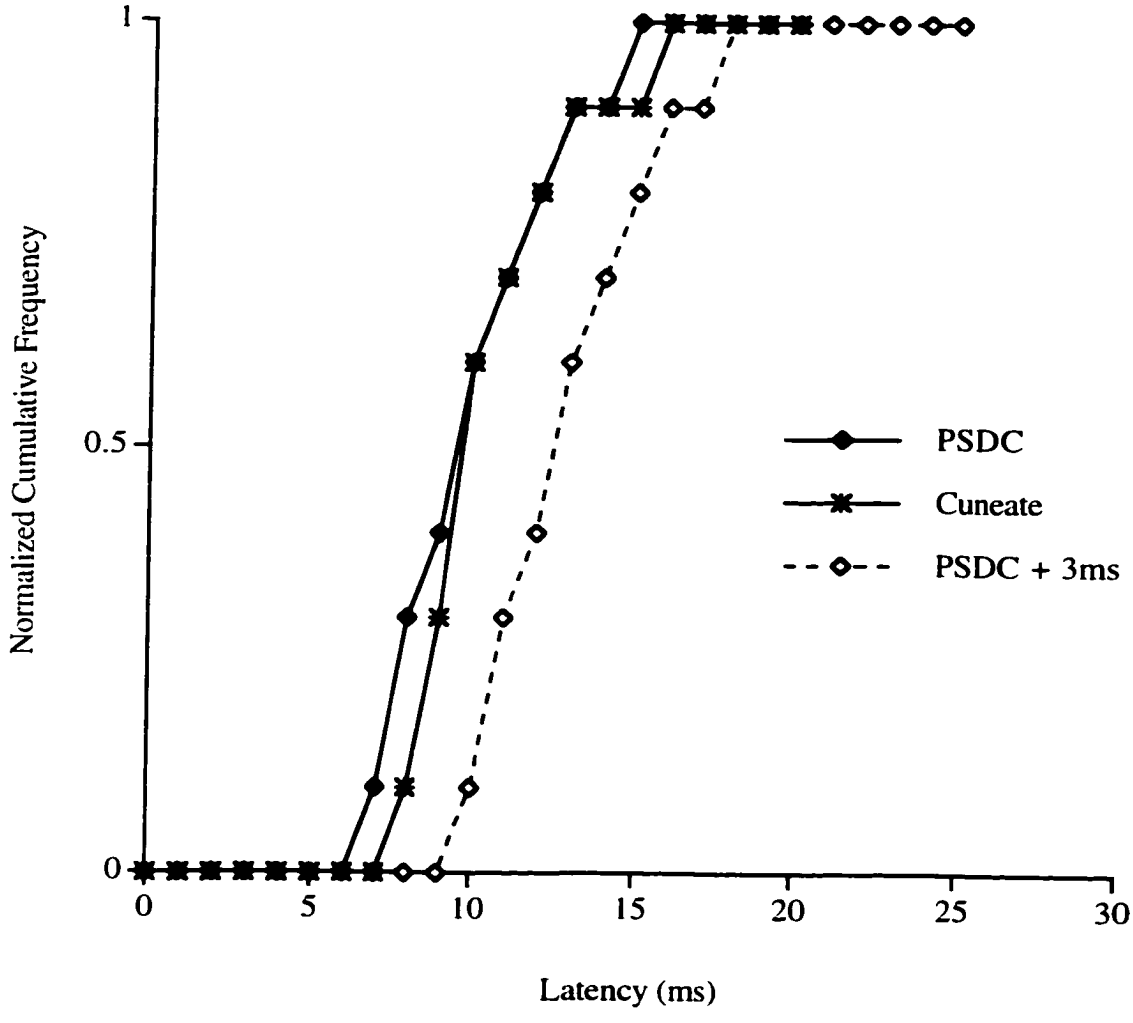
1
0.5
0
Normalized Cumulative Frequency
0
5
10
15
20
25
30
Latency (ms)
PSDC
Cuneate
PSDC + 3ms

Figure 13

higher for cuneate neurons (on-focus: 391.3 μA, off-focus: 797.8 μA, F=9.1, df=1, 66, p<0.01) than for PSDC neurons (Fig. 11C). The probability of response of cuneate neurons to off-focus stimulation (75%) was not statistically different from PSDC neurons (ANOVA, p>0.05) (Fig. 11D). Table 1B shows a summary of cuneate neuron activity in response to electrical stimulation of the on- and off- focus digits and during spontaneous discharge.

3.8 Comparison of PSDC and cuneate neuron spontaneous activity

Cuneate neurons exhibited a significantly higher rate of spontaneous discharge (mean 23 spikes/s, t=1.7, df=165, p<0.001) than PSDC neurons (Fig. 12B). The cuneate neurons, like PSDC neurons, fired in bursts of 2-5 spikes during spontaneous discharge; however, the mean ISI was significantly shorter for cuneate neurons (1.8 ms, t=1.7, df=98, p<0.001) than for PSDC neurons. Statistically significant differences between on- and off-focus responses are indicated in Tables 1A and B.

3.9 Comparison of cuneate and PSDC RF sizes

RF sizes of cuneate neurons were observed to be significantly smaller (mean 6.7 (±3.5) mm^2, t=1.7, df=56, p<0.001) than those of PSDC neurons (Fig. 6B). In addition, cuneate neurons RFs were always confined to a single digit or palmar region unlike PSDC neuron RFs that, in three of 102 cases, were found to include regions of two adjacent digits or regions of the palm.

Table 1A: Summary of Response Properties for PSDC Neurons

	On-focus				Off-focus			
	Mean	s.d.	Range	n	Mean	s.d.	Range	n
Latency (ms)	8.2	1.1	6.1-11.3	55	9.9*	2.9	6.1-16	55
Variability of first spike (ms)	1.1	0.7	0.2-3.3	55	1.6*	1.1	0-4.2	55
P(r) (%)	96	6	70-100	55	87*	18.6	8-100	55
Threshold (μA)	306.7†	191.9	100-1000	45	553.3*†	307.9	100-1000	45
Response (spikes/30 ms)	6†	4.2	1.5-20.7	55	4.1*	4.7	0-23.1	55
ISI (ms)	1.6	0.3	0.9-2.3	51	1.9*	0.4	1.1-2.7	23
Spontaneous (spikes/s)	7.4†	7.3	0-30.4	55				
Spontaneous ISI (ms)	2.17†	0.5	1.1-3.5	51				

Table 1B: Summary of Response Properties for Cuneate Neurons

	On-focus				Off-focus			
	Mean	s.d.	Range	n	Mean	s.d.	Range	n
Latency (ms)	8.7	2.9	7-10.3	19	9.9*	3	7.7-13.2	19
Variability of first spike (ms)	0.8	0.4	0.1-2.1	19	1.2*	0.6	0.2-2.7	19
P(r) (%)	99	9	91-100	19	75*	28	15-100	19
Threshold (μA)	391.3	253.9	100-1000	23	797.8*	396.1	200-2000	23
Response (spikes/30 ms)	4.6	4.6	1-13	40				
ISI (ms)	1.6	0.4	0.9-2.6	49				
Spontaneous spikes/s	23	23.2	1.1-66.7	25				
Spontaneous ISI (ms)	1.8	0.4	1.1-1.3	26				

*Significant difference between on- vs. off-focus digit stimulation, $p<0.01$.
†Significant difference between PSDC vs. cuneate neurons, $p<0.01$.

Chapter 4: RESULTS - Experiment 2

4.1 PSDC-cuneate neuron pairs

A total of 51 neuron pairs were examined for neural interactions following RF stimulation and during spontaneous activity (i.e. in the absence of stimulation). Of the 51 neuron pairs tested, 27 had RFs that overlapped spatially (mean 66.5%, range 16.2-100%) and the remaining 24 had RFs on glabrous skin of adjacent digits.

4.2 Cross-correlation analysis: RF stimulation

The response to electrical RF stimulation was recorded for each of the 51 PSDC-cuneate neuron pairs. To test for possible interactions between PSDC and cuneate neurons, raw CCGs were constructed. An example of the raw, shifted and neural CCGs for a single neuron pair can be seen in Figures 14A, B and C, respectively. Even though there is a peak at 3 ms in the raw CCG (Fig. 14A), there is a similar peak in the shifted CCG (Fig. 14B) that indicates this is a stimulus effect. Subtraction of the shifted CCG from the raw CCG yielded a flat neural CCG with no bins above the 95% confidence interval (Fig. 14C). This result indicates that the peak in the raw CCG resulted entirely from stimulus effects and not from neural interactions. In fact, none of the 51 PSDC-cuneate pairs tested exhibited any significant interactions following electrical RF stimulation in any of the four quadrants of the neural CCG. In other words, there is no support for the hypothesis that there are interactions, either excitatory or inhibitory, between PSDC and cuneate neurons at any time following electrical stimulation of the RF.

Fig. 14. CCGs post stimulation for a representative PSDC-cuneate neuron pair. A: The raw CCG shows a distinct peak at 3 ms after the reference PSDC neuron has fired. B: The shifted CCG represents stimulus effects. Note the similarity in shape of the raw and shifted CCGs, indicating that at least some of the interaction seen in the raw CCG is due to stimulus effects. C: The neural CCG is constructed by subtracting the shifted CCG from the raw CCG. Lines show the 95% confidence limits. The neural CCG is flat and has no bins that exceed the 95% confidence interval, indicating that all the interactions seen in the raw CCG were due to stimulus effects only and not to neural interactions.

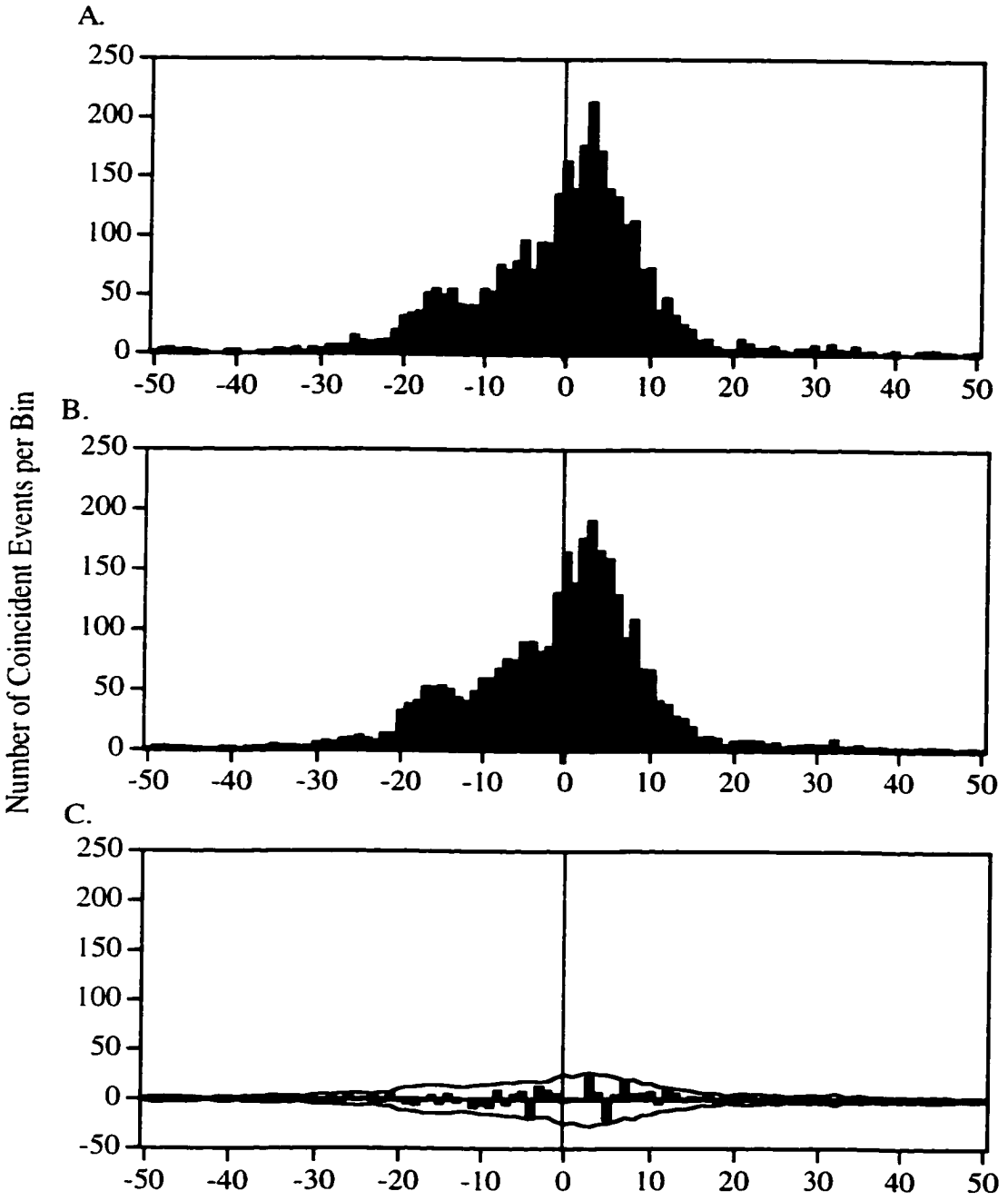
A.
B.
C.
250
200
150
100
50
0
-50
-40
-30
-20
-10
0
10
20
30
40
50
Number of Coincident Events per Bin
Time (ms)

Figure 14

4.3 Cross-correlation analysis: spontaneous activity

The same 51 neuron pairs used in the post-stimulus cross-correlation analysis were tested for temporal interactions during spontaneous discharge. Using the same methodology as applied to the post-stimulus trials, neural CCGs were constructed from the spontaneous activity of each simultaneously recorded PSDC-cuneate neuron pair. Each of the four quadrants in the neural CCG was examined for statistically significant inter-neuronal interactions within 50 ms of the PSDC event at time zero. Of the 51 neuron pairs tested, a total of 26 (51%) exhibited significant interactions in the neural CCG. Of the pairs exhibiting interactions, 19 of 26 (73%) occurred between PSDC and cuneate neurons with overlapping RFs. The remaining 7 of 26 (27%) interactions occurred between PSDC and cuneate neurons that had RFs on adjacent digits (i.e. non-overlapping). There were significantly more interacting PSDC-cuneate neuron pairs with overlapping RFs than non-overlapping RFs (χ^2=8.6, $p<0.001$). Table 2 shows a summary of PSDC-cuneate neuron pairs, separating them into four groups based on the presence (or absence) of significant interactions and RF overlap.

Table 2: Summary of Spontaneous Neural Interactions

Interactions:	Significant	Not Significant
Overlapping RFs	19	8
Non-overlapping RFs	7	17

χ^2=8.6, p<0.001

4.3.1 Spinocuneate spontaneous interactions

The majority of interactions that occurred during spontaneous activity (20/26) were in quadrant I of the neural CCG. The peak interaction was *excitatory* and the cuneate neuron fired at specific times *after* the PSDC neuron event at time zero, suggesting a spinocuneate influence. Figure 15A shows the raw CCG during spontaneous activity for a representative PSDC-cuneate neuron pair with overlapping RFs (100% overlap). There is a distinct peak in the raw CCG that occurs to the right of time zero. The shifted CCG (Fig. 15B) does not exhibit the distinct peak seen in the raw CCG. The neural CCG that resulted from the subtraction of the shifted from the raw CCG (Fig. 15C) shows a significant peak interaction for this neuron pair in quadrant I at 4 ms.

The single event connection strength (C_{single}) was calculated for each excitatory spinocuneate interaction. The peak connection efficacy (C_{peak}) was also calculated to give an indication of the overall efficacy of the interaction. The value of C_{single} for the PSDC-cuneate interaction shown in Figure 15C was 0.08, indicating the maximum strength of a single PSDC to cuneate interaction, occurring at 4 ms (i.e. the time of the maximum interaction) after the PSDC neuron has fired. The value of C_{peak} for the PSDC-cuneate neuron pair in Figure 15C was 0.4, indicating the peak strength of the PSDC to cuneate influence that lasted for 26 ms (from -8 ms to 18 ms).

Fig. 15. CCGs during spontaneous activity for a representative PSDC-cuneate neuron pair with 100% RF overlap. A: Raw CCG showing a peak to the right of time zero, after the PSDC neuron has fired. B: Shifted CCG that is flat, showing no peaks within ±50 ms of time zero. C: Neural CCG with a distinct peak in quadrant I, suggesting a spinocuneate influence. Lines show the 95% confidence limits. Note the similarity in shape between the raw and neural CCGs.

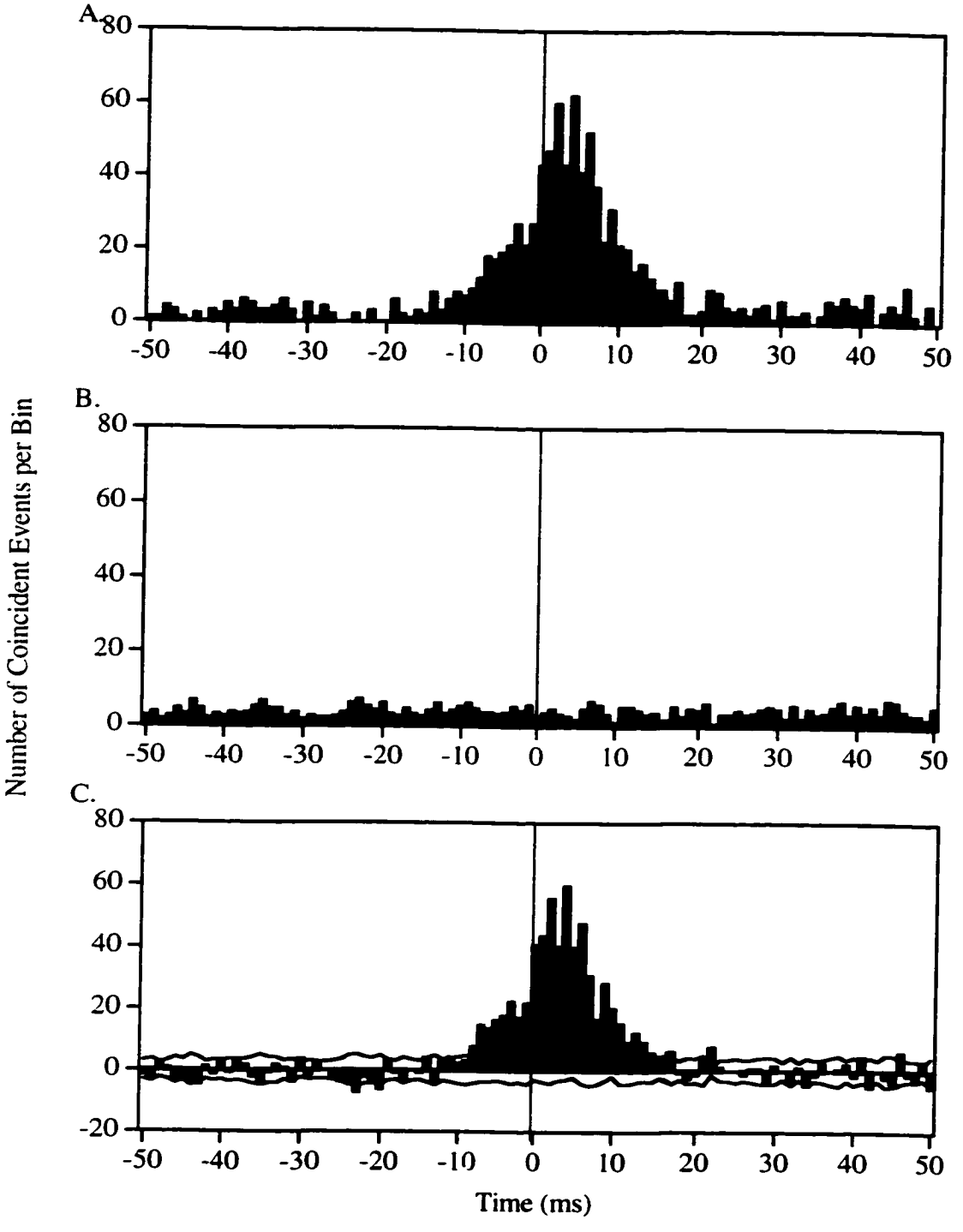
A.
B.
C.
Number of Coincident Events per Bin
Time (ms)
80
60
40
20
0
-20
-50
-40
-30
-20
-10
0
10
20
30
40
50

Figure 15

When all excitatory spinocuneate interactions were examined together, it was found that the mean peak interaction occurred 10.4 ms following the PSDC event. The interactions commenced at a mean time of 5.9 (±14.1) ms (range -25-30 ms) and ended at a mean of 16.1 (±9.4) ms (range 5-33 ms) after the spike occurred in the PSDC neuron. The average duration of the excitatory spinocuneate interactions was 9.7 ms. The mean C_{single} for excitatory spinocuneate interactions was 0.08 and the mean C_{peak} was 0.28. Table 3 shows a summary of all significant interactions between PSDC and cuneate neurons. Figure 16 shows the relationship between C_{peak} and the duration of statistically significant PSDC-cuneate interactions. The Pearson correlation coefficient was 0.84, suggesting a close relationship between C_{peak} and the longevity of PSDC-cuneate neuron interactions. It appears that the longer PSDC-cuneate neuron pairs are interacting with one another, the stronger the contribution of PSDC neurons to cuneate neuron activity.

In one of the 26 cases, the significant interaction was in quadrant IV of the neural CCG, indicating an *inhibitory* spinocuneate interaction with the cuneate neuron being inhibited *after* the PSDC neuron. Figure 17A shows the raw CCG for a PSDC-cuneate neuron pair in which a small depression can be identified to the right of time zero. The shifted and neural CCGs for this neuron pair are shown in Figs.17B and C, respectively. The peak inhibitory interaction occurred at 17 ms and lasted from 14 to 19 ms following the occurrence of the PSDC spike. The value of C_{single} was 0.16, indicating a 16% chance that the cuneate neuron will not fire at precisely 17 ms (i.e. the time of maximum inhibitory interaction). The value of C_{peak} was 0.36. In this case

Table 3: Summary of Significant Interactions Between PSDC and Cuneate Neurons

Interaction Type:	n	C_{single}	C_{peak}	Peak time (ms)	Duration (ms)
Excitatory Spinocuneate	20	0.08±0.04* (range 0.02-0.17)	0.28±0.25* (range 0.2-1.1)	10.4±9.9 (range 1-30)	9.7±10.8 (range 3-46)
Excitatory Cuneospinal	5	0.03±0.01 (range 0.01-0.05)	0.06±0.02 (range 0.03-0.08)	-15.2±10.5 (range -12 to -17.4)	5.4±3.8 (range 3-12)
Inhibitory Spinocuneate	1	0.16	0.36	17	6

*Significant difference between spinocuneate and cuneospinal values, t-test, $p<0.05$.

Fig. 16. Relationship between C_{peak} and duration of PSDC-cuneate neuron interactions. The Pearson correlation coefficient was 0.84, indicating a strong relationship between the duration of interaction between PSDC-cuneate neuron pairs and the value of C_{peak}. It appears that the longer PSDC-cuneate neuron pairs are interacting with one another, the stronger the contribution of PSDC neurons to cuneate neuron activity.

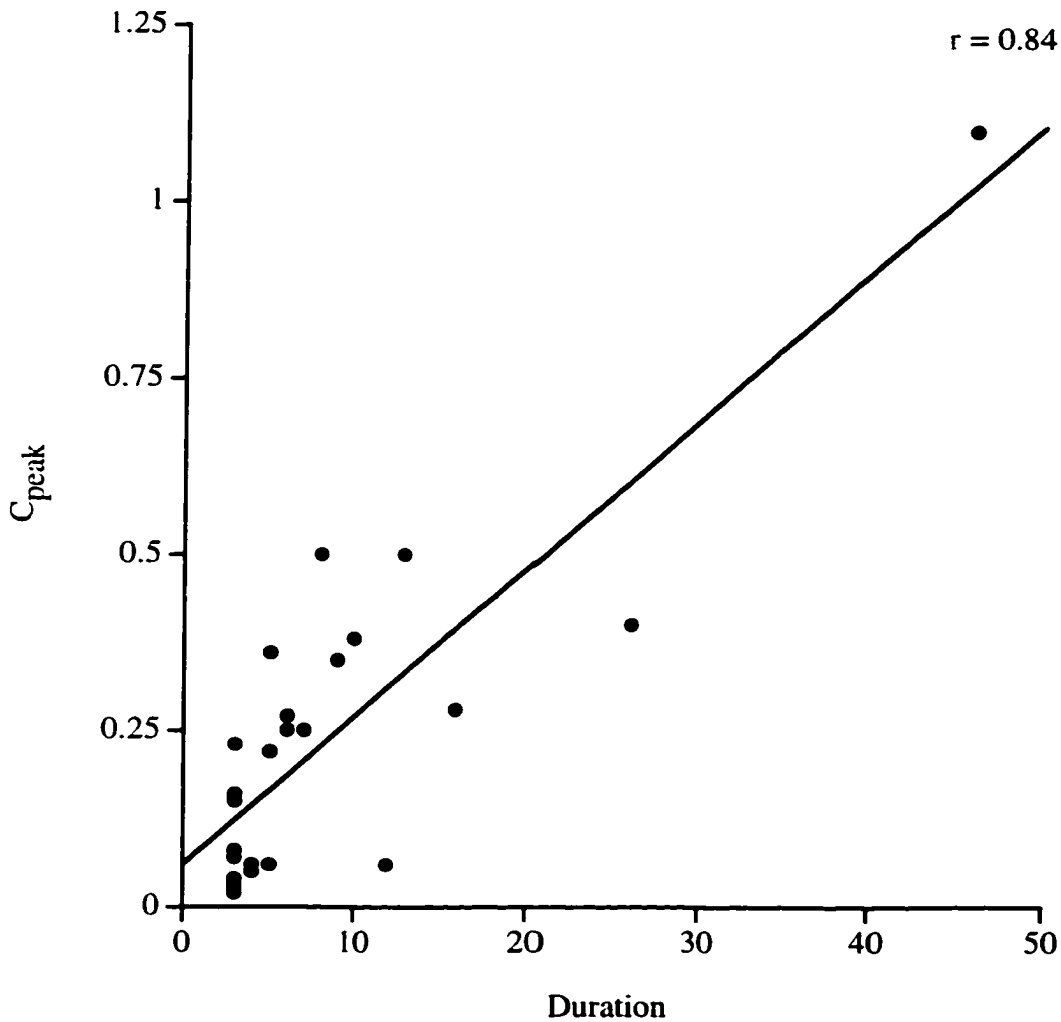

Figure 16

Fig. 17. CCGs for a representative PSDC-cuneate neuron pair exhibiting an inhibitory spinocuneate interaction during spontaneous activity. A: Raw CCG showing a small depression to the right of time zero. B: Shifted CCG that does not have the same depression as in the raw CCG. C: Neural CCG showing an interaction in quadrant IV, suggesting an inhibitory spinocuneate influence. Lines show the 95% confidence interval.

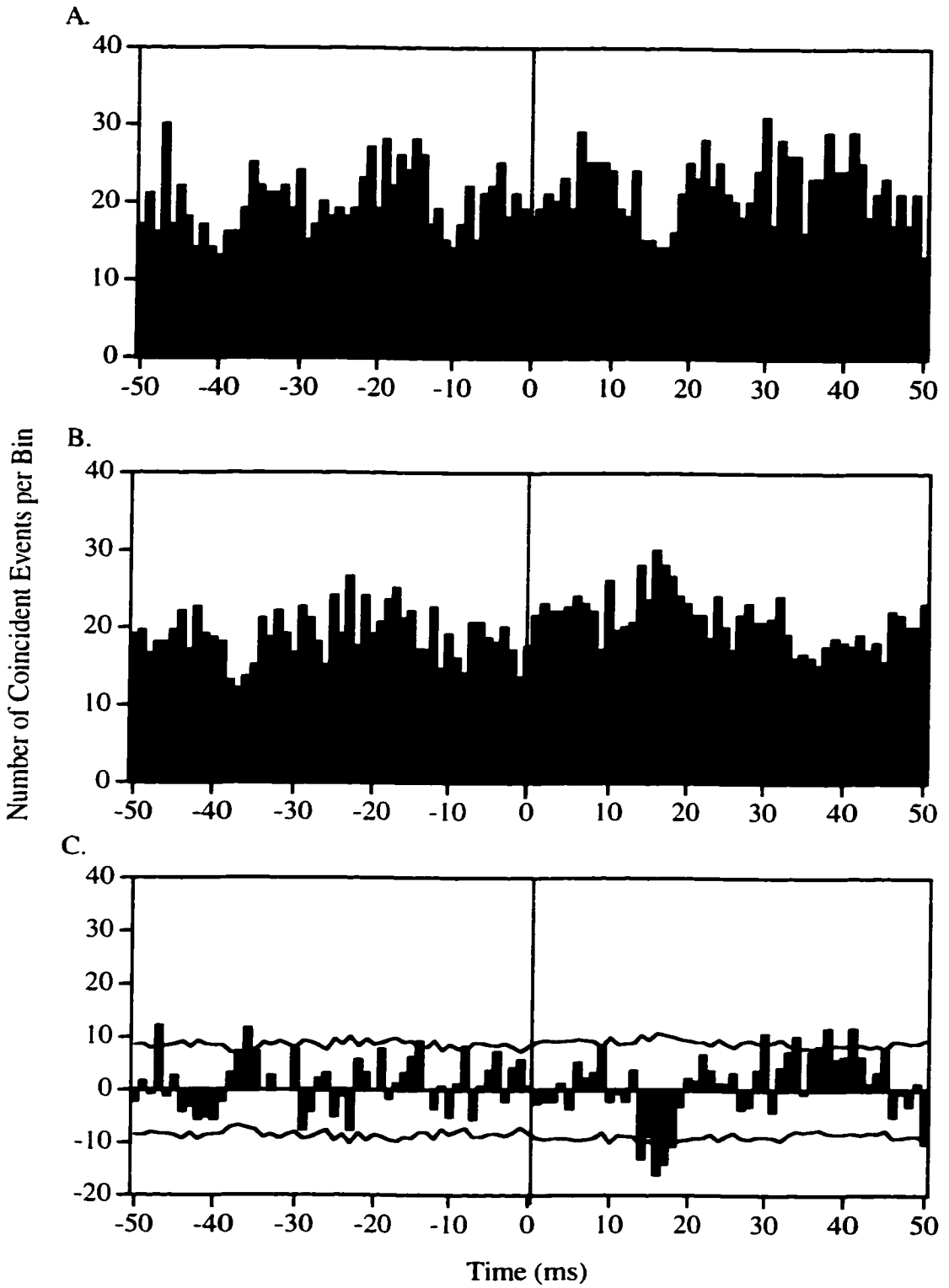
A.
B.
C.
Number of Coincident Events per Bin
Time (ms)
40
30
20
10
0
-10
-20
-50
-40
-30
-20
-10
0
10
20
30
40
50

Figure 17

of an inhibitory spinocuneate interaction, the PSDC-cuneate neuron pair had a 100% RF overlap. The majority (14/20) of excitatory spinocuneate interactions occurred between PSDC-cuneate neuron pairs with overlapping RFs. The mean overlap in these 14 pairs was 76.1% (range 18.3-100%). In six cases, the interacting neurons had RFs that were on adjacent digits and did not share regions of overlap. However, there were no statistically significant differences between interaction parameters measured for neurons with overlapping RFs as compared to neurons with RFs on adjacent digits (t-test, $p>0.05$).

The neural CCGs for all significant spinocuneate interactions not shown in the Results are shown in the Appendix.

4.3.2 Cuneospinal spontaneous interactions

In 5 of the 26 pairs exhibiting spontaneous neural interactions, the significant peak was in quadrant II of the neural CCG, indicating that the predominant interaction was *excitatory* with the cuneate neuron firing at times *before* the PSDC neuron (i.e. an excitatory cuneospinal interaction). Figure 18A shows the raw CCG of a representative PSDC-cuneate neuron pair with an excitatory cuneospinal interaction in which there is a distinct peak to the left of time zero. The shifted and neural CCGs for this neuron pair are shown in Figs. 18B and C, respectively. The time of maximal interaction for the PSDC-cuneate neuron pair shown in Figure 18 was -8 ms. The significant interaction lasted for 12ms, from 0 to -11 ms. The functional strength of a single excitatory cuneospinal interaction (i.e. C_{single}) was calculated in the same manner as for the excitatory interactions in the opposite direction (i.e. spinocuneate

interactions). The C_{peak} calculation was also performed in the same manner for all statistically relevant quadrants of the neural CCG. The neuron pair shown in Figure 18, whose RFs shared a 100% overlap, had C_{single} and C_{peak} values of 0.013 and 0.06, respectively.

When all of the neuron pairs that exhibited a cuneospinal interaction were examined together, the mean time of occurrence of the peak interaction was -15.2 (±10.5) ms, indicating that the predominant time of cuneate neuron firing was 15.2 ms *before* the PSDC spinal cord neuron fired. The mean duration of the inhibitory cuneospinal interaction was 5.4 (±3.8) ms. The mean C_{single} for excitatory cuneospinal interactions was calculated to be 0.03 (±0.01) and the mean C_{peak} was 0.06 (±0.02). Of the 5 cuneospinal excitatory interactions, 4 of the neuron pairs had overlapping RFs (mean 60.4%, range 39.2-100%). The remaining neuron pair had RFs on adjacent digits that did not overlap.

The neural CCGs for all significant cuneospinal interactions not shown in the Results are shown in the Appendix.

Fig. 18. CCGs for a representative PSDC-cuneate neuron pair exhibiting an excitatory cuneospinal interaction. A: The raw CCG shows a distinct peak to the left of zero. B: In the shifted CCG there are no large peaks, although a small peak at -15 ms is evident. C: Neural CCG showing a statistically significant interaction to the left of zero, in quadrant II. Note the similarities with respect to the shape of the peaks in the raw CCG vs. neural CCG.

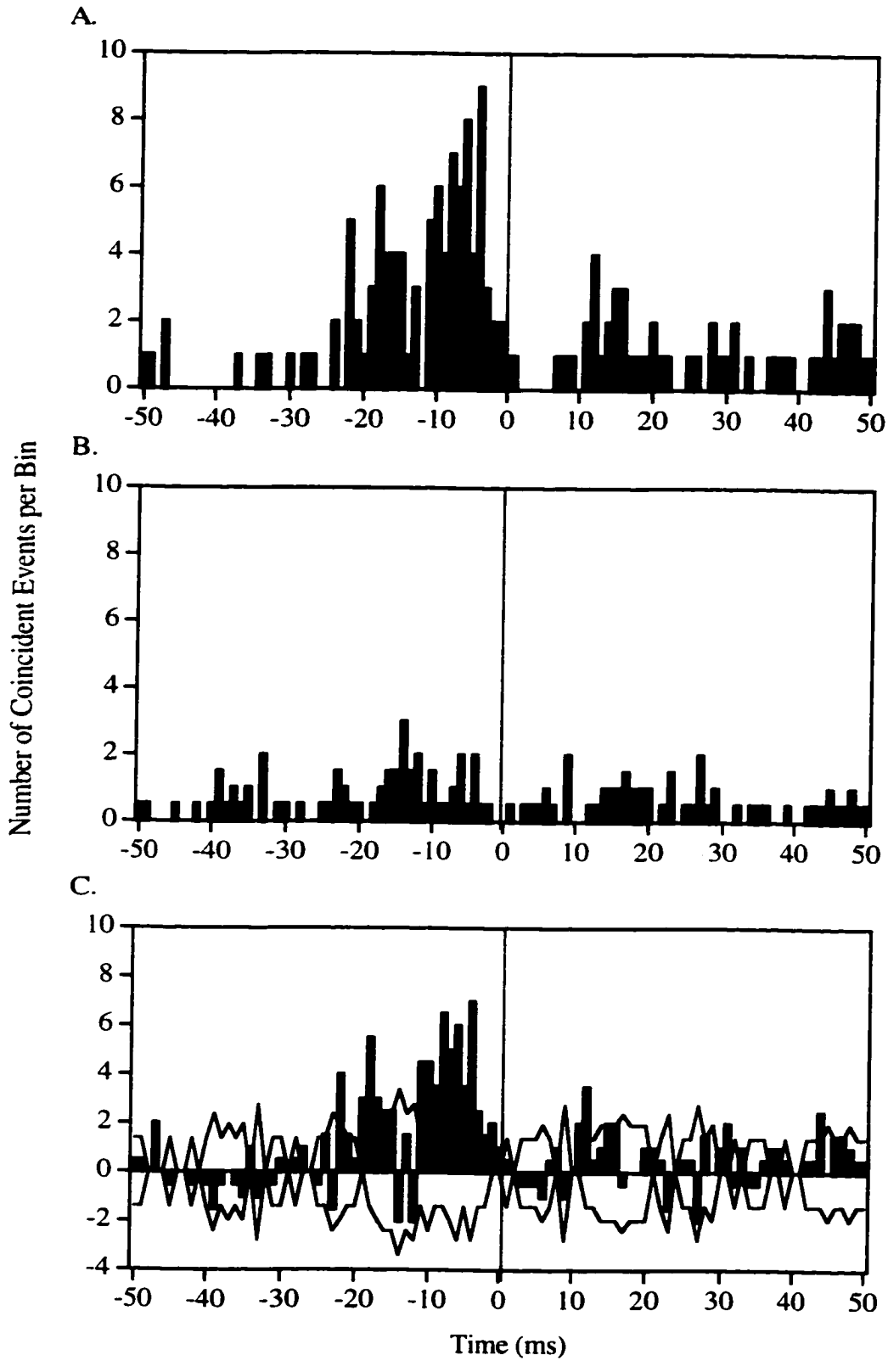
A.
B.
C.
Number of Coincident Events per Bin
Time (ms)
10
8
6
4
2
0
-2
-4
-50
-40
-30
-20
-10
0
10
20
30
40
50

Figure 18

4.3.3 Comparison of spinocuneate vs. cuneospinal excitatory connection strength

The excitatory PSDC-cuneate interactions in quadrant I of the neural CCG (i.e. spinocuneate interactions) had significantly higher mean C_{single} values than the excitatory cuneospinal interactions in quadrant II ($t=1.7$, $df=24$, $p<0.01$). Similarly, the excitatory spinocuneate interactions had significantly higher C_{peak} values than did the excitatory cuneospinal interactions ($t=1.7$, $df=23$, $p<0.05$). Taken together, the results indicate that excitatory spinocuneate interactions are significantly stronger than cuneospinal interactions. Figs. 19A and B show the relationship between the time of the peak in quadrant I of the neural CCG and values of C_{single} and C_{peak}, respectively. In Fig. 19A, two distinct groupings with respect to the values of C_{single} can be seen. The first group includes all the cuneospinal interactions and is characterized by low values of C_{single}. The second group includes only spinocuneate interactions and is characterized by higher values of C_{single}. The same two groupings are also evident in Figure 19B where C_{peak} is plotted against the time of maximal interaction. Figs. 19C and D show the relationship between the amount of RF overlap and the values of C_{single} and C_{peak}, respectively. There does not appear to be any relationship between the degree of RF overlap for a PSDC-cuneate neuron pair and the strength of their interaction as measured using the values of C_{single} and C_{peak}.

Fig. 19. Plot of connection strength vs. time of maximal interaction and degree of RF overlap between interacting PSDC-cuneate neuron pairs. A: Scatter plot of C_{single} versus time of maximal interaction (i.e. peak time). Two distinct groups can be seen, one with low C_{single} values and wide ranging peak times and the other with higher C_{single} values and peak times that are all to the right of zero. Note the different grouping of neuron pairs with spinocuneate versus cuneospinal interactions. B: Scatter plot of C_{peak} versus time of maximal interaction. The same two groups as in A can be seen when C_{peak} is plotted against the time of maximal interaction, indicating that the strongest interactions between PSDC-cuneate neuron pairs occur when the peak is in quadrant I of the neural CCG. C,D: Scatter plot of %RF overlap versus C_{single} and C_{peak}, respectively. There does not appear to be any relationship between the amount of RF overlap between PSDC-cuneate neuron pairs and the strength of interaction.

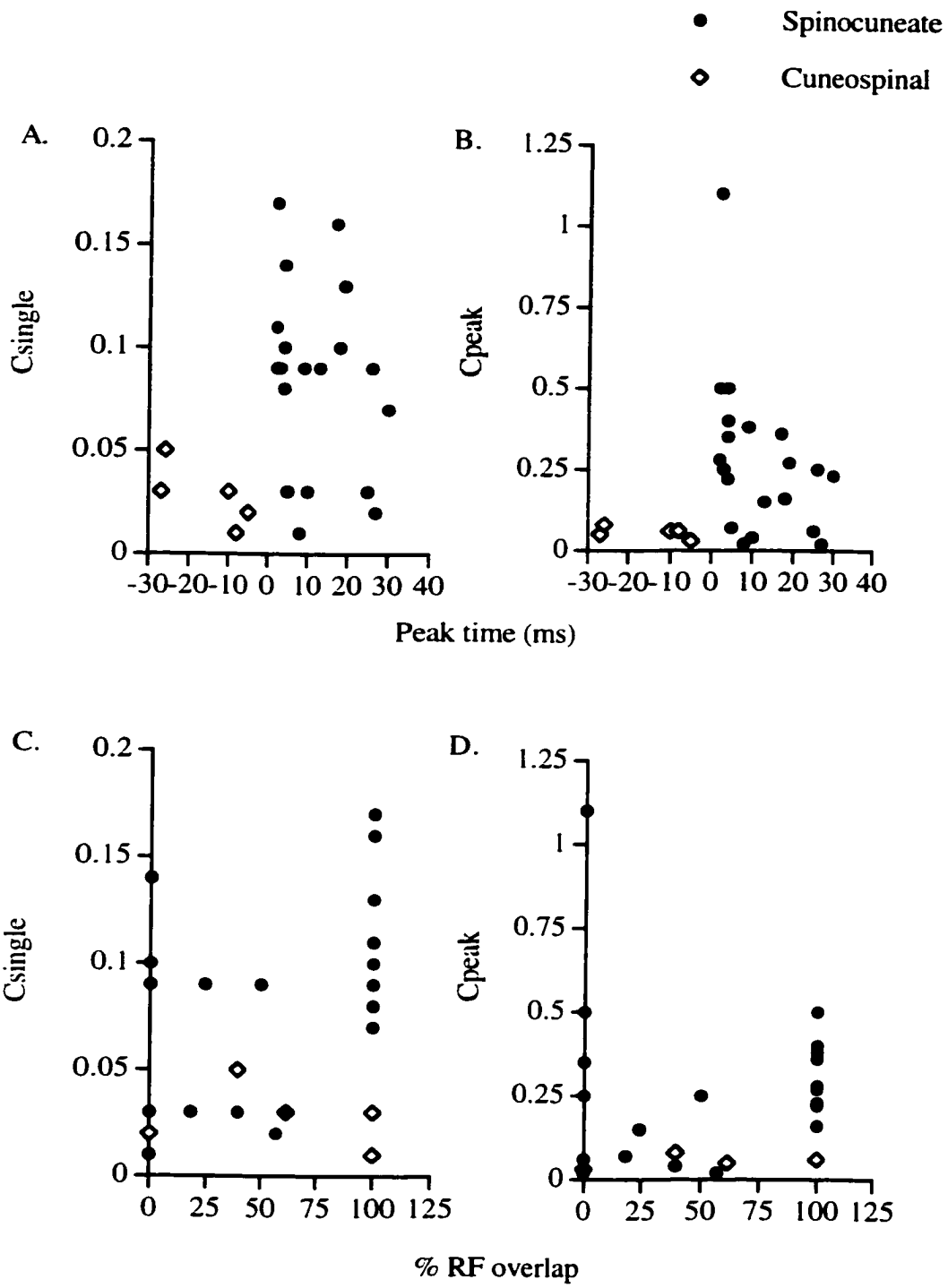
Spinocuneate
Cuneospinal
A.
B.
Csingle
Cpeak
0.2
0.15
0.1
0.05
0
1.25
1
0.75
0.5
0.25
-30 -20 -10 0 10 20 30 40
Peak time (ms)
C.
D.
0 25 50 75 100 125
% RF overlap

Figure 19

4.4 Frequency response analysis: spontaneous interactions

The PSDC-cuneate neuron pairs that exhibited significant temporal interactions in the spontaneous neural CCGs were further analyzed in the frequency domain. The coherence between input PSDC and output cuneate signals was examined to test the linearity of the PSDC to cuneate connection. A coherence value of 1 would indicate that the input-output relationship is completely linear and a value of zero would indicate that there is no linearity in the PSDC to cuneate connection. Values between zero and 1 are more difficult to interpret because they could represent non-linearity, uncorrelated signal in the system or both. Figure 20 shows the coherence between the input (PSDC) signal and the output (cuneate) signal of a representative PSDC-cuneate neuron pair with a spinocuneate interaction. In this example, the maximum coherence was 0.7 and occurred at a frequency of 1.8 Hz. Figure 21 shows the frequency response for the same PSDC-cuneate neuron pair as in Figure 20. From the Bode plots seen in Figure 21 (linear scale), it is apparent that the gain and phase of the cuneate output signal change as a function of the input frequency. The Bode plots (linear scale) show a decline in cuneate output signal phase and gain as a function of the PSDC input signal frequency.

Fig. 20. Graph showing the coherence between the input PSDC signal and the output cuneate signal for a representative PSDC-cuneate neuron pair exhibiting a spinocuneate interaction. The normalized PSDC input power spectrum is also shown (hatched line). In this example, the coherence had a maximum value of 0.7 at 1.8 Hz, indicating linearity in the input-output relationship at low frequencies. The coherence value was less than a unitary value, indicating the presence of non-linearity, uncorrelated signal in the system, or both. The number of ensembles used to calculate the coherence value in this example was 74.

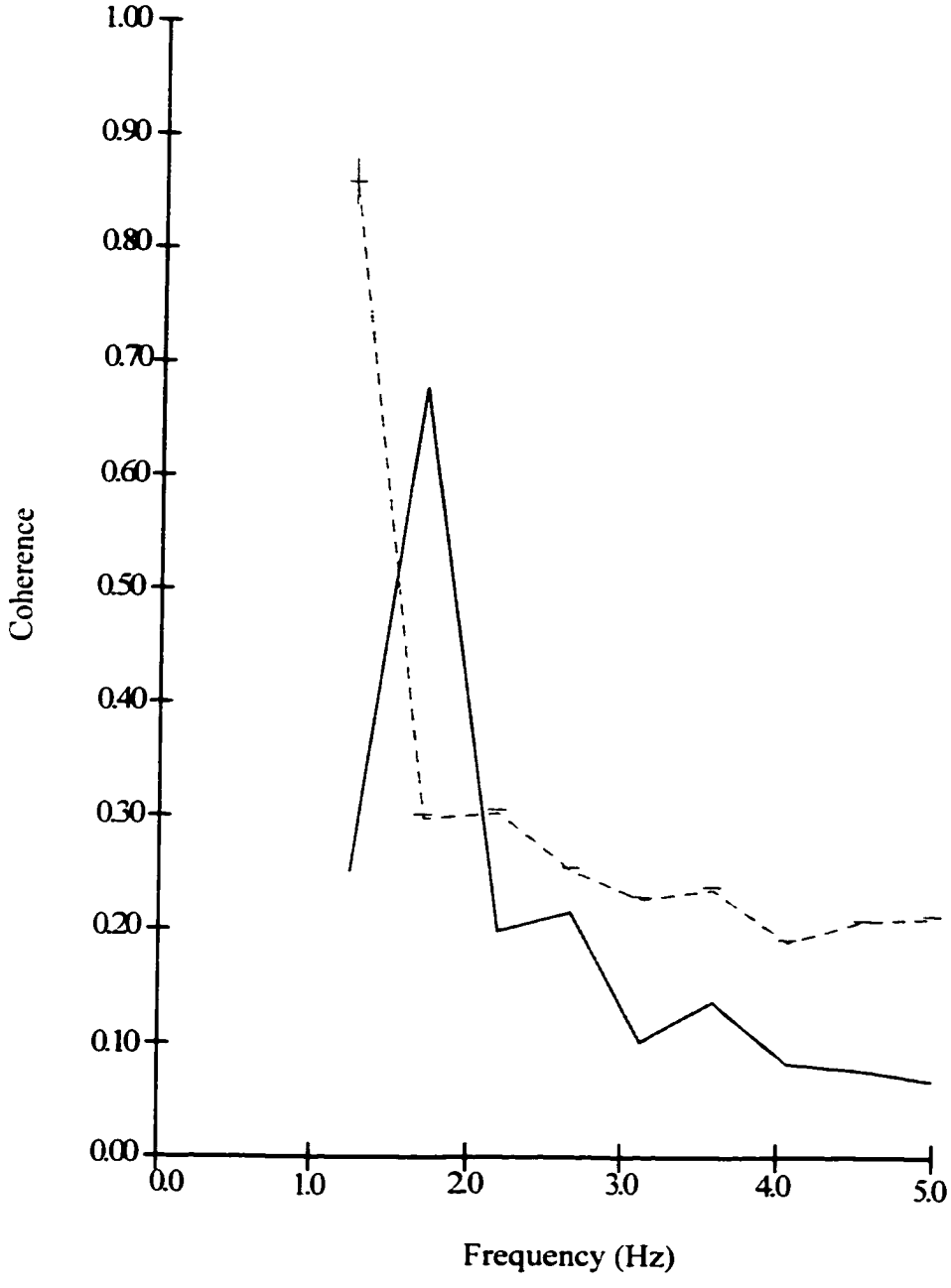
1.00
0.90
0.80
0.70
0.60
0.50
0.40
0.30
0.20
0.10
0.00
Coherence
0.0
1.0
2.0
3.0
4.0
5.0
Frequency (Hz)

Figure 20

Fig. 21. Frequency response of a representative PSDC-cuneate neuron pair with a spinocuneate interaction (linear scale). The neuron pair used in this example is the same as in Figure 20. A: Gain of the output cuneate signal plotted against frequency of the input PSDC signal. Note the steady decline of the cuneate signal gain as a function of the PSDC input signal frequency. This type of input-output relationship can be modeled by a low-pass linear system. B: Phase of the output cuneate signal plotted against frequency of the input PSDC signal. Note the decrease in the phase of the cuneate signal as a function of the PSDC input signal frequency between 1-4 Hz.

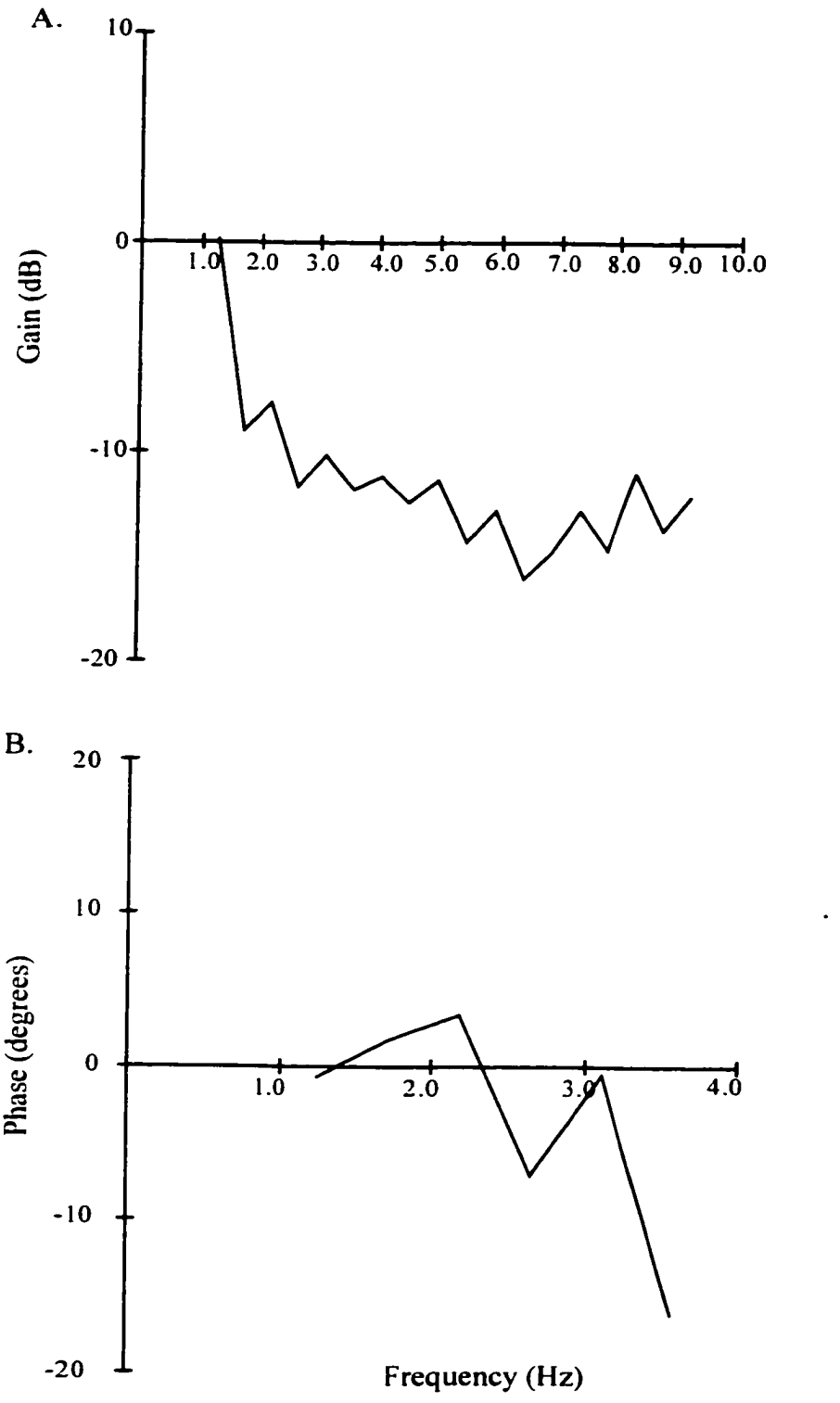
A.
10
0
-10
-20
Gain (dB)
1.0
2.0
3.0
4.0
5.0
6.0
7.0
8.0
9.0
10.0
B.
20
10
0
-10
-20
Phase (degrees)
1.0
2.0
3.0
4.0
Frequency (Hz)

Figure 21

The mean coherence between input and output signals of the spinocuneate connection (mean 0.27 (±0.2), range 0-0.7, n=20) was significantly higher than for the cuneospinal connection (mean 0.09 (±0.02), range 0.03-0.16, $t=1.7$, $df=16$, $p<0.05$). The mean spinocuneate coherence was also significantly greater than the mean coherence between signals that were not correlated in time (mean 0.17 (±0.1), range 0-0.5, $t=1.7$, $df=31$, $p<0.01$). The maximum coherence, regardless of connection type, occurred at low frequencies with a mean of 2.5 (±2.3) Hz (range 1.2-10 Hz) for spinocuneate and 3.9 (±0.8) Hz (range 1-8.9 Hz) for cuneospinal interactions. Neurons that did not interact in time had a maximum coherence between input and output signals at a mean frequency of 2.12 (±0.6) Hz (range 1.2-8.3). There was no statistically significant difference in the frequency at which peak coherence occurred between the spinocuneate and cuneospinal interaction conditions (t-test, $p>0.05$).

Chapter 5: RESULTS - Experiment 3

A total of 55 PSDC neurons were recorded before and after temporary blockade of the on-focus input. In 26/55 of the cases, cuneate neurons were recorded simultaneously and in the majority of cases (92%, 24/26) they had RFs on an adjacent, off-focus digit with respect to the PSDC cells. The remaining two cuneate neurons had RFs that spatially overlapped those of the PSDC neurons being recorded simultaneously. The immediate effects of peripheral deafferentation on neurons in the raccoon cuneate nucleus have been reported elsewhere (Northgrave and Rasmusson 1996) and will not be specifically addressed here.

5.1 Off-focus response of PSDC neurons during temporary deafferentation

The extent of temporary deafferentation is defined as the time period during which the PSDC neuron did not respond to electrical or mechanical stimulation of the RF. In general, this began 1-2 minutes after the lidocaine injection and lasted 5-10 minutes. Deafferentation had the effect of significantly lengthening the latency of response to stimulation of the adjacent digit. Table 4 shows a summary of PSDC neurons responses to off-focus digit stimulation and spontaneous activity before and during temporary deafferentation. The mean latency of response to off-focus electrical stimulation before temporary deafferentation was 9.9 ms and increased to 10.3 ms ($t=1.7$, $df=54$, $p<0.05$) after the dominant input to the PSDC neurons was blocked (Fig. 24). The variability in the latency of response to off-focus stimulation (mean 1.6 ms) did not change following deafferentation (mean 1.6 ms, paired t-test, $p>0.05$).

Table 4: PSDC neuron off-focus responses before and during deafferentation

	Before		During		
	mean (±s.d.)	range	mean (±s.d.)	range	n
Latency (ms)	9.9 (±2.9)	(6.1-16)	10.3 (±3)*	(6.2-17.6)	55
Variability in first spike (ms)	1.6 (±1.1)	(0-4.2)	1.6 (±1.3)	(0.1-1.3)	55
P(r) (%)	90 (±19)	(8-100)	80 (±29)*	(0-100)	55
Response (spikes/30s)	4.4 (±4.7)	(0-23.1)	3.1 (±4)*	(0-19)	45
ISI (ms)	1.9 (±0.4)	(1.1-2.7)	1.8 (±0.4)	(1.1-3.1)	55
Spontaneous (spikes/s)	7.3 (±7.9)	(0-30.4)	3.3 (±3.9)*	(0-20.2)	23

*Significant difference before vs. during deafferentation, $p<0.05$

Fig. 22. PSDC neuron latency of response to off-focus digit stimulation before versus during deafferentation. Deafferentation significantly lengthened the latency of response from 9.9 ms before to 10.3 ms during ($t=1.7$, $df=54$, $p<0.05$). However, it should be noted that in some cases, there was either no change or a decrease in the latency of response during deafferentation.

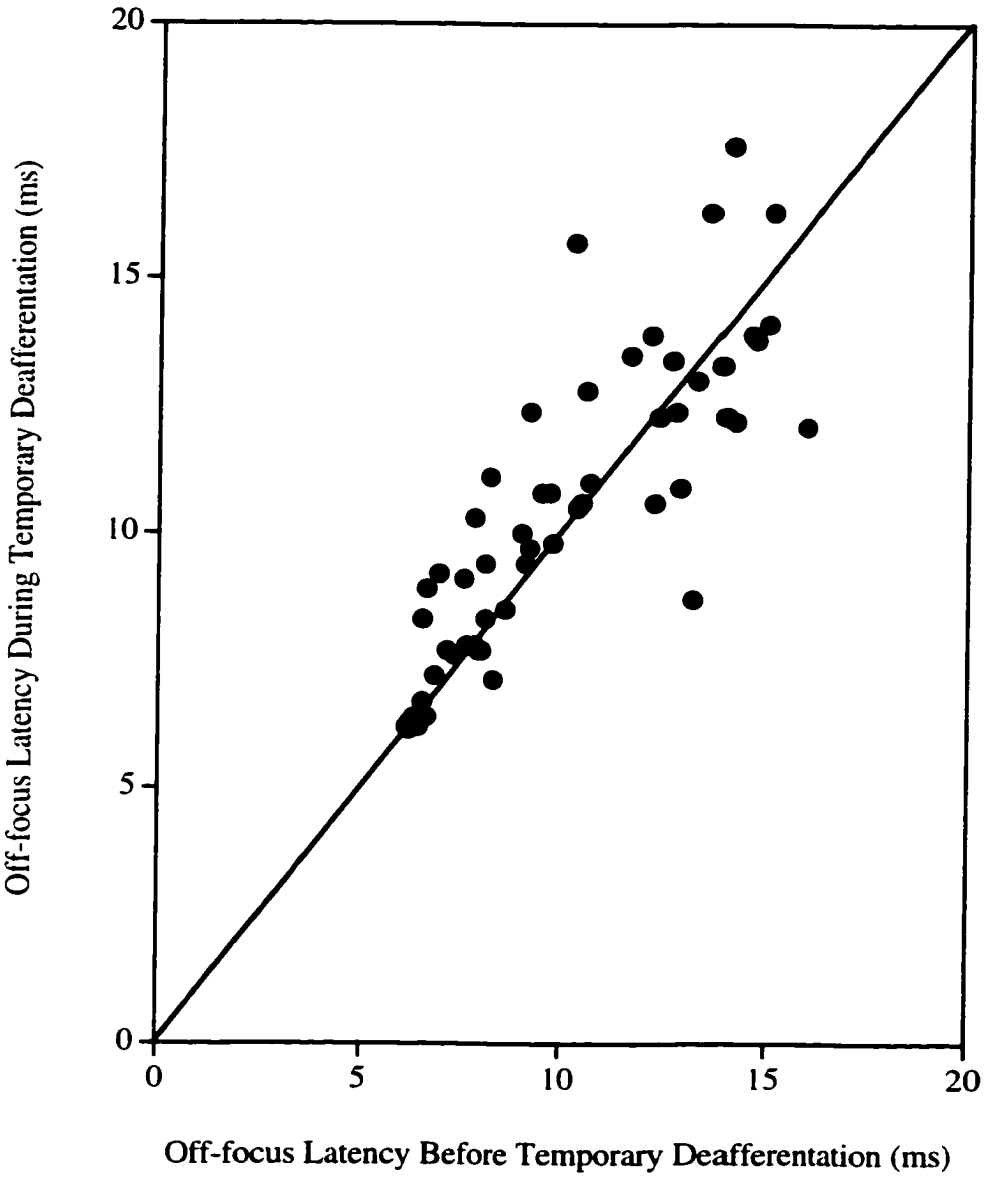
20
15
10
5
0
0
5
10
15
20
Off-focus Latency During Temporary Deafferentation (ms)
Off-focus Latency Before Temporary Deafferentation (ms)

Figure 22

However, deafferentation had the effect of decreasing the mean probability of response to stimulation of the adjacent digit from 90% to 80% ($t=1.7$, $df=54$, $p<0.01$).

The number of PSDC neuron spikes in response to off-focus electrical stimulation was significantly higher before (mean 4.4 spikes/30 ms) than during temporary deafferentation (mean 3.1 spikes/30 ms, $t=1.7$, $df=51$, $p<0.001$). The mean inter-spike interval (ISI) of PSDC neurons in response to off-focus stimulation was 1.9 ms and did not significantly change during the lidocaine-induced blockade of on-focus input (paired t-test, $p>0.05$).

5.2 Spontaneous activity of PSDC neurons during temporary deafferentation

The mean rate of spontaneous discharge of raccoon PSDC neurons before removal of on-focus input was 7.3 spikes/s. During temporary deafferentation, the spontaneous activity of these cells was significantly decreased to a mean rate of 3.3 spikes/s ($t=1.6$, $df=147$, $p<0.001$). The average spontaneous activity of cuneate neurons also decreased during deafferentation, falling from 23 spikes/s to 7.2 spikes/s. The PSDC neuron ISI during spontaneous firing (mean 2.3 ($\pm$0.5 ms)) was not affected by deafferentation (paired t-test, $p>0.05$).

5.3 Effect of temporary deafferentation on PSDC-cuneate functional interactions

Chapter 4 described the presence of neural interaction between PSDC and cuneate neurons during spontaneous discharge. In 26 of the cases used in the previous analysis, lidocaine was injected into an on-focus digit and the spontaneous cross-correlation was re-calculated during temporary deafferentation. Lidocaine was

injected into the on-focus digit for the PSDC cell and off-focus for the cuneate cell when the PSDC-cuneate neuron pair had RFs on adjacent digits. In the cases where PSDC and cuneate neurons had overlapping RFs, the lidocaine induced a blockade of the on-focus digit for both the PSDC and cuneate neurons.

Most of the PSDC-cuneate neuron pairs used in the lidocaine analysis (24/26) had RFs that did not overlap. Of these neuron pairs, 35% (9/26) had significant temporal interactions before lidocaine injection, as identified by cross-correlation analysis (chapter 4). Of the neuron pairs that were defined as functionally connected prior to lidocaine injection, the majority (8/9) had excitatory spinocuneate interactions and included the 2 cases with overlapping RFs. The remaining neuron pair had an excitatory cuneospinal interaction before the lidocaine-induced temporary deafferentation. The effects of deafferentation on these individual neuron pairs is summarized in Table 5.

Six of eight neuron pairs with significant spinocuneate interactions before lidocaine injection had the same interaction during deafferentation but with a significantly higher single event efficacy. The value of C_{single} prior to lidocaine (0.1 ±0.02) was significantly increased during deafferentation of the on-focus digit (0.2 ±0.02, range 0.09-0.32, $t=2$, $df=5$, $p<0.01$). The peak connection strength (C_{peak}) remained unchanged during deafferentation (paired t-test, $p>0.05$).

Table 5: Individual PSDC-cuneate interactions that were influenced by deafferentation

Interaction Type Before	Interaction Type During	C_{single} Before	C_{single} During	C_{peak} Before	C_{peak} During
spinocuneate	spinocuneate	0.09	0.09	1.1	0.86
spinocuneate	spinocuneate	0.09	0.22	0.25	0.34
spinocuneate	spinocuneate	0.13	0.15	0.27	0.27
spinocuneate	spinocuneate	0.09	0.09	0.25	0.22
spinocuneate	spinocuneate	0.14	0.23	0.50	0.37
spinocuneate	spinocuneate	0.10	0.32	0.35	0.90
spinocuneate	none	0.01	0	0.02	0
spinocuneate	none	0.03	0	0.06	0
cuneospinal	none	0.02	0	0.03	0
none	spinocuneate	0	0.01	0	0.03
none	cuneospinal	0	0.16	0	0.51

The start time of the interaction was significantly later during deafferentation (9 ±13.4 ms, range -10-23 ms, t=2, df=5, $p<0.05$) than before lidocaine was injected (2.2 ±16.6 ms, range, -25-22 ms). However, the duration of the interaction remained unchanged as did the time of maximal interaction (i.e. peak time) (paired t-test, $p>0.05$). Figure 25 shows a representative PSDC-cuneate neuron pair that exhibited a spinocuneate interaction both before and during deafferentation. In this example, the value of C_{single} increased from 0.10 before to 0.32 during deafferentation. The value of C_{peak} was also affected by deafferentation, increasing from 0.35 before to 0.9 during. The time of maximal interaction shifted from 4 ms to 6 ms after the PSDC neuron fired and the duration of interaction decreased from 9 ms to 7 ms.

In two cases, deafferentation blocked the spinocuneate interaction. Both of these interactions had low single and peak connection strengths prior to the injection of lidocaine (C_{single} 0.01 and 0.03; C_{peak} 0.02 and 0.06). The only excitatory interaction that was initially in the cuneate to spinal direction was also lost after lidocaine injection. As was the case where the spinocuneate interaction was lost, the cuneospinal interaction was weak prior to the injection of lidocaine (C_{single} 0.02, C_{peak} 0.03).

Two previously non-interacting neuron pairs showed significant interaction during temporary deafferentation. In one case, the new interaction was an excitatory spinocuneate interaction and in the other it was an excitatory cuneospinal interaction. The new spinocuneate interaction was weak (C_{single} 0.01, C_{peak} 0.03) whereas the new, deafferentation-induced cuneospinal interaction was much stronger (C_{single} 0.16, C_{peak} 0.51).

Fig. 23. Neural CCG for a representative PSDC-cuneate neuron pair before (A) and after (B) the injection of lidocaine (i.e. during temporary deafferentation). Note the similar shape of the neural CCG before and during deafferentation.

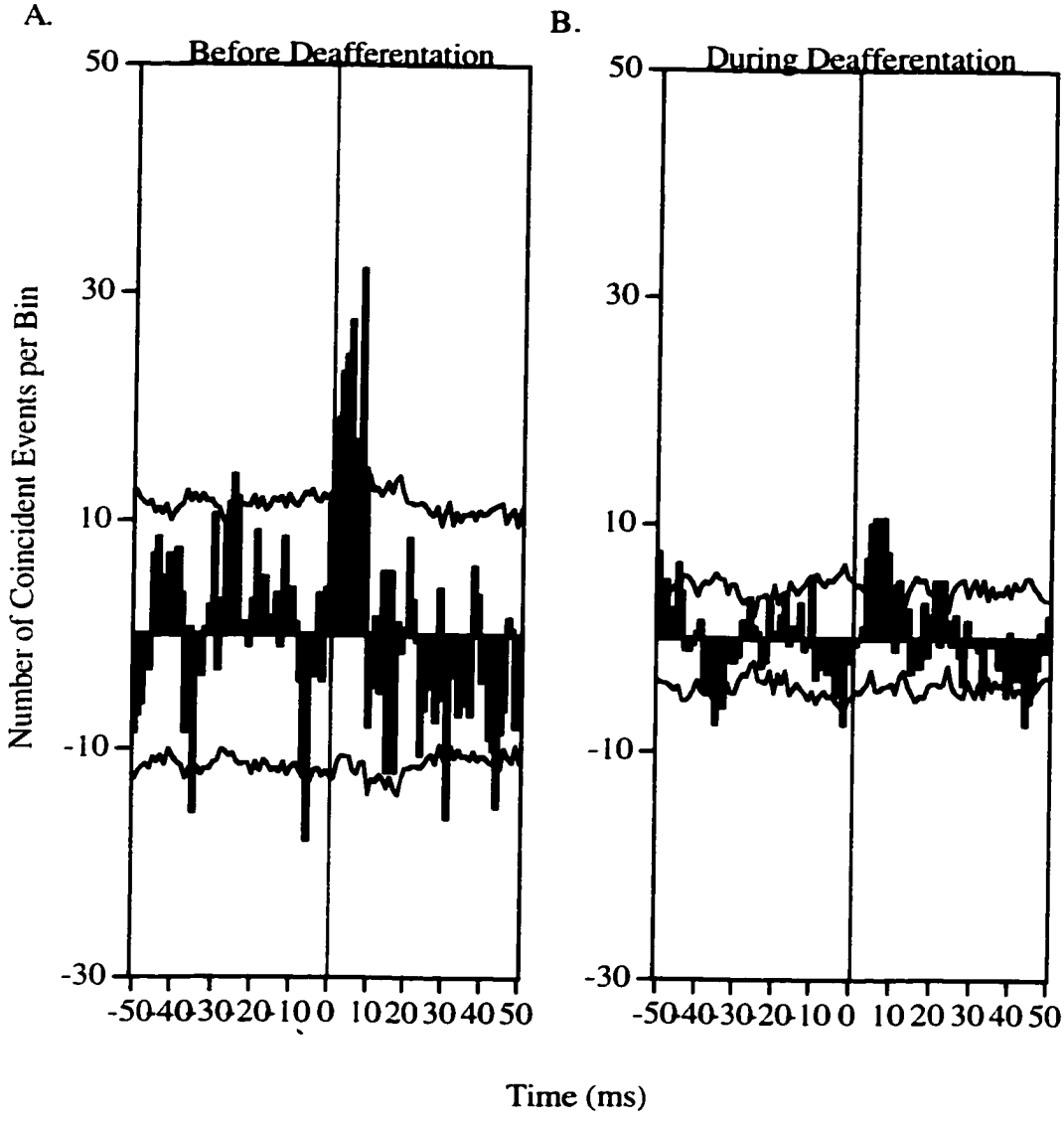
A.
Before Deafferentation
B.
During Deafferentation
50
30
10
-10
-30
Number of Coincident Events per Bin
-50 -40 -30 -20 -10 0 10 20 30 40 50
Time (ms)

Figure 23

Chapter 6: DISCUSSION

The present study provides a description of the response properties of raccoon PSDC neurons and a comparison to neurons in the cuneate nucleus. This information is useful because it is an extension of previously reported findings on the PSDC system in rat and cat in an animal with large areas of glabrous skin on the forepaw and a highly differentiated somatosensory system. Interactions between PSDC and cuneate neurons are also demonstrated, providing direct evidence of a functional excitatory connection between these cell populations in raccoon. This finding is important because it helps to elucidate the role of PSDC neurons in mechanosensation. Finally, changes in PSDC neuron response properties and PSDC-cuneate interactions were examined following temporary deafferentation. This information is important because it could lead to an increased understanding of the mechanisms involved in cuneate nucleus reorganization, a process that occurs following peripheral deafferentation.

6.1 Location of PSDC neurons in raccoon

The histological and electrophysiological results from the present study suggest that PSDC neurons in raccoon are located within Rexed's laminae III-IV, as they are in rat, cat and monkey (Giesler et al., 1984; de Pommery et al., 1984; Brown and Fyffe, 1981; Bennett et al., 1983; Rustioni et al., 1979; Bennett et al., 1983). PSDC neurons in this study were most often found at depths that roughly correspond to Rexed's lamina III according to a previous anatomical description of dorsal horn neurons in the raccoon cervical enlargement (Hirata and Pubols 1989).

Hirata and Pubols (1989) showed evidence that the nucleus proprius in raccoon includes depths of between 1725 μm and 3500 μm, making it likely that lamina III extends to at least 2000 μm in this animal based on the relative thickness of lamina III vs. IV in cat (Rexed, 1954). And, since the majority of neurons in the present study were found between 1500 μm and 2500 μm, it is probable that many were located in Rexed's lamina III. The superficial position of raccoon PSDC neurons makes them more similar to monkey than cat because monkey PSDC neurons are often found in Rexed's lamina III, whereas those in cat are more often found in lamina IV (Bennett et. al., 1983, 1984; Enevoldson and Gordon, 1989).

The gross rostrocaudal somatotopy of PSDC neurons has not been explicitly demonstrated in rat, cat or monkey. However, the general somatotopic organization of mechanosensory neurons in the raccoon cervical enlargement has been described by Pubols et al. (1989), and the results were consistent with a previous report on the dermatomal organization of forepaw afferents in this animal (Pubols et al., 1965). Although they did not identify the neurons tested in their study, Pubols et al. (1989) described all those that responded to mechanosensory input to the forelimbs, and likely included PSDC neurons as well as SCT and STT neurons. The results of the present study are in agreement with Pubols et al. (1989) who found that mechanosensory neurons with RFs on glabrous skin regions of the paw were concentrated in the medial half of the cervical enlargement. Also similar to the present study was the authors' finding that neurons with RFs on glabrous skin of the digits were lateral to those with RFs on the palm, but with some overlap in the distribution

of digit and palm representations medially (Pubols et al. 1989). The rostrocaudal organization of PSDC neurons in this study corresponded to the general dermatomal organization of the raccoon forepaw, similar to the findings of Pubols et al. (1989).

6.2 PSDC neuron RF and response properties in raccoon

6.2.1 PSDC neuron RFs in raccoon and a comparison to cat

The raccoon PSDC neurons that were examined in this study had very different RF characteristics than PSDC neurons in cat. In raccoon, PSDC neurons were found to have small, low-threshold RFs, some of which were surrounded by a higher threshold subliminal fringe. The PSDC neuron RFs were, in almost all cases, confined to a single digit or palmar region. In contrast, the majority of PSDC neurons described in cat had large, discontinuous RFs with separate regions of high- and low-threshold (Brown and Fyffe, 1981, 1983; Noble and Riddell, 1988). Most studies of PSDC neurons in cat have described RFs on hairy skin, with very few reports of RFs exclusively on the glabrous skin of the pads. In contrast, most of the PSDC neurons found in this study had RFs that were restricted to glabrous skin regions on the forepaw digits and/or palm. Furthermore, the few PSDC neurons in cat with RFs on glabrous skin always included more than one pad, unlike the predominant finding in raccoon of PSDC neuron RFs on single digits or palmar regions (Noble and Riddell, 1988).

The observed differences between cat and raccoon PSDC neuron RFs may be due, at least in part, to their anatomical location. Most studies in cat have described PSDC neuron RFs on the hindlimb, whereas all of the PSDC neuron RFs in this study

were located on the forelimb. Because mechanosensory RF characteristics differ according to anatomical location within the same animal, it is not unexpected that cat hindlimb and raccoon forelimb PSDC RFs would have different properties.

There are additional factors that could contribute to the unique features of raccoon PSDC neuron RFs. For example, raccoons can grasp and handle objects with exceptional manipulatory ability and use the forepaw as a specialized tactile organ (Iwaniuk and Whishaw, 1999). In contrast, the limbs of cats are primarily adapted for locomotion and not for skilled object manipulation and/or fine tactile discrimination. Given the differences in limb usage, it is not surprising that raccoon PSDC neurons were found to have RFs that were smaller and better defined than in cat. The discrete and smaller RFs would render the raccoon forepaw a more suitable instrument for tasks involving fine spatial discrimination than the cat forepaw.

Given the differences in limb usage between raccoons and cats, it is possible that there is a greater proportion of low-threshold mechanosensory input from forepaw glabrous skin regions to PSDC neurons in raccoon than in cat. Similarly, one might expect a higher proportion of proprioceptive input from the forelimb to PSDC neurons in cat as compared to raccoon. It would be interesting to compare PSDC neuron RFs on the torso of cats vs. raccoons to see if the observed differences are less pronounced for functionally similar anatomical regions.

The predominance of RFs on hairy skin in cat vs. glabrous skin in raccoon seems to be a consistent finding within both the SCT and PSDC systems. Furthermore, it appears that SCT and PSDC neurons in cat are more similar to each other with respect to RF properties than they are to the homologous neuron

populations in raccoon. The physical properties of hairy vs. glabrous skin are different, and it is likely that the functional properties of both SCT and PSDC neurons reflect these differences. This is important because it suggests that discrepancies with respect to PSDC neuron properties in cat vs. raccoon could be partly due to the different RF locations of these cells (i.e. hairy skin in cat vs. glabrous skin in raccoon) and not reflect true species differences. For this reason, it would be useful to compare the response properties of PSDC neurons with RFs on hairy skin in raccoon vs. cat to test more directly for species differences in the PSDC system.

One might expect raccoons to resemble rats and monkeys more closely with respect to PSDC neuron RF properties because these animals also use the forelimb for tactile purposes and have glabrous skin covering the entire palmar surface of the forepaw. However, since there have been no functional descriptions of PSDC neurons with distal RFs in rat or monkey, comparisons to the present study in raccoon are not possible.

6.2.2 Response properties of PSDC neurons in raccoon

It appears that PSDC neurons have a synaptically secure connection to the periphery in raccoon because they were found to exhibit a reliable (mean P(r)=96%), short latency (8.2 ms) response to on-focus stimulation that was tightly coupled to the stimulus onset. The combination of synaptically secure input and small, well-defined RFs (mean RF size=9.9 mm^2) make PSDC neurons good candidates for a role in discriminative aspects of light touch. The small receptive field size would facilitate

the spatial localization of tactile input and the secure connection would enable its reliable transmission to PSDC neurons and to the DCN.

It was estimated from the antidromic latencies observed in the present study that PSDC neurons in raccoon relay information to the cuneate nucleus at velocities of between 9 and 23 m/s. This is within the range of myelinated axons of small to moderate size and similar to Aδ fibers in the periphery(Boivie and Perl, 1975). The range of PSDC axonal conduction velocities in raccoon is similar to previous reports in rat (range: 11-44 m/s, Cliffer and Giesler, 1985) and cat (range: 16-80 m/s, Uddenberg, 1968b; Angaut-Petit, 1975; Brown and Fyffe, 1981, Brown et al., 1983a; Jankowska et al., 1979; Lu et al., 1983), highlighting the similarity across species with respect to the ability of these cells to rapidly transfer peripheral information to the DCN.

The reliable response of PSDC neurons to off-focus electrical but not to mechanical stimulation demonstrates the existence of normally ineffective inputs to PSDC neurons. These inputs can be uncovered by electrical stimulation presumably because of the increased temporal coincidence of inputs as compared to natural (i.e. mechanical) stimulation. The latency of response to electrical stimulation was significantly longer for the off-focus vs. the on-focus digit and the mean difference (1.7 ms) suggests that the off-focus connection could involve as many as three additional synapses. The greater variability and lower probability of response to off-focus stimulation supports the existence of additional synapses in this pathway because the phenomenon of synaptic failure could, at least in part, account for the

difference. Alternatively, longer off-focus latencies could be explained by weaker synapses that are located farther out on the dendrite than on-focus synapses, resulting in a lesser depolarization at the axon hillock.

The higher threshold in response to electrical stimulation of the off-focus digit (mean difference=247μA) indicates that there are more inputs (and/or more effective synapses) from on-focus digits than from adjacent off-focus digits. This difference likely accounts for the stronger response of PSDC neurons to on-focus (mean response: 6 spikes/30 ms) than off-focus digit stimulation (mean response: 4.7 spikes/30 ms).

The results of this study reveal that raccoon PSDC neurons are more similar to PSDC neurons in rat and monkey than they are to cat PSDC neurons in terms of their location, RF characteristics and response properties, supporting hypothesis 1A (p. 56). In addition, raccoon PSDC neurons with RFs on forepaw glabrous skin are similar to published reports of raccoon SCT neurons with respect to RF size and responsiveness to innocuous mechanosensory stimulation, supporting hypothesis 1B.

6.3 Comparison of PSDC and cuneate neurons in raccoon

This study provides evidence that PSDC neurons exert an excitatory influence on cuneate neurons in the absence of peripheral stimulation. However, there is no evidence that PSDC neurons drive cuneate cells in response to mechanosensory input. The combined evidence suggests that PSDC neurons play a supportive role, perhaps by modulating the responsiveness of cuneate neurons to mechanosensory input from

the periphery. The hypothesis that PSDC neurons play a secondary or supportive role in mechanosensation makes sense in light of the fact that cuneate neurons are better suited for the precise localization of touch and the rapid relay of this information to the thalamus. For example, cuneate neurons were found to have significantly smaller RFs than PSDC neurons and the RFs of cuneate cells were always constrained to a single digit or palmar region, unlike PSDC cells.

Our results demonstrate that cuneate and PSDC neurons in raccoon receive somatosensory information from the periphery almost simultaneously and that it takes an additional 3 ms for information from PSDC cells to reach the cuneate nucleus. This finding suggests that the direct, monosynaptic pathway from the periphery to cuneate neurons is the most likely route by which high fidelity sensory information is relayed to the cortex. Cuneate neurons in cat respond best to innocuous stimulation of the skin, hair movement and/or to small changes in joint angle (Kruger et al., 1961). PSDC neurons in cat respond to these same stimuli but are additionally responsive to noxious thermal and/or noxious mechanosensory input (Uddenberg, 1968; Angaut-Petit, 1975; Brown and Fyffe, 1981, Brown et al., 1983a; Jankowska et al., 1979; Lu et al., 1983). Therefore, based on evidence in cat, it appears that cuneate neurons receive less convergence from different sensory submodalities than PSDC neurons, making cuneate cells better suited to encode specific stimulus features.

6.4 Interaction between PSDC and cuneate neurons in raccoon

The results presented in chapter 4 demonstrate the lack of interaction between PSDC and cuneate neurons in response to RF stimulation. When taken together with

results from chapter 3, it is clear that no interaction, either excitatory or inhibitory, occurs during the initial response to stimulation or during later stimulus-dependent cuneate responses (i.e. hypothesis 2E is not supported). In contrast, these experiments reveal the presence of PSDC-cuneate interactions during spontaneous discharge, suggesting a functional connection between PSDC and cuneate neurons in raccoon, supporting hypotheses 2A and 2F. The results of this study are important because they represent the first direct evidence of a functional connection between PSDC and mechanosensory cuneate neurons.

6.4.1 Post-stimulus interactions

One possible explanation for the negative results of the post-stimulus neural CCGs is that cuneate neurons are known to undergo a prolonged period of inhibition (often exceeding 100-200 ms) that immediately follows electrical RF stimulation (Andersen et al. 1964, 1970, 1972; Jabbur and Banna 1968, 1970; Bromberg et al. 1975). Therefore, it is likely that cuneate neurons are incapable of responding to PSDC input that arrives after primary afferent input because these cells have already entered a prolonged post-stimulus period of inhibition. It could be that the post-excitatory period of inhibition is a mechanism that is specifically designed to prevent depolarization of cuneate neurons by transient input from PSDC neurons as well as other convergent sources (Willis and Coggeshall 1991). The faithful transmission of high fidelity information from the periphery requires that it be relayed to the DCN, thalamus and cortex as quickly and efficiently as possible. Sensory information being transmitted centrally has a temporal structure that encodes information about the

peripheral stimulus (Adrian and Zotterman 1926b). Responses of cuneate neurons to transient PSDC input would likely degrade the precise temporal structure of the DC-ML somatosensory relay, possibly resulting in decreased spatiotemporal discrimination.

6.4.2 Spontaneous spinocuneate interactions

The predominant interaction between spontaneously active PSDC and cuneate neurons was an excitatory spinocuneate interaction, meaning that the probability of cuneate neuron firing was increased by the occurrence of a spike in the PSDC neuron and supporting hypothesis 2C. The fact that the maximum interaction between PSDC and cuneate occurred at times after the PSDC neuron had fired suggests the possibility that PSDC neurons exert a tonic excitatory influence on cuneate neurons during spontaneous discharge. The mean delay with respect to the commencement of the significant interaction (10.4 ms) is sufficient to account for the minimum 3 ms it takes for PSDC impulses to travel to the cuneate nucleus via the dorsal columns. In fact, interactions in quadrant I of the neural CCG would not be expected to occur prior to 3 ms for this reason.

It is not possible to make conclusive statements about the anatomical connectivity of interacting neurons based solely on the results of cross-correlations; however, it is reasonable to propose possible geometric configurations that could account for specific findings. For example, the predominance of peak spinocuneate interactions at times later than 3 ms could be indicative of a PSDC to cuneate connection. The more recent finding of PSDC terminations in the vicinity of

cuneothalamic neurons makes this supposition anatomically possible for both direct and/or indirect PSDC to cuneate connection (Cliffer and Willis, 1994).

It should be noted that in 8 of 20 cases, the excitatory spinocuneate interaction commenced at times before 3 ms in the neural CCG. This finding is interpreted to mean that the spinocuneate interactions commenced before impulses from PSDC neurons reached the cuneate nucleus, making it unlikely that they are entirely the result of an anatomical PSDC to cuneate projection. At least some of the spontaneous interaction between PSDC and cuneate neurons must result from a common input to the neuron populations.

One of the most likely sources of common input to PSDC and cuneate neurons is from a group of small-diameter Aδ and C-fibers that are unresponsive to mechanical and thermal stimulation (Handwerker et al., 1991; Meyer et al., 1991). It is possible that these fibers project to both PSDC and cuneate neurons, simultaneously contributing to the spontaneous discharge of these cells (Briner et al., 1988; Patterson et al., 1990; Garrett et al., 1992). Impulses from peripheral input would arrive in the dorsal horn before the cuneate nucleus, causing a potential time lag between PSDC and cuneate neuron firing. This time lag could account for the predominance of excitatory peak interactions at times later than zero in the neural CCG (i.e. after the PSDC neuron has fired).

The same type of argument could be made to explain the 5/20 excitatory spinocuneate interactions where the significant interaction started *before* but reached its peak *after* the PSDC neuron had fired. In this case, the putative common input

would have to arrive in the cuneate nucleus before the dorsal horn in order to explain the observed results. In the case of common input from the periphery, it is possible that one or more interneurons in the dorsal horn could create a sufficient time delay, with the result being that cuneate neurons are activated before PSDC neurons. A possible explanation for the occurrence of peak interactions to the right of time zero (i.e. after the PSDC neuron has fired) is that the interaction is initiated by common input but the peak interaction depends on a combination of common and spinocuneate input.

In addition to the excitatory spinocuneate interactions, one case was observed in which the interaction was inhibitory (i.e. in quadrant IV of the neural CCG). The fact that the inhibitory spinocuneate interaction was observed in only 1/26 cases suggests that it is not the primary type of connection between PSDC and cuneate neurons. However, of all the spinocuneate interactions, the inhibitory interaction had among the highest values of C_{single} and C_{peak}, indicating an important relative contribution of PSDC neurons to this connection type when it occurs.

The number of inhibitory interactions may have been underestimated in this study because of the asymmetry in the sensitivity of the cross-correlation function for excitatory vs. inhibitory connections (Aertsen and Gerstein 1985). It has been demonstrated by Aertsen and Gerstein (1985) that the cross-correlation is much less sensitive for inhibition as compared to excitation of comparable strength. The strong connection strength of the single inhibitory interaction found in this study likely reflects the bias towards detection of only the strongest inhibitory interactions and does not reflect the typical strength of inhibitory connections between PSDC and

cuneate neurons. Inhibitory spinocuneate interactions could result from the same PSDC to cuneate projection or common input as proposed for the excitatory connection because the timing of the maximum interaction (17 ms) falls within the range for the time of maximum excitatory spinocuneate interactions (1-30 ms). The addition of inhibitory interneurons in the cuneate nucleus would alter the putative circuitry and account for the inhibition of cuneate neurons.

The coherence between the input and output signals provides strong evidence that there is a linear relationship between the PSDC neuron input and the cuneate neuron output in raccoon, supporting hypothesis 2D. The fact that the coherence reached a maximum value of 0.7 is not unexpected given previous estimates of input-output coherence using different neuronal models (Stein et al. 1972). In two types of neuronal model (i.e. leaky and perfect integrator) the coherence between input and output signals declined below a value of unity as noise was added to the system (Stein et al. 1972). In addition, the frequency response of the PSDC-cuneate neuron pairs indicates that the interaction can be modeled by a low-pass linear system.

6.4.3 Spontaneous cuneospinal interactions

CCGs consistent with cuneospinal interactions were seldom found in raccoon, perhaps reflecting the dominance of spinocuneate interactions in this animal. In cuneospinal interactions the cuneate neuron fires before the PSDC neuron, suggesting the existence of a direct or indirect projection from cuneate to PSDC neurons. There is some anatomical evidence to support a DCN projection to the spinal cord dorsal horn (Dart 1971; Enevoldson and Gordon 1984). Enevoldson and Gordon (1984) found that

the DCN to dorsal horn projection rarely originated from the cell clusters, arising mostly from caudal reticular regions. In this case, the cuneospinal interaction found in this study could result from an indirect cuneate to PSDC projection via neurons in the caudal reticular region of the cuneate nucleus. In this scenario, neurons in the cuneate cluster region would project to the caudal reticular region which, in turn, would project to PSDC neurons in the dorsal horn.

An alternative anatomical substrate that could account for cuneospinal interactions in the cross-correlation is the existence of a common input to both PSDC and cuneate neurons. Cuneospinal interactions are unlikely to result from common input from the periphery (i.e. Aδ or C-fibers) because these axons would have to excite cuneate neurons at least 17.4 ms in advance of PSDC neurons based on their conduction velocities and the greater distance to the cuneate nucleus. Although this is not impossible, there would have to be many interneurons in the spinal cord dorsal horn to cause a prolonged delay in excitation of PSDC neurons via peripheral input.

Given the fact that cuneate neurons fire before PSDC neurons in cuneospinal interactions, it seems logical to propose that common input could arise from cortical and/or sub-cortical regions of the CNS. Central sources of common input could include the somatosensory cortex (SI and SII), periaqueductal gray, raphe and juxta-raphe regions of the medial reticular formation and the brainstem lateral reticular formation (Engberg et al., 1968; Hall et al., 1982; Morton et al., 1983; Gray and Dostrovsky, 1983). Impulses along such inputs would have to travel a shorter distance to reach the medulla than the cervical cord and could explain the earlier

excitation of cuneate vs. PSDC neurons. When common central input to PSDC and cuneate neurons is inhibitory (e.g. from the cortex), excitatory cuneospinal interactions could still occur secondary to a simultaneous disinhibition of the two cell populations.

The predominant interaction between PSDC and cuneate neurons occurs predominantly, but not exclusively, when the neuron pair has an overlapping RF (i.e. hypothesis 2B is unsupported). This finding suggests a somatotopic organization of the PSDC-cuneate interaction that is incomplete i.e. there is divergence in the system whereby PSDC neurons responsive to one digit interact with cuneate neurons that are responsive to an adjacent digit. The majority of PSDC-cuneate interactions are excitatory and most often occur when PSDC neurons fire in advance of cuneate neurons. In addition to being more abundant, spinocuneate interactions are also significantly stronger than interactions that occur in the cuneate to spinal direction (i.e. cuneospinal) based on the mean values of C_{single} and C_{peak} for each interaction type. Because the amount of RF overlap was the same for both spinocuneate and cuneospinal interactions, it cannot account for the observed differences with respect to connection strength. However, it is possible that differences in connection strength could reflect the relative importance of spinocuneate vs. cuneospinal interactions in raccoon.

6.5 Effect of temporary deafferentation on PSDC neurons in raccoon

One of the hypotheses of this study was that temporary deafferentation of the on-focus digit would cause an increased responsiveness of PSDC neurons to electrical stimulation of the off-focus digit. The rationale for this hypothesis was based on the observation that cuneate neurons develop RFs on the off-focus digits following digit amputation (Rasmusson and Northgrave, 1997). Although immediate shifts in cuneate neuron RFs were not observed in raccoon during temporary deafferentation, it has been proposed that the long term reorganization could involve the immediate unmasking of normally ineffective, off-focus input to PSDC neurons (Rasmusson and Northgrave, 1997). In this scenario, input to PSDC neurons from adjacent digits would become more effective following the removal of dominant inputs (e.g. by digit amputation), enabling PSDC cells to contribute to cuneate neuron activity. If the PSDC to cuneate connection increased in effectiveness over time, it would contribute to long term reorganization but would not be apparent in the cuneate nucleus immediately following digit removal. PSDC neurons in raccoon are good candidates to mediate cuneate nucleus reorganization because they had a significantly lower threshold of response (difference=245μA) to stimulation of the off-focus digit than cuneate neurons.

The results of the temporary deafferentation experiments demonstrated that it is unlikely that immediate unmasking of ineffective input to raccoon PSDC neurons contributes to the RF organization in the cuneate nucleus following digit removal. In

fact, PSDC neurons became even less responsive to stimulation of adjacent digits during deafferentation (i.e. hypothesis 3C is unsupported). Deafferentation had the effect of lengthening the latency of response of PSDC neurons to stimulation of the adjacent digit. In addition, the probability of response to stimulation of the adjacent digit was significantly decreased and there were fewer spikes per response during as compared to before deafferentation.

It has previously been shown by Northgrave and Rasmusson (1996) that temporary deafferentation significantly decreases the spontaneous firing rate of raccoon cuneate neurons in the digit cluster regions. The authors proposed that direct input from primary afferents and/or from PSDC neurons could contribute to the resting discharge of mechanosensory cuneate neurons. In the present study, PSDC neurons were found to have a resting discharge, adding support to the hypothesis that these cells could contribute to the resting discharge of cuneate neurons. However, the fact that PSDC neurons had a significantly lower rate of resting discharge than cuneate neurons in the same animal makes it unlikely that PSDC cells are entirely responsible for cuneate neuron spontaneous activity. In addition, deafferentation caused a significant decrease in the spontaneous activity of PSDC neurons in raccoon (i.e. hypothesis 3A is supported). Thus, it is likely that input from peripheral nerves is at least partly responsible for the spontaneous activity of both PSDC and cuneate neurons. However, the fact that many PSDC-cuneate interactions persisted even during temporary deafferentation indicates that PSDC neurons themselves may have an intrinsically generated spontaneous rate that is capable of driving cuneate neurons in the absence of stimulation (i.e. hypothesis 3B is not supported).

6.6 Putative role of PSDC neurons in raccoon

Based on the results of the present study, it is clear that PSDC and cuneate neurons are functionally connected, but interact only during spontaneous activity in raccoon. The fact that there is no interaction between PSDC and cuneate neurons in response to RF stimulation indicates that PSDC neurons do not play a direct role in the rapid transmission of information about peripheral mechanosensory input. However, the functional connection between PSDC and cuneate neurons could act as a mechanism to gate the response of cells in the cuneate nucleus to incoming somatosensory information. The results of the present study indicate that there is a tonic excitatory facilitation of cuneate neurons that could result from a direct or indirect PSDC to cuneate projection. Changes in the level of PSDC neuron resting discharge could therefore modulate cuneate neuron excitability. Since PSDC neurons in cat receive convergent input from many different sensory submodalities (including both noxious and innocuous), it is possible that these cells play a role in monitoring the general state of the body surface. Using information from the periphery, PSDC neurons could adjust the excitability of neurons in the DCN accordingly. For example, a tissue damaging injury on the body surface could cause an increase in PSDC neuron spontaneous discharge via an increased drive from Aδ and/or C-fibers. An increase in PSDC spontaneous activity would facilitate DCN neurons, increasing the gain of the DC-ML system. In this way, DCN neurons would acquire an increased sensitivity to

input from the periphery, requiring less stimulus contact to reach firing threshold and minimizing further damage to the injured body part.

Dykes and Craig (1998) suggested that PSDC neurons indirectly inhibit cells in the cluster regions via GABA-ergic interneurons at the base of the cuneate nucleus. However, this scenario is unlikely given the results of the present study in which most of the tonic interactions between PSDC and cuneate neurons were excitatory. It is more likely that PSDC neurons exert a tonic facilitatory influence on cuneothalamic neurons, but are themselves regulated via inhibitory GABA-ergic and glycinergic input in the dorsal horn.

Dykes and Craig (1998) may have been led to the conclusion that PSDC neurons indirectly inhibit cuneothalamic neurons because of their use of cobalt chloride to block synaptic transmission in the dorsal horn. Cobalt chloride acts non-specifically to block both excitatory and inhibitory synapses. PSDC neurons receive input via GABA and glycinergic neurons (Maxwell and Kerr, 1995) and the loss of inhibitory input to these cells could cause an increased drive onto cuneate neurons, increasing their responsiveness and accounting for the observations of Dykes and Craig (1998). In support of this hypothesis, Sherman et al. (1997) found that mechanosensory thalamic neurons had increased RF sizes following strychnine-induced blockade of glycinergic synapses in the spinal cord. The finding was unexpected and the authors proposed that disinhibition of PSDC neurons by blocking glycinergic synaptic transmission was the cause (Sherman et al., 1997).

Deafferentation causes a significant decrease in the rate of spontaneous discharge of both PSDC and cuneate neurons, indicating that peripheral input

contributes to the tonic activity in both neural populations. However, interactions between PSDC and cuneate neurons often persisted during temporary deafferentation, despite significantly reduced rates of spontaneous discharge in both neuron populations. This finding suggests that PSDC neurons are partly responsible for driving cuneate neurons in the absence of stimulation, perhaps secondary to an intrinsically generated resting discharge. The neural CCGs before and during temporary deafferentation were similar in shape, indicating that the PSDC-cuneate interaction type was preserved. The single event efficacy (C_{single}) for preserved interactions actually increased on average during deafferentation. This is a surprising result since the spontaneous activity of both PSDC and cuneate neurons was significantly reduced during deafferentation. It is possible that pre-existing PSDC to cuneate connections could become more effective immediately following the removal of common input to these two neuron populations from peripheral Aδ or C-fibers. Unfortunately, the linearity of the PSDC to cuneate connection could not be tested before and during deafferentation because the spontaneous discharge of PSDC and cuneate neurons was too low to perform a frequency response analysis following the injection of lidocaine.

6.7 Technical considerations

The antidromic identification of PSDC neurons in this study involved the stimulation of dorsal column axons rostral to the level of C1. Because the DLF was left intact, the possibility exists that current spread from the stimulating electrode,

exciting axons of SCT neurons in this tract. However, this scenario is unlikely because the stimulating current amplitude used in this study was very low, typically less than 20 μA. It has been estimated that current of this magnitude would spread a distance of approximately 150 μm in the cortex of cat (Asanuma and Sakata, 1967). The current spread along axons in the dorsal columns would likely be less because of the high capacitance of myelin. Furthermore, the spread of current along axons would predominantly occur in the rostrocaudal direction within the dorsal columns and not laterally to the DLF. Based on previous studies in raccoon, it was estimated that the distance from the stimulating electrode to the DLF in the present study was a minimum of 1000 μm (Johnson et al., 1968; Hirata and Pubols, 1989). Therefore, it is not likely that DLF axons were excited by the stimulation, leading to the incorrect identification PSDC neurons.

6.8 Future directions

6.8.1 Testing of putative PSDC to cuneate anatomical connections

To examine the anatomical connectivity between PSDC and thalamic-projecting cuneate neurons in raccoon, an anterograde tracer (e.g. *Phaseolus vulgaris* leucoagglutinin) could be injected into the spinal cord dorsal horn to label axon terminals of PSDC neurons in the cuneate nucleus. A retrograde tracer could then be injected into the VPL thalamus to label thalamic-projecting cuneate neurons. Using light and/or electron microscopy, anatomical connections between PSDC axon terminals and cuneothalamic neurons could be examined.

6.8.2 Testing the effect of disinhibition on PSDC-cuneate interactions

The results of this study suggest that there is a tonic facilitation of cuneate neurons by PSDC neurons during spontaneous activity. The modulation of this interaction could occur via inhibitory input to PSDC neurons in the dorsal horn. One way to test this hypothesis would be to identify spontaneously interacting PSDC-cuneate neuron pairs and test the effect that injection of glycine and/or GABA antagonists (e.g. strychnine and bicuculine, respectively) into the dorsal horn has on the interaction. Increased interaction strength following disinhibition would suggest that inhibitory input acts to gate the PSDC to cuneate excitatory facilitation. Similarly, the addition of glycine and/or GABA into the dorsal horn would be expected to decrease the magnitude of PSDC-cuneate interactions by increasing the inhibitory drive to PSDC neurons.

BIBLIOGRAPHY:

Adrian, E.D. (1928). *The Basis of Sensation. The Action of the Sense Organs.* Reprinted by Hafner Publishing Co., New York, 1964.

Adrian, E.D. (1946). *The Physical Background of Perception.* Oxford Univ. Press, Oxford.

Adrian, E.D. and Zotterman, Y. (1926a). The impulses produced by sensory nerve-endings. Part 2. The response of a single end-organ. J. Physiol. 61: 151-171.

Adrian, E.D. and Zotterman, Y. (1926b). The impulses produced by sensory nerve endings. Part 3. Impulses set up by touch and pressure. J. Physiol. 61: 465-483.

Aersten, A.M.H.J. and Gerstein, G.L. (1985). Evaluation of neuronal connectivity: sensitivity of cross-correlation. Brain Res. 340: 341-354.

Aertsen, A.M.H.J., Gerstein, G.L., Habib, M.K. and Palm, G. D. (1989). Dynamics of neuronal firing correlation: modulation of "effective connectivity". J. Neurophysiol. 61: 900-917.

Al-Chaer, E.D., Lawand, N.B., Westlund, K.N. and Willis, W.D. (1996a). Visceral nociceptive input into the ventral posterolateral nucleus of the thalamus: a new function for the dorsal column pathway. J. Neurophysiol. 76: 2661-2674.

Al-Chaer, E.D., Lawand, N.B., Westlund, K.N. and Willis, W.D. (1996b). Pelvic visceral input into the nucleus gracilis is largely mediated by the postsynaptic dorsal column pathway. J. Neurophysiol. 76: 2675-2690.

Al-Chaer, E.D., Feng, Y. and Willis, W.D. (1998). A role for the dorsal column in nociceptive visceral input into the thalamus of primates. J. Neurphysiol. 79: 3143-3150.

Alloway, K.D., Johnson, M.J. and Wallace, M.B. (1993). Thalamocortical interactions in the somatosensory system: interpretations of latency and cross-correlation analyses. J. Neurophysiol. 70: 892-908.

Alloway, K.D., Wallace, M.B. and Johnson, M.J. (1994). Cross-correlation analysis of cuneothalamic interactions in the rat somatosensory system: influence of receptive field topography and comparisons with thalamocortical interactions. J. Neurophysiol. 72:1949-1972.

Andersen, P., Eccles, J.C., Oshima, T. and Schmidt, R.F. (1964). Mechanisms of synaptic transmisision in the cuneate nucleus. J. Neurophysiol. 27: 1096-1116.

Andersen, P., Etholm, B. and Gordon, G. (1970). Presynaptic and post-synaptic inhibition elicited in the cat's dorsal column nuclei by mechanical stimulation of the skin. J. Physiol. 210: 433-455.

Andersen, P., Gjerstad, L. and Pasztor, E. (1972). Effects of cooling on inhibitory processes in the cuneate nucleus. Acta Physiol. Scand. 84: 448-461.

Angaut-Petit, D. (1975). The dorsal column system: I Existence of long ascending postsynaptic fibres in the cat's fasciculus gracilis. Exp. Brain Res. 22: 457-470.

Apkarian, A.V. and Hodge, J.J. (1989a). The primate spinothalamic pathways: II. The cells of origin of the dorsolateral and ventral spinothalamic pathways. J. Comp. Neurol. 288: 474-492.

Apkarian, A.V. and Hodge, C.J. (1989b). The primate spinothalamic pathways: III. Thalamic terminations of the dorsolateral and ventral spinothalamic pathways. J. Comp. Neurol. 288: 493-511.

Apkarian, A.V. and Hodge, C.J. (1989c). A dorsolateral spinothalamic tract in macaque monkey. Pain 37: 323-333.

Appelberg, B., Bessou, P. and Laporte, Y. (1966). Action of static and dynamic fusimotor fibres on secondary endings of cat's spindles. J. Physiol. 185: 160-171.

Applebaum, A.E., Beall, J.E., Foreman, R.D. and Willis, W.D. (1975). Organization and receptive fields of primate spinothalamic tract neurons. J. Neurophysiol. 38: 572-586.

Asanuma, H. and Sakata, H. (1967). Functional organization of a cortical efferent system examined with focal depth stimulation in cats. J. Neurophysiol. 30: 35-54.

Azulay, A. and Schwartz, A. (1975). The role of the dorsal funiculus of the primate in tactil discrimination. Exp. Neurol. 46: 315-332.

Barker, D. (1962). The structure and distribution of muscle receptors. In: *Symposium on Muscle Receptors*. D. Barker, ed. Hong Kong Univ. Press, Hong Kong.

Beck, C.H.M. (1981). Mapping of forelimb afferents to the cuneate nuclei of the rat. Brain Res. Bull. 6: 503-516.

Bendat, J.S. and Piersol, A.G. (1980). *Engineering applications of correlation and spectral analysis*. John Wiley and Sons, Inc., New York.

Bennett, G.J., Abdelmoumene, M., Hayashi, H. and Dubner, R. (1980). Physiology and morphology of substantia gelatinosa neurons intracellularly stained with horseradish peroxidase. J. Comp. Neurol. 194: 809-827.

Bennett, G.J., Seltzer, Z., Lu, G.W., Nishikawa, N. and Dubner, R. (1983). The cells of origin of the dorsal column postsynaptic projection in the lumbosacral enlargements of cats and monkeys. Somatosensory Res. 1: 131-149.

Bennett, G.J., Nishikawa, N., Lu, G.W., Hoffert, M.J. and Dubner, R. (1984). The morphology of dorsal column postsynaptic (DCPS) spino-medullary neurons in the cat. J. Comp. Neurol. 224: 568-578.

Berkley, K.J. (1975). Different targets of different neurons in nucleus gracilis of the cat. J. Comp. Neurol. 163: 285-304.

Berkley, K.J. and Hand, P.J. (1978). Efferent projections of the gracile nucleus in the cat. Brain Res. 153: 263-283.

Berkley, K.J. (1980). Spatial relationships between the terminations of somatic sensory and motor pathways in the rostral brainstem of cats and monkeys. I. Ascending somatic sensory inputs to lateral diencephalon. J. Comp. Neurol. 193: 283-317.

Blair, R.W., Weber, R.N. and Foreman, R.D. (1981). Characteristics of primate spinothalamic tract neurons receiving viscerosomatic convergent inputs in the T3-T5 segments. J. Neurophysiol. 46: 797-811.

Blomqvist, A. (1980). Gracilo-diencephalic relay cells: a quantitative study in the cat using retrograde transport of horseradish peroxidase. J. Comp. Neurol. 193: 1097-1125.

Blomqvist, A. and Westman, J. (1975). Combined HRP and Fink-Heimer staining applied on the gracile nucleus in the cat. Brain Res. 99: 339-342.

Boivie, J. (1970). The termination of the cervicothalamic tract in the cat. An experimental study with silver degeneration methods. Exp. Brain Res. 12:331-353.

Boivie, J. (1971a). The termination of the spinothalamic tract in the cat. An experimental study with silver degeneration methods. Exp. Brain Res. 12:331-353.

Boivie, J. (1971b). The termination in the thalamus and the zona incerta of fibers from the dorsal column nuclei (DCN) in the cat. An experimental study with silver impregnation methods. Brain Res. 28: 459-490.

Boivie, J. (1978). Anatomical observations on the dorsal column nuclei, their thalamic projection and the cytoarchitecture of some somatosensory thalamic nuclei in the monkey. J. Comp. Neurol. 186: 343-370.

Boivie, J. (1979). An anatomical reinvestigation of the termination of the spinothalamic tract in the monkey. J. Comp. Neurol. 186: 343-370.

Boivie, J. (1980). Thalamic projections from lateral cervical nucleus in monkey. A degeneration study. Brain Res. 198: 13-26.

Boivie, J. and Perl, E.R. (1975). Neural substrates of somatic sensation. In: *MTP International Review of Science*, Physiology Series One, Vol. 3, *Neurophysiology*. C.C. Hunt, ed. Univ. Park Press, Baltimore.

Boring, E.G. (1942) *A History of Experimental Psychology*, 2nd edition, Prentice-Hall, London.

Briner, R.P., Carlton, S.M., Coggeshall, R.E. and Chung, K. (1988) Evidence for unmyelinated sensory fibres in the posterior columns in man. Brain 111: 999-1007.

Bromberg, M.B., Blum, P. and Whitehorn, D. (1975). Quantitative characteristics of inhibition in the cuneate nucleus of the cat. Exp. Neurol. 48: 37-56.

Brown, A.G. (1973). Ascending and long spinal pathways: dorsal columns, spinocervical tract and spinothalamic tract. In: *Handbook of Sensory Physiology*, Vol. II. *Somatosensory System*. A. Iggo, ed. Springer-Verlag, New York

Brown, A.G. (1981). *Organization in the Spinal Cord: The Anatomy and Physiology of Identified Neurones*. Springer-Verlag, Berlin.

Brown, A.G. and Franz, D.N. (1969). Responses of spinocervical tract neurones to natural stimulation of identified cutaneous receptors. Exp. Brain Res. 7: 231-249.

Brown, A.G., Hamann, W.C. and Martin, H.F. (1973a). Interactions of cutaneous myelinated (A) and non-myelinated (C) fibres on transmission through the spinocervical tract. Brain Res. 53: 222-226.

Brown, A.G., Hamann, W.C. and Martin, H.F. (1973b). Descending influences on spinocervical tract cell discharges evoked by non-myelinated cutaneous afferent nerve fibres. Brain Res. 53: 222-226.

Brown, A.G., Kirk, E.J. and Martin, H.F. (1973c). Descending and segmental inhibition of transmission through the spinocervical tract. J. Physiol. 230: 689-705.

Brown, A.G., Hamann, W.C. and Martin, H.F. (1975). Effects of activity in non-myelinated afferent fibres on the spinocervical tract. Brain Res. 98: 243-259.

Brown, A.G., House, C.R., Rose, P.K. and Snow, P.J. (1976). The morphology of spinocervical tract neurones in the cat. J. Physiol. 260: 719-738.

Brown, A.G., Coulter, J.D., Rose, P.K., Short, A.D. and Snow, P.J. (1977a). Inhibition of spinocervical tract discharges from localized areas of the sensorimotor cortex in the cat. J. Physiol. 264: 1-16.

Brown, A.G., Rose, P.K. and Snow, P.J. (1977b). The morphology of spinocervical tract neurones revealed by intracellular injection of horseradish peroxidase. J. Physiol. 270: 747-764.

Brown, A.G., Fyffe, R.E.W., Noble, R., Rose, P.K. and Snow, P.J. (1980). The density, distribution and topographical organization of spinocervical tract neurones in the cat. J. Physiol. 300: 409-428.

Brown, A.G. and Fyffe, R.E.W. (1981). Form and function of dorsal horn neurones with axons ascending the dorsal columns in cat. J. Physiol. 321: 31-47.

Brown, A.G., Brown, P.B., Fyffe, R.E.W. and Pubols, L.M. (1983). Receptive field organization and response properties of spinal neurones with axons ascending the dorsal columns in the cat. J. Physiol. 337: 575-588.

Brown, A.G., Noble, R. and Riddell, J.S. (1986). Relations between spinocervical and postsynaptic dorsal column neurones in the cat. J. Physiol. 381: 333-349.

Brown, A.G., Koerber, H.R. and Noble, R. (1987). An intracellular study of spinocervical tract cell responses to natural stimuli and single hair afferent fibres in cats. J. Physiol. 382: 331-354.

Bryan, R.N., Trevino, D.L., Coulter, J.D. and Willis, W.D. (1973). Location and somatotopic organization of the cells of origin of the spinocervical tract. Exp. Brain Res. 17: 177-189.

Bryan, R.N., Coulter, J.D. and Willis, W.D. (1974). Cells of origin of the spinocervical tract in the monkey. Exp. Neurol. 42: 574-586.

Burgess, P.R. and Perl, E.R. (1967). Myelinated afferent fibres responding specifically to noxious stimulation of the skin. J. Physiol. 190: 541-562.

Burgess, P.R. and Perl, E.R. (1973). Cutaneous mechanoreceptors and nociceptors. In *Handbook of Sensory Physiology II, Somatosensory System*. A. Iggo, ed. Springer-Verlag, Berlin.

Burgess, P.R., Petit, D. and Warren, R.M. (1968). Receptor types in cat hairy skin supplied by myelinated fibers. J. Neurophysiol. 31: 833-848.

Burgess, P.R. and Horch, K.W. (1978). The distinction between the short and intermediate ascending pathways in the fasciculus gracilis of the cat. Brain Res. 151: 579-580.

Carpenter, M.B., Stein, B.M. and Shriver, J.E. (1968). Central projections of spinal dorsal roots in the monkey. II. Lower thoracic, lumbosacral and coccygeal dorsal roots. Amer. J. Anat. 123: 75-118.

Carstens, E. and Trevino, D.L. (1978). Laminar origins of spinothalamic projections in the cat as determined by the retrograde transport of horseradish peroxidase. J. Comp. Neurol. 182: 151-166.

Cervero, F., Iggo, A. and Molony, V. (1977). Responses of spinocervical tract neurones to noxious stimulation of the skin. J. Physiol. 267: 537-558.

Cervero, F., and Iggo, A. (1980). The substantia gelatinosa of the spinal cord. A critical review. Brain 103: 717-772.

Cheek, M.D., Rustioni, A. and Trevino, D.L. (1975). Dorsal column nuclei projections to the cerebellar cortex in cats as revealed by the use of the retrograde transport of horseradish peroxidase. J. Comp. Neurol. 164: 31-46.

Cheema, S., Whitsel, B.L. and Rustioni, A. (1983). The corticocuneate pathway in the cat: relation among terminal distribution patterns, cytoarchitecture, and single functional properties. Somatosensory Res. 1: 169-205.

Christensen, B.N. and Perl, E.R. (1970). Spinal neurons specifically excited by noxious or thermal stimuli: marginal zone of the dorsal horn. J. Neurophysiol. 33: 293-307.

Chung, J.M., Kenshalo, D.R., Jr., Gerhart, K.D. and Willis, W.D. (1979). Excitation of primate spinothalamic neurons by cutaneous C-fiber volleys. J. Neurophysiol. 42: 1354-1369.

Chung, J.M., Surmeier, D.J., Lee, K.H., Sorkin, L.S., Honda, C.N., Tsong, Y. and Willis, W.D. (1986). Classification of primate spinothalamic and somatosensory thalamic neurons based on cluster analysis. J. Neurophysiol. 56: 308-327.

Chung, K., McNeill, D.L., Hulsebosch, C.E. and Coggeshall, R.E. (1989). Changes in dorsal horn synaptic disc numbers following unilateral dorsal rhizotomy. J. Comp. Neurol. 283: 568-577.

Clark, F.J., Burgess, R.C., Chapin, J.W. and Lipscomb, W.T. (1985). Role of intramuscular receptors in the awareness of limb position. J. Neurophysiol. 54: 1529-1540.

Cliffer, K.D. and Giesler, G.J. (1989). Postsynaptic dorsal column pathway of the rat. III. Distribution of ascending afferent fibers. J. Neurosci. 9: 3146-3168.

Cliffer, K.D and Willis, W.D. (1994). Distribution of the postsynaptic dorsal column projection in the cuneate nucleus of monkeys. J. Comp. Neurol. 345: 84-93.

Clifton, G.L., Coggeshall, R.E., Vance, W.H. and Willis, W.D. (1976). Receptive fields of unmyelinated ventral root afferent fibres in the cat. J. Physiol. 256: 573-600.

Coggeshall, R.E., Hong, K.A.P., Langford, L.A., Schaible, H.G. and Schmidt, R.F. (1983). Discharge characteristics of fine medial articular afferents at rest and during passive movements of inflamed knee joints. Brain Res. 272: 185-188.

Cooley, J.W. and Tukey, J.W. (1965). An algorithm for the machine calculation of complex Fourier series. Math. Of comput. 19: 297-301.

Craig, A.D. (1989). Ascending lamina I axons in the cat are concentrated in the middle of the lateral funiculus. Neurosci. Abstr. 15, 1190.

Craig, A.D. and Burton, H. (1981). Spinal and medullary lamina I projection to nucleus submedius in medial thalamus: a possible pain center. J. Neurophysiol. 45: 433-466.

Craig, A.D. and Burton, H. (1985). The distribution and topographical organization in the thalamus of anterogradely-transported horseradish peroxidase after spinal injections in cat and raccoon. Exp. Brain Res. 58: 227-254.

Craig, A.D. and Tapper, D.N. (1985). A dorsal spinal neural network in cat. III. Dynamic nonlinear analysis of responses to random stimulation of single type I cutaneous fibers. J. Neurophysiol. 53: 995-1015.

Culberson, J.L. and Brushart, T.M. (1989). Somatotopy of digital nerve projections to the cuneate nucleus in the monkey. Somatosensory Motor Res. 6: 319-330.

Dart, A.M. (1971). Cells of the dorsal column nuclei projecting down into the spinal cord. J. Physiol. 219: 29-30P.

De Biasi, S., Vitellaro-Zuccarello, L., Bernardi, P., Valtschanoff, J.G., Weinberg, R.J. (1975). Ultrastructural and immunocytochemical characterization of terminals of postsynaptic ascending dorsal column fibers in the rat cuneate nucleus. J. Comp. Neurol. 353: 109-118.

de Pommery, J., Roudier, F. and Menetrey, D. (1984). Postsynaptic fibers reaching the dorsal column nuclei in rat. Neurosci. Lett. 50: 319-323.

Dodt, E. and Zotterman, Y. (1952). Mode of action of warm receptors. Acta Physiol. Scand. 26: 345-357.

Dodt, E. (1952). The behaviour of thermoreceptors at low and high temperatures with special reference to Ebbecke's temperature phenomena. Acta Physiol. Scand. 27: 295-314.

Downie, J.W., Ferrington, D.G., Sorkin, L.S. and Willis, W.D. (1988). The primate spinocervicothalamic pathway: responses of cells of the lateral cervical nucleus and spinocervical tract to innocuous and noxious stimuli. J. Neurophysiol. 59: 861-885.

Dykes, R.W., Rasmusson, D.D., Sretavan, D. and Rehman, N.B. (1982). Submodality segregation and receptive-field sequences in cuneate, gracile and external cuneate nuclei of the cat. J. Neurophysiol. 47: 389-416.

Dykes, R.W. and Craig, A.D. (1998). Control of size and excitability of mechanosensory receptive fields in dorsal column nuclei by homolateral dorsal horn neurons. J. Neurophysiol. 80: 120-129.

Edwards, S.B. (1972). The ascending and descending projections of the red nucleus in the cat: an experimental study using an autoradiographic tracing method. Brain Res. 48: 45-63.

Ellis, L.C. and Rustioni, A. (1981). A correlative HRP, Golgi and EM study of the intrinsic organization of the feline dorsal column nuclei. J. Comp. Neurol. 197: 341-367.

Enevoldson, T.P. and Gordon, G. (1984). Spinally projecting neurones in the dorsal column nuclei: distribution, dendritic trees and axonal projections. Exp. Brain Res. 54: 201-205.

Enevoldson, T.P. and Gordon, G. (1989a). Postsynaptic dorsal column neurons in the cat: a study with retrograde transport of horseradish peroxidase. Exp. Brain Res. 75: 611-620.

Enevoldson, T.P. and Gordon, G. (1989b). Spinocervical neurons and dorsal horn neurons projecting to the dorsal column nuclei through the dorsolateral fascicle: a retrograde HRP study in the cat. Exp. Brain Res. 75: 621-630.

Engberg, I., Lundberg, A. and Ryall, R.W. (1968). Reticulospinal inhibition of transmission in reflex pathways. J. Physiol. 194: 201-223.

Erlanger, J. and Gasser, H.S. (1937). *Electrical Signs of Nervous Activity*, Univ. Pennsylvania Press, Philadelphia.

Erulkar, S.D., Sprague, J.M., Whitsel, B.L., Dogan, S. and Jannetta, P.J. (1966). Organization of the vestibular projection to the spinal cord of the cat. J. Neurophysiol. 29: 626-664.

Ferraro, A. and Barrera, S.E. (1935a). The nuclei of the posterior funiculi in Macacus rhesus. An anatomic and experimental investigation. Arch. Neurol. Psychiat. 33: 262-275.

Ferraro, A. and Barrera, S.E. (1935b). Posterior column fibers and their termination in Macacus rhesus. J. Comp. Neurol. 62: 507-530.

Ferrington, D.G. Sorkin, L.S. and Willis, W.D. (1987). Responses of spinothalamic tract cells in the superficial dorsal horn of the primate lumbar spinal cord. J. Physiol. 388: 681-703.

Fetz, E.E. (1968). Pyramidal tract effects on interneurons in the cat lumbar dorsal horn. J. Neurophysiol. 31: 69-80.

Fleetwood-Walker, S.M., Mitchell, R., Hope, P.J., Molony, V. and Iggo, A. (1985). An α_2 receptor mediates the selective inhibition by noradrenaline of nociceptive responses of identified dorsal horn neurones. Brain Res. 334: 243-254.

Florence, S.L., Wall, J.T. and Kaas, J.H. (1989). Somatotopic organization of inputs from the hand to the spinal gray and cuneate nucleus of monkeys with observations on the cuneate nucleus of humans. J. Comp. Neurol. 286: 48-70.

French, A.S. and Holden, V. (1971). Alias-free sampling of neuronal spike trains. Kybernetik 8: 165-171.

Fyffe, R.E.W., Cheema, S.S. and Rustioni, A. (1986). Intracellular staining study of the feline cuneate nucleus. I. Terminal patterns of primary afferent fibers. J. Neurophysiol. 56: 1268-1283.

Gasser, H.S. (1950). Unmedullated fibers originating in dorsal root ganglia. J. Gen. Physiol. 3: 651-690.

Giesler, G.J., Cannon, J.T., Urca, G. and Liebeskind, J.C. (1978). Long ascending projections from substantia gelatinosa Rolandi and the subjacent dorsal horn in the rat. Science 202: 984-986.

Giesler, G.J. Yezierski, R.P., Gerhart, K.D. and Willis, W.D. (1981). Spinothalamic tract neurons that project to medial and/or lateral thalamic nuclei: evidence for a physiologically novel population of spinal cord neurons. J. Neurophysiol. 46: 1285-1308.

Giesler, G.J., Nahin, R.L. and Madsen, A.M. (1984). Postsynaptic dorsal column pathway of the rat. I. Anatomical studies. J. Neurophysiol. 51: 260-275.

Giesler, G.J. and Cliffer, K.D. (1985). Postsynaptic dorsal column pathway of the rat. II Evidence against an important role in nociception. Brain Res. 326: 347-356.

Giesler, G.J., Bjorkeland, M., Xu, Q. and Grant, G. (1988). Organization of the spinocervicothalamic pathway in the rat. J. Comp. Neurol. 268: 223-233.

Glees, P. and Soler, J. (1951). Fibre content of the posterior column and synaptic connections of nucleus gracilis. Z. Zellforsch. 36: 381-400.

Gobel, S. (1975). Golgi studies of the substantia gelatinosa neurons in the spinal trigeminal nucleus of the adult cat. Brain Res. 83: 83: 333-338.

Gobel, S. (1978a). Golgi studies of the neurons in layer I of the dorsal horn of the medulla (trigeminal nucleus caudalis). J. Comp. Neurol. 180: 375-394.

Gobel, S. (1978b). Golgi studies of the neurons in layer II of the dorsal horn of the medulla (trigeminal nucleus caudalis). J. Comp. Neurol. 180: 395-414.

Gobel, S. (1979). Neural circuitry in the substantia gelatinosa of Rolando: anatomical insights. Adv. Pain Res. Ther. 3: 175-195.

Gobel, S. Falls, W.M., Bennett, G.J., Hayashi, H. and Humphrey, E. (1980). An EM analysis of the synaptic connections of horseradish peroxidase-filled stalked cells and islet cells in the substantia gelatinosa of adult cat spinal cord. J. Comp. Neurol. 194: 781-807.

Gochin, P.M., Kaltenbach, J.A. and Gerstein, G.L. (1989). Coordinated activity of neuron pairs in anesthetized rat dorsal cochlear nucleus. Brain Res. 497: 1-11.

Gordon, G. and Grant, G. (1982). Dorsolateral spinal afferents to some medullary sensory nuclei: an anatomical study in the cat. Exp. Brain Res. 46: 12-23.

Gowers, W.R. (1878). A case of unilateral gunshot injury to the spinal cord. Trans. Clin. London 11: 24-32.

Gray, B.G. and Dostrovsky, J.O. (1983) Descending inhibitory influences from periaqueductal gray, nucleus raphe magnus, and adjacent reticular formation. I. Effects on lumbar spinal cord nociceptive and nonnociceptive neurons. J. Neurophysiol. 49: 932-947.

Grigg, P., Schaible, H.G. and Schmidt, R.F. (1986). Mechanical sensitivity of group III and IV afferents from posterior articular nerve in normal and inflamed cat knee. J. Neurophysiol. 55: 635-643.

Groenewegen, H.J., Boesten, A.J.P. and Voogd, J. (1975). The dorsal column nuclear projections to the nucleus ventralis posterior lateralis thalami and the inferior olive in the cat. An autoradiographic study. J. Comp. Neurol 162: 505-518.

Gulley, R.L. (1973) Golgi studies of the nucleus gracilis in the rat. Anat. Rec. 177: 325-342.

Ha, H., Kitai, S.T. and Morin, F. (1965). The lateral cervical nucleus of the raccoon. Exp. Neurol. 11: 441-450.

Hagen, E., Knoche, H., Sinclair, D.C., and Weddell, G. (1953). The role of specialized nerve terminals in cutaneous sensibility. Proc. R. Soc. B. 141: 279-87.

Hall, J.G., Duggan, A.W., Morton, C.R. and Johnson, S.M. (1982). The location of brainstem neurones tonically inhibiting dorsal horn neurones of the cat. Brain Res. 244: 214-222.

Hancock, M.B. (1982). A serotonin-immunoreactive fiber system in the dorsal columns of the spinal cord. Neurosci. Lett. 31: 247-252.

Hand, P.J. (1966). Efferent projections of the nucleus gracilis. Anat. Rec. 154: 353-354.

Hand, P.J. and van Winkle, T. (1977). The efferent connections of the feline nucleus cuneatus. J. Comp. Neurol. 171: 83-110.

Handwerker, H.O., Iggo, A. and Zimmerman, M. (1975). Segmental and supraspinal actions on dorsal horn neurons responding to noxious and non-noxious skin stimuli. Pain 1: 147-165.

Heinbecker, P., Bishop, G.H. and O'Leary, J.L. (1933). Pain and touch fibers in peripheral nerves. Arch. Neurol. Psychiat. 29: 771-789.

Heinbecker, P., Bishop, G.H. and O'Leary, J.L. (1934). Analysis of sensation in terms of the nerve impulse. Arch Neurol. Psychiat. 31: 34-53.

Hendry, S.H., Hsiao, S.S. and Brown, M.C. (1999). Fundamentals of sensory systems. In: *Fundamental Neuroscience.* M.J. Zigmond, F.E. Bloom, S.C. Landis, J.L. Roberts and L.R. Squire eds. Academic Press, New York.

Hensel, H. and Zotterman, Y. (1951). The response of the cold receptors to constant cooling. Acta Physiol. Scand. 22: 96-105.

Hensel, H., Iggo, A. and Witt, I. (1960). A quantitative study of sensitive cutaneous thermoreceptors with C afferent fibres. J. Physiol. 153: 113-126.

Herrnstein, R.J., Boring, E.G. (1965) *A Source Book in the History of Psychology*, Harvard University Press, Cambridge.

Hirata, H. and Pubols, B.H. (1989). Spinocervical tract neurons responsive to light mechanical stimulation of the raccoon forepaw. J. Neurophysiol. 61(1): 138-148.

Hongo, T. Jankowska, E. and Lundberg, A. (1968). Post-synaptic excitation and inhibition from primary afferents in neurones of the spinocervical tract. J. Physiol. 199: 569-592.

Horch, K.W., Burgess, P.R. and Whitehorn, D. (1976). Ascending collaterals of cutaneous neurons in the fasciculus gracilis of the cat. Brain Res. 117: 1-17.

Houk, J. and Henneman, E. (1967). Responses of Golgi tendon organs to active contractions of the soleus muscle of the cat. J. Neurophysiol. 30: 466-481.

Howe, J.R. and Zieglgansberger, W. (1987). Responses of rat dorsal horn neurons to natural stimulation and to iontophoretically applied norepinephrine. J. Comp. Neurol. 255: 1-17.

Hummelsheim, H., Wiesendanger, R., Wiesendanger, M. and Bianchetti, M. (1985). The projection of low-threshold muscle afferents of the forelimb to the main and external cuneate nuclei of the monkey. Neuroscience 16: 979-987.

Hunt, C.C. (1954). Relation of function to diameter in afferent nerve fibers of muscle nerves. J. Gen. Physiol. 38: 117-131.

Hunt, C.C. (1961). On the nature of vibration receptors in the hind limb of the cat. J. Physiol. 155: 175-186.

Hunt, C.C. and McIntyre, A.K. (1960). An analysis of fibre diameter and receptor characteristics of myelinated cutaneous afferent fibres in cat. J. Physiol. 153: 99-112.

Hursh, J.B. (1939). Conduction velocity and diameter of nerve fibers. Amer. J. Physiol. 127: 131-139.

Iggo, A. (1959). Cutaneous heat and cold receptors with slowly conducting C afferent fibres. Quart. J. Exp. Physiol. 44: 362-370.

Iggo, A. (1960). Cutaneous mechanoreceptors with afferent C fibres. J. Physiol. 152: 337-353.

Iggo, A. and Ogawa, H. (1977). Correlative physiological and morphological studies of rapidly adapting mechanoreceptors in cat's glabrous skin. J. Physiol. 266: 275-296.

Imai, Y. and Kusama, T. (1969). Distribution of the dorsal root fibers in the cat. An experimental study with the Nauta method. Brain Res. 13: 338-359.

Iriuchijima, J. and Zotterman, Y. (1960). The specificity of afferent cutaneous C fibres in mammals. Acta Physiol. Scand. 49: 267-278.

Iwaniuk, A.N. and Whishaw, I.Q. (1999). How skilled are the skilled limb movements of the raccoon (Procyon lotor)? Behav. Brain Res. 99: 35-44.

Jabbur, S.J. and Banna, N.R. (1968). Presynaptic inhibition of cuneate transmission by wide-spread cutaneous inputs. Brain Res. 10: 273-276.

Jabbur, S.J. and Banna, N.R. (1970). Widespread cutaneous inhibition in dorsal column nuclei. J. Neurophysiol. 33: 616-624.

Jankowska, E., Rastad, J. and Zarzecki, P. (1979). Segmental and supraspinal input to cells of origin of nonprimary fibres in the feline dorsal columns. J. Physiol. 290: 185-200.

Jankowska, E., Hammar, I., Djouhri, L., Heden, C., Szabo Lackberg, Z. and Yin, X.-K. (1997). Modulation of responses of four types of feline ascending tract neurons by serotonin and noradrenaline.

Jiao, S.S., Zhang, G.F., Liu, Y.J., Wang, Y.S. and Lu, G.W. (1984). Double labelling of cat spinal dorsal horn neurons with fluorescent substances. Pain 2: suppl. S130.

Johnson, J.I., Welker, W.I. and Pubols, B.H. (1968). somatotopic organization of raccoon dorsal column nuclei. J. Comp. Neurol. 132: 1-44.

Jones, M.W., Hodge, C.J., Apkarian, A.V. and Stevens, R.T. (1985). A dorsolateral spinothalamic pathway in cat. Brain Res. 335: 188-193.

Jones, M.W., Apkarian, A.V., Stevens, R.T. and Hodge, C.J. (1987). the spinothalamic tract: an examination of the cells of origin of the dorsolateral and ventral spinothalamic pathways in cats. J. Comp. Neurol. 260: 349-361.

Joseph, B.S. and Whitlock, D.G. (1968). Central projections of selected spinal dorsal roots in anuran amphibians. Anat. Rec. 160: 279-288.

Kajander, K.C. and Giesler, G.J. (1987). Responses of neurons in the lateral cervical nucleus of the cat to noxious cutaneous stimulation. J. Neurophysiol. 57: 1686-1704.

Kamogawa, H. and Bennett, G.J. (1986). Dorsal column postsynaptic neurons in the cat are excited by myelinated nociceptors. Brain Res. 364: 386-390.

Kappers, C.U.A., Huber, G.C. and Crosby, E.C. (1936). *The Comparative Anatomy of the Nervous System of Vertebrates, Including Man*. Hafter, New York. (Reprinted in 1960).

Keele, K.D. (1957). *Anatomies of Pain*. Charles A. Thomas, Springfield

Kerr, F.W.L. (1968). The descending pathway to the lateral cuneate nucleus, the nucleus of Clarke and the ventral horn. Anat. Rec. 160: 375.

Kitai, S.T., Ha, H. and Morin, F. (1965). Lateral cervical nucleus of the dog: anatomical and microelectrode studies. Amer. J. Physiol. 209: 307-311.

Kress, M. and Zeilhofer, H.U. (1999). Capsaicin, protons and heat: new excitement about nociceptors. TIPS 20: 112-118.

Kruger, L. and Witkovsky, P. (1961). A functional analysis of neurons in the dorsal column nuclei and spinal nucleus of the trigeminal in the reptile. J. Comp. Neurol. 117: 97-105.

Kruger, L., Perl, E.R. and Sedivec, M.J. (1981). Fine structure of myelinated mechanical nociceptor endings in cat hairy skin. J. Comp. Neurol. 198: 137-154.

Kumazawa, T., Mizumura, K. and Sato, J. (1987). Response properties of polymodal receptors using in vitro testis superior spermatic nerve preparations of dogs. J. Neurophysiol. 57: 702-711.

Kuypers, H.G.J.M. and Tuerck, J.D. (1964). The distribution of the cortical fibers within the nuclei cuneatus and gracilis in the cat. J. Anat. 98: 143-162.

Landon, D.N. (1976). *The Peripheral Nerve*. John Wiley and Sons, New York.

Levick, W.R., Cleland, B.G. and Dubin, M.W. (1972). Lateral geniculate neurons of cat: retinal inputs and physiology. Invest. Ophthamol. 11: 302-311.

Lewis, T. and Pochin, E.E. (1938a). The double pain response of the human skin to a single stimulus. Clin. Sci. 3: 67-76.

Lewis, T. and Pochin, E.E. (1938b). Effects of asphyxia and pressure on sensory nerves of man. Clin. Sci. 3: 141-155.

Light, A.R. and Perl, E.R. (1979). Spinal termination of functionally identified primary afferent neurons with slowly conducting myelinated fibres. J. Comp. Neurol. 186: 133-150.

Light, A.R. and Kavookjian, A.M. (1988). Morphology and ultrastructure of physiologically identified substantia gelatinosa (lamina II) neurons with axons that terminate in deeper dorsal horn laminae (III-V). J. Comp. Neurol. 267: 172-189.

Lima, D. and Coimbra, A. (1988). The spinothalamic system of the rat: structural types of retrogradely labeled neurons in the marginal zone (lamina I). Neuroscience 27: 215-230.

Lloyd, D.P.C. and Chang, H.T. (1948). Afferent fibers in muscle nerves. J. Neurophysiol. 11: 199-208.

Lu, G.W., Bennett, G.J., Nishikawa, N., Hoffert, M.J. and Dubner, R. (1983). Extra- and intracellular recordings from dorsal column postsynaptic spinomedullary neurons in the cat. Exp. Neurol. 82: 456-477.

Lu, G.W., Bennett, G.J., Nishikawa, N. and Dubner, R. (1985). Spinal neurons with branched axons traveling in both the dorsal and dorsolateral funiculi. Exp. Neurol. 87: 571-577.

Lundberg, A. and Oscarsson, O. (1961). Three ascending spinal pathways in the dorsal part of the lateral funiculus. Acta Physiol. Scand. 51: 1-16.

Lund, R.D. and Webster, K.E. (1967). Thalamic afferents from the spinal cord and trigeminal nuclei. An experimental anatomical study in the rat. J. Comp. Neurol. 130: 313-328.

Matsushita, M. (1969). Some aspects of the interneuronal connections in cat's spinal grey matter. J. Comp. Neurol. 136: 57-80.

Matsushita, M. (1970). The axonal pathways of spinal neurons in the cat. J. Comp. Neurol. 138: 391-418.

Maxwell, D.J. and Bannatyne, B.A. (1983). Ultrastructure of muscle spindle afferent terminations in lamina VI of the cat spinal cord. Brain Res. 288: 297-301.

Maxwell, D.J. and Koerber, H.R. (1986). Fine structure of collateral axons originating from feline spinocervical tract neurons. Brain Res. 363: 199-203.

Maxwell, D.J. and Kerr (1995) Colocalization of glycine and GABA in synapses on spinomedullary neurons. Brain Res. 690: 127-132.

Maxwell, D.J., Koerber, H.R. and Bannatyne, B.A. (1995). Light and electron microscopy of contacts between primary afferent fibres and neurones with axons ascending the dorsal columns of the feline spinal cord. Neurosci. 16: 375-394.

McNeill, D.L., Chung, K., Carlton, S.M. and Coggeshall, R.E. (1988a). Calcitonin gene-related peptide immunostained axons provide evidence for fine primary afferent fibers in dorsal and dorsolateral funiculi of rat spinal cord. J. Comp. Neurol. 272: 303-308.

McNeill, D.L., Chung, K., Hulsebosch, C.E., Bolender, R.P. and Coggeshall, R.E. (1988b). Number of synapses in laminae I-IV of the rat dorsal horn. J. Comp. Neurol. 278: 453-460.

Mehler, W.R. (1962). The anatomy of the so-called "pain tract" in man: an analysis of the course and distribution of the ascending fibers of the fasciculus anterolateralis. In: *Basic Research in Paraplegia*. J.D. French and R.W. Porter, eds., New York.

Mehler, W.R. (1966). Some observations on secondary ascending afferent systems in the central nervous system. In: *Pain*. R.S. Knighton and P.R. Dumke, eds. Little Brown, Boston.

Mehler, W.R. (1969). Some neurological species differences – a posteriori. Ann. N.Y. Acad. Sci. 167: 424-468.

Mehler, W.R. (1974). Central pain and the spinothalamic tract. Adv. Neurol. 4: 127-146.

Mendell, L.M. (1966). Physiological properties of unmyelinated fiber projection to the spinal cord. Exp. Neurol. 16: 316-322.

Mense, S. and Stahnke, M. (1983). Responses in muscle afferent fibres of slow conduction velocity to contractions and ischaemia in the cat. J. Physiol. 342: 383-397.

Mense, S. and Meyer, H. (1985). Different types of slowly conducting afferent units in cat skeletal muscle and tendon. J. Physiol. 363: 403-417.

Millar, J. and Basbaum, A.I. (1975). Topography of the projection of the body surface of the cat to cuneate and gracile nuclei. Exp. Neurol. 49: 281-290.

Morin, F. (1955). A new spinal pathway for cutaneous impulses. Amer. J. Physiol. 183: 245-252.

Morin, F., Kitai, S.T., Portnoy, H. and Demirjian, C (1963). Afferent projections to the lateral cervical nucleus: a microelectrode study. Amer. J. Physiol. 204: 667-672.

Morrison J.F.B. (1977). The afferent innervation of the gastrointestinal tract. In: *Nerves and the Gut*. F.P. Brooks and P.W. evers, eds. C.B. Slack, Thorofare, New Jersey.

Morton, C.R., Johnson, S.M. and Duggan, A.W. (1983). Lateral reticular regions and the descending control of dorsal horn neurones of the cat: selective inhibition by electrical stimulation. Brain Res. 275: 13-21.

Narotzky, R.A. and Kerr, R.W. (1978). Marginal neurons of the spinal cord: types, afferent synaptology and functional consideration. Brain Res. 139: 1-20.

Nathan, P.W. and Smith, M.C. (1979). Clinico-anatomical correlation in anterolateral cordotomy. Adv. Pain Res. Ther. 3: 921-926.

Noble, R. and Riddell, J.S. (1988). Cutaneous excitatory and inhibitory input to neurones of the postsynaptic dorsal column system in the cat. J. Physiol. 396: 497-513.

Noble, R. and Riddell, J.S. (1989). Descending influences on the cutaneous receptive fields of postsynaptic dorsal column neurones in the cat. J. Physiol. 408: 167-183.

Nord, S.G. (1967). Somatotopic organization in the spinal trigeminal nucleus, the dorsal column nuclei and related structures in the rat. J. Comp. Neurol. 130: 343-356.

Northgrave, S.A. and Rasmusson, D.D. (1996). The immediate effects of peripheral deafferentation on neurons of the cuneate nucleus in raccoons. Somatosensory and Motor Res. 13(2): 103-113.

Nyberg, G. and Blomqvist, A. (1982). The termination of forelimb nerves in the feline cuneate nucleus demonstrated by the transganglionic transport method. Brain Res. 248: 209-222.

Nyberg, G. (1988). Representation of the forepaw in the feline cuneate nucleus: a transganglionic transport study. J. Comp. Neurol. 271: 143-152.

Patterson, J.T., Head, P.A., McNeill, D.L., Chung, K. and Coggeshall, R.E. (1989). Ascending unmyelinated primary afferent fibers in the dorsal funiculus. J. Comp. Neurol. 290: 384-390.

Patterson, J.T., Coggeshall, R.E., Lee, W.T. and Chung, K. (1990). Long ascending unmyelinated primary afferent axons in the rat dorsal column: immunohistochemical localizations. Neurosci. Lett. 108: 6-10.

Perkel, D.H., Gerstein, G.L. and Moore, G.P. (1967). Neuronal spike trains and stochastic point processes. II. Simultaneous spike trains. Biophys. J. 7: 419-440.

Peschanski, M., Mantyh, P.W. and Besson, J.M. (1983). spinal afferents to the ventrobasal thalamic complex in the rat: an anatomical study using wheat-germ agglutinin conjugated to horseradish peroxidase. Brain Res. 278: 240-244.

Pierce, J.P., Weinberg, R.J. and Rustioni, A. (1990). Single fiber studies of ascending input to the cuneate nucleus of cats: II. Postsynaptic afferents. J. Comp. Neurol. 300: 134-152.

Price, D.D., Hayes, R.L., Ruda, M. and Dubner, R. (1978). Spatial and temporal transformations of input to spinothalamic tract neurons and their relation to somatic sensations. J. Neurophysiol. 41: 933-947.

Pubols, L.M. and Pubols, B.H. (1973). Modality composition and functional characteristics of dorsal column mechanoreceptive afferent fibers innervating the raccoon's forepaw. J. Neurophysiol. 36: 1023-1037.

Pubols, B.H. and Haring, J.H. (1995). The raccoon spinocervical and spinothalamic tracts: a horseradish peroxidase study. Brain Res. Rev. 20: 196-208.

Ralston, H.J. and Ralston, D.D. (1982). The distribution of dorsal root axons to laminae IV, V, and VI of the macaque spinal cord: A quantitative electron microscopic study. J. Comp. Neurol. 212: 435-448.

Rasmusson, D.D. (1988). Projections of digit afferents to the cuneate nucleus in the raccoon before and after partial deafferentation. J. Comp. Neurol. 277: 549-556.

Rasmusson, D.D. (1989). The projection pattern of forepaw nerves to the cuneate nucleus of the raccoon. Neurosci. Lett. 98: 129-134.

Rasmusson, D.D. and Northgrave, S.A. (1997). Reorganization of the raccoon cuneate nucleus after peripheral denervation. J Neurophysiol. 78: 2924-2936.

Rastad, J., Jankowska, E. and Westman, J. (1977). Arborization of initial axon collaterals of spinocervical tract cells stained intracellularly with horseradish peroxidase. Brain Res. 135: 1-10.

Rastad, J. (1981a). Morphology of synaptic vesicles in axodendritic and axosomatic collateral terminals of two feline spinocervical tract cells stained intracellularly with horseradish peroxidase. Exp. Brain Res. 41: 390-398.

Rastad, J. (1981b). Quantitative analysis of axodendritic and axosomatic collateral terminals of two feline spinocervical tract cells. J. Neurocytol. 10: 475-496.

Rethelyi, M. and Szentagothai, J. (1973). Distribution and connections of afferent fibres in the spinal cord. In: *Handbook of Sensory Physiology*, Vol. II. *Somatosensory System*. A. Iggo, ed. Springer-Verlag, New York.

Rethelyi, M. (1977). Preterminal and terminal axon arborizations in the substantia gelatinosa of cat's spinal cord. J. Comp. Neurol. 172: 511-528.

Rethelyi, M. and Capowski, J.J. (1977). The terminal arborization pattern of primary afferent fibers in the substantia gelatinosa of the spinal cord in the cat. J. Physiol. 73: 269-277.

Rexed, B. and Therman, P. (1948). Calibre spectra of motor and sensory nerve fibres to flexor and extensor muscles. J. Neurophysiol. 11: 133-139.

Rexed, B. (1952). The cytoarchitectonic organization of the spinal cord in the rat. J. Comp. Neurol. 96: 415-466.

Rexed, B. (1954). A cytoarchitectonic atlas of the spinal cord in the cat. J. Comp. Neurol. 100: 297-380.

Rothwell, J. (1992). *Control of Human Voluntary Movement* 2nd edition. Chapman and Hall, New York.

Rowinski, M.J., Haring, J.H. and Pubols, B.H. (1981). Correlation of peripheral receptive field area and rostrocaudal locus of neurons within the raccoon cuneate nucleus. Brain Res. 211: 463-467.

Rowinski, M.J., Haring, J.H. and Pubols, B.H. (1985). Response properties of raccoon cuneothalamic neurons. Somatosensory Res. 2: 263-280.

Rustioni, A. (1973). Non-primary afferents to the nucleus gracilis from the lumbar cord of the cat. Brain Res. 51: 81-95.

Rustioni, A. (1974). Non-primary afferents to the cuneate nucleus in the brachial dorsal funiculus of the cat. Brain Res. 75: 247-259.

Rustioni, A. and Kaufman, A.B. (1977). Identification of cells of origin of non-primary afferents to the dorsal column nuclei of the cat. Exp. Brain Res. 27: 1-14.

Rustioni, A., Schmechel, D.E., Cheema, S. and Fitzpatrick, D. (1984). Glutamic acid decarboxylase containing neurons in the dorsal column of the cat. Somatosensory Res. 1: 329-357.

Schaible, H.G. and Schmidt, R.F. (1983a). Activation of groups III and IV sensory units in medial articular nerve by local mechanical stimulation of knee joint. J. Neurophysiol. 49: 35-44.

Schaible, H.G. and Schmidt, R.F. (1983b). Responses of fine medial articular nerve afferents to passive movements of knee joint. J. Neurophysiol. 49: 1118-1126.

Scheibel, M.E. and Scheibel, A.B. (1968). Terminal axon patterns in cat spinal cord. II: The dorsal horn. Brain Res. 9: 32-58.

Schoenen, J. (1982). The dendritic organization of the human spinal cord: the dorsal horn. Neuroscience 7: 2057-2087.

Schoultz, T.W. and Swett, J.E. (1972). The fine structure of the Golgi tendon organ. J. Neurocytol. 1: 1-26.

Sheehan, D. (1932). The afferent nerve supply of the mesentery and its significance in the causation of abdominal pain. J. Anat. 67: 233-249.

Sherman, S.E., Luo, L. and Dostrovsky, J.O. (1997). Altered receptive fields and sensory modalities of rat VPL thalamic neurons during spinal strychnine-induced allodynia. J. Neurophysiol. 78: 2296-2308.

Sherrington, C.S. (1906). *The Integrative Action of the Nervous System.* Yale Univ. Press, New Haven.

Shriver, J.E., Stein, B.M. and Carpenter, M.B. (1968). Central projections of spinal dorsal roots in the monkey. I. Cervical and upper thoracic dorsal roots. Amer. J. Anat. 123: 27-74.

Simone, D.A. and Pubols, B.H. (1991). The raccoon lateral cervical nucleus: a single-unit analysis. J. Neurophysiol. 65(6):1411-1421.

Sinclair, D.C. (1955). Cutaneous sensation and the doctrine of specific nerve energy. Brain 78: 584-614.

Sinclair, D.C. (1981). *Mechanisms of Cutaneous Sensation*, Oxford University Press, New York.

Skoglund, S. (1956). Anatomical and physiological studies of knee joint innervation in the cat. Acta Physiol. Scand. 36: (Suppl 124): 1-101.

Skoglund, S. (1973). Joint receptors and kinaesthesis. In: *Handbook of Sensory Physiology* Vol. II. *Somatosensory System*. A. Iggo, ed. Springer-Verlag, Berlin.

Smith, K.R. (1968). The structure and function of the Haarscheibe. J. Comp. Neurol. 131: 459-474.

Snyder, R.L., Faull, R.L.M. and Mehler, W.R. (1978). Comparative study of the neurons of origin of the spinocerebellar afferents in the rat, cat and squirrel monkey based on the retrograde transport of horseradish peroxidase. J. Comp. Neurol. 181: 833-852.

Sorkin, L.S., Ferrington, D.G. and Willis, W.D. (1986). Somatotopic organization and response characteristics of dorsal horn neurons in the cervical spinal cord of the cat. Somatosensory Res. 3: 323-338.

Sotgiu, M.L. and Marini G. (1977). Reticulo-cuneate projections as revealed by horseradish peroxidase axonal transport. Brain Res. 128: 341-345.

Sprague, J.M. and Ha, H. (1964). The terminal fields of dorsal root fibers in the lumbosacral spinal cord of the cat and the dendritic organization of the motor nuclei. In: Organization of the Spinal Cord. Progress in Brain Research, Vol. II, J.C. Eccles and J.P. Schade, eds. Elsevier, New York.

Stacey, M.J. (1969). Free nerve endings in skeletal muscle of the cat. J. Anat. 105: 231-254.

Stein, R.B., French, A.S. and Holden, A.V. (1972). The frequency response, coherence and information capacity of two neuronal models. Biophys. J. 12(3): 295-322.

Sterling, P. and Kuypers, H.G.J.M. (1967). Anatomical organization of the brachial spinal cord of the cat. I. The distribution of dorsal root fibers. Brain Res. 4: 1-15.

Stevens, J.C. and Green, B.G. (1978). History of research on feeling. In *Handbook of Perception*, Vol 6B, E.C. Carterette and M.P. Friedman, eds., Academic Press, New York.

Stevens, R.T., Hodge, C.J. and Apkarian, A.V. (1989). Medial, intralaminar and lateral terminations of lumbar spinothalamic tract neurons: a fluorescent double label study. Somatosensory and Motor Res. 6: 285-308.

Surmeier, D.J., Honda, C.N. and Willis, W.D. (1988). Natural grouping of primate spinothalamic neurons based on cutaneous stimulation. Physiological and anatomical features. J. Neurophysiol. 59: 833-860.

Svensson, B.A., Rastad, J., Westman, J. and Wiberg, M. (1985). Somatotopic termination of spinal afferents to the feline lateral cervical nucleus. Exp. Brain Res. 57: 576-584.

Szentagothai, J. (1964). Neuronal and synaptic arrangement in the substantia gelatinosa Rolandi. J. Comp. Neurol. 122: 219-239.

Talbot, W.H., Darian-Smith, I., Kornhuber, H.H. and Mountcastle, V.B. (1968). The sense of flutter-vibration: comparison of the human capacity with response patterns of mechanoreceptive afferents from the monkey hand. J. Neurophysiol. 31: 301-334.

Tamatani, M., Senba, E. and Tohyama, M. (1989). Calcitonin gene-related peptide- and substance P-containing primary afferent fibers in the dorsal column of the rat. Brain Res. 495: 122-130.

Torebjork, H.E. and Hallin, R.G. (1973). Perceptual changes accompanying controlled preferential blocking of A and C fibre responses in intact human skin nerves. Exp. Brain Res. 16: 321-332.

Uddenberg, N. (1966). Studies on modality segregation and second order neurones in the dorsal funiculus. Experientia 22: 441-442.

Uddenberg, N. (1968). Functional organization of long, second-order afferents in the dorsal funiculus. Exp. Brain Res. 4: 377-382.

Valverde, F. (1966). The pyramidal tract in rodents. A study of its relations with the posterior column nuclei dorsolateral reticular formation of the medulla oblongata, and cervical spinal cord (Golgi and electron microscopic observations). Z. Zellforsch. 71: 297-363.

Walker, A.E. and Weaver, T.A. (1942). The topical organization and termination of the fibers of the posterior columns in Macaca mulatta. J. Comp. Neurol. 76: 145-158.

Weisberg, J.A. and Rustioni, A (1979). Cortical cells projecting to the dorsal column nuclei of Rhesus monkey. Exp. Brain Res. 28: 521-528.

Welker, W.I. and Johnson, J.I. (1965). Correlation between nuclear morphology and somatotopic organization in ventro-basal complex of the raccoon's thalamus. J. Anat. Lond. 99: 761-790, 1965.

Werner, G. and Whitsel, B.L. (1967). The topology of dermatomal projection in the medial lemniscal system. J. Physiol. 192: 123-144.

Willis, W.D. (1999). Anatomy, physiology and descending control of lumbosacral sensory neurons involved in tactile and pain sensations. In: *Handbook of Behavioural State Control: Cellular and Molecular Mechanisms*. R.Lydic and H.A. Baghdoyan, eds. CRC Press, New York.

Willis, W.D., Trevino, D.L., Coulter, J.D. and Maunz, R.A. (1974). Responses of primate spinothalamic tract neurons to matural stimulation of hindlimb. J. Neurophysiol. 37: 358-372.

Willis, W.D., Maunz, R.A., Foreman, R.D. and Coulter, J.D. (1975). Static and dynamic responses of spinothalamic tract neurons to mechanical stimuli. J. Neurophysiol. 38: 587-600.

Willis, W.D., Leonard, R.B. and Kenshalo, D.R. Jr. (1978). Spinothalamic tract neurons in the substantia gelatinosa. Science 202: 986-988.

Willis, W.D., Kenshalo, D.R., Jr. and Leonard, R.B. (1979). The cells of origin of the primate spinothalamic tract. J. Comp. Neurol. 188: 543-574.

Willis, W.D., Coggeshall, R.E. (1991) *Sensory Mechanisms of the Spinal Cord*, 2nd edition, Plenum Press, New York.

Woodward, W.R. (1975). Hermann Lotze's critique of Johannes Muller's doctrine of specific sense energies. Med. Hist. 19: 147-57.

Zelman, F.P., Leonard, C.M., Kow, L.M. and Pfaff, D.W. (1978). Ascending tracts of the lateral columns of the rat spinal cord: a study using the silver impregnation and horseradish peroxidase techniques. Exp. Neurol. 62: 298-334.

APPENDIX:

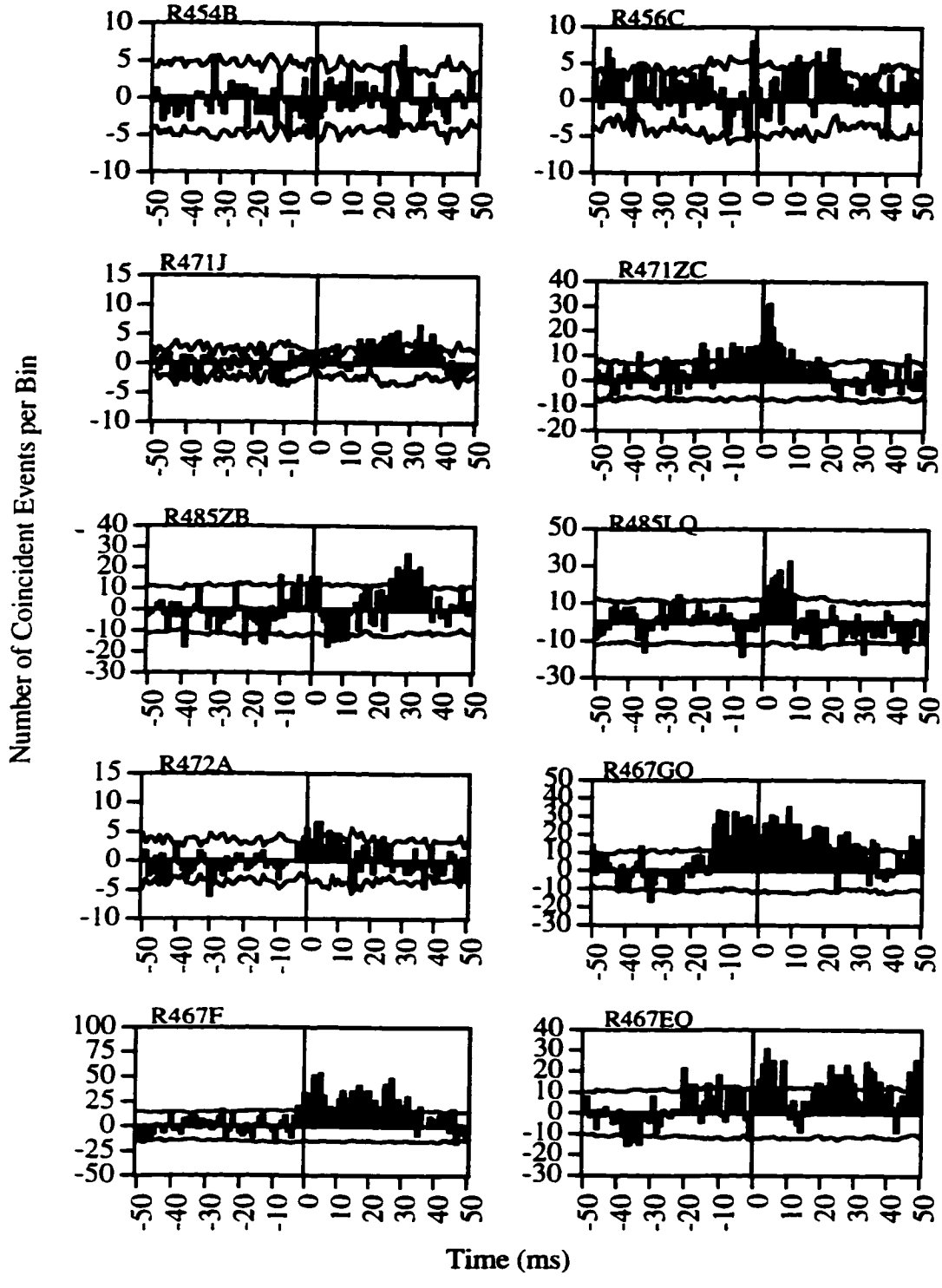

*Neural CCGs for significant excitatory spinocuneate interactions not shown in RESULTS (Figure 15)

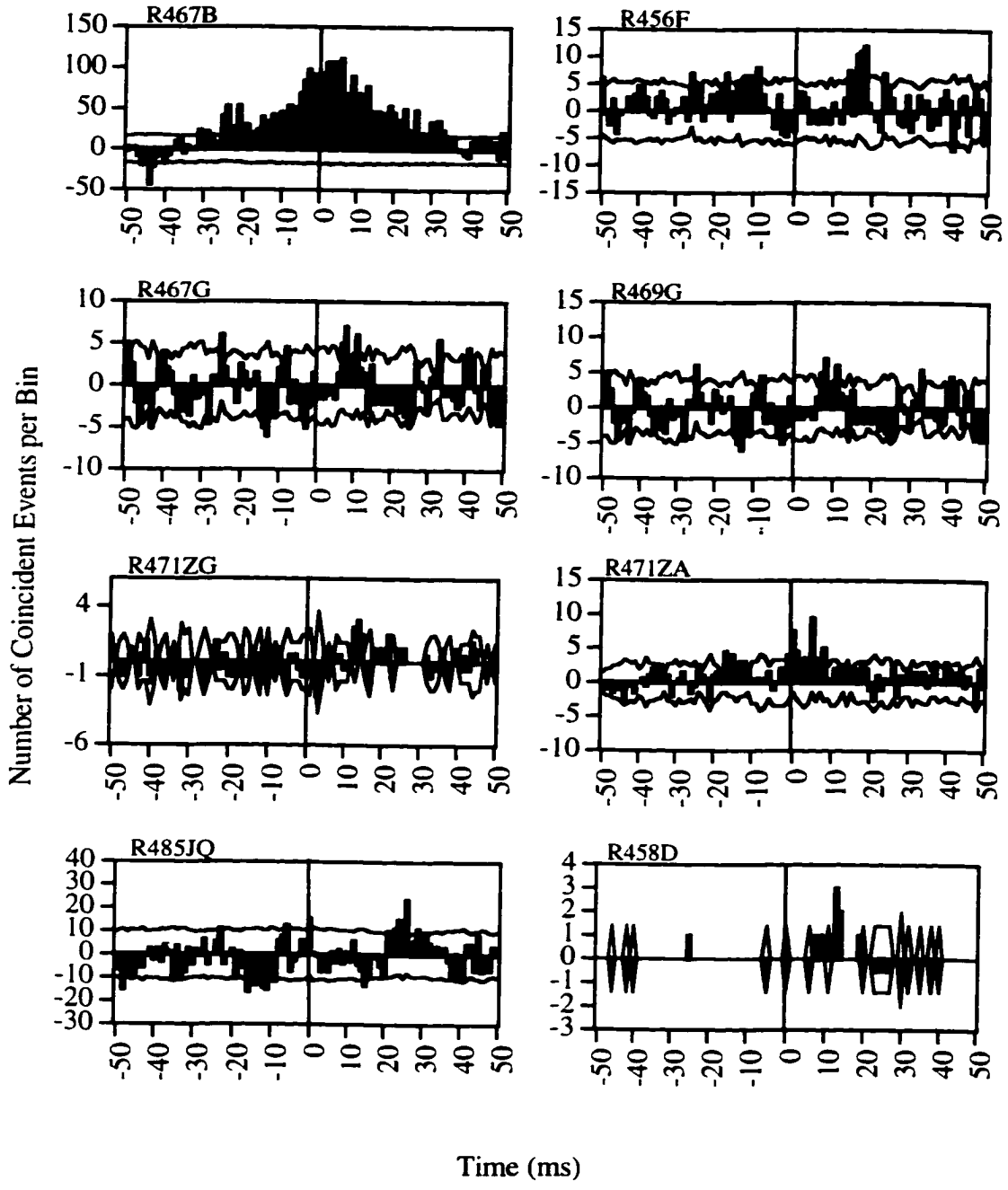

*Neural CCGs for significant excitatory spinocuneate interactions

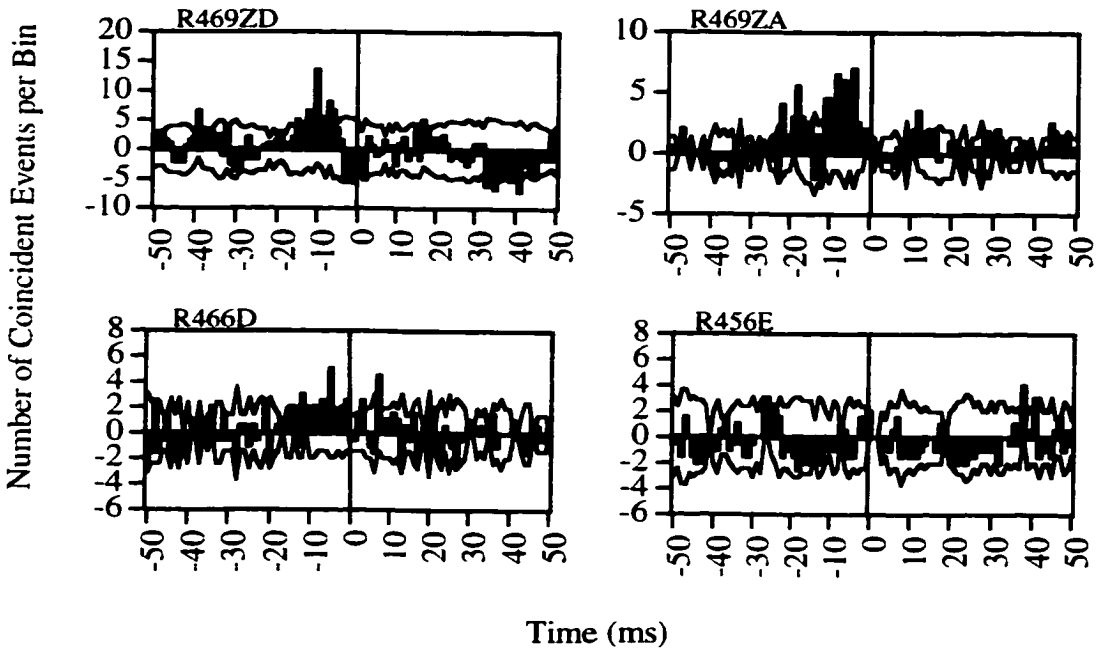

*Neural CCGs for significant excitatory cuneospinal interactions not shown in RESULTS (Figure 18)

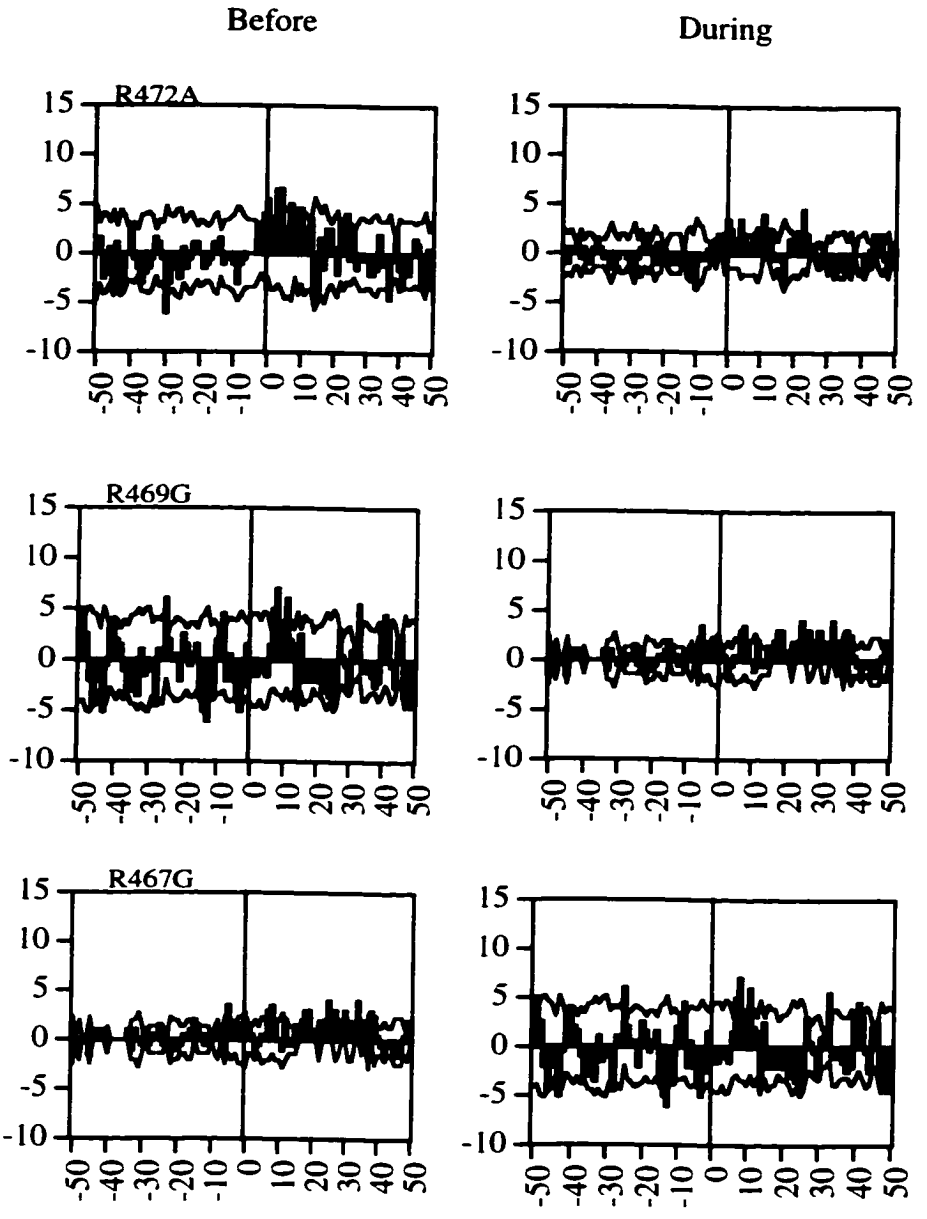

*Neural CCGs for significant spinocuneate interactions before vs. during deafferentation not shown in RESULTS (Figure 25)

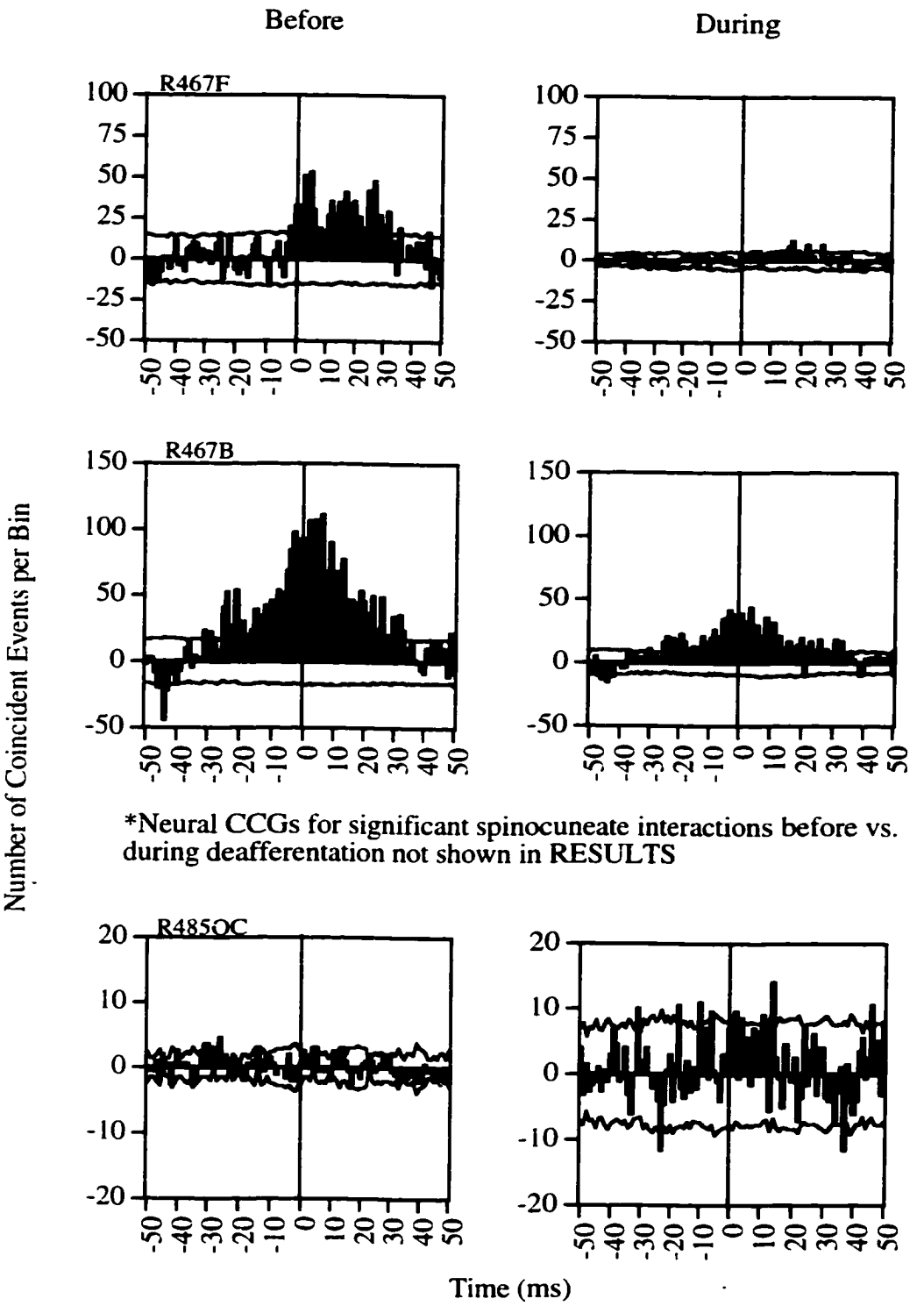

*Neural CCGs for significant spinocuneate interactions before vs. during deafferentation not shown in RESULTS

*Neural CCGs for significant cuneospinal interactions before vs. during deafferentation not shown in RESULTS